To the Graduate Council:

I am submitting herewith a thesis written by David Charles Johnson entitled "Structural Behavior and Damage Assessment of Residential Foundations Subjected to Subsidence." I have examined the final copy of this thesis for form and content and recommend that it be accepted in partial fulfillment of the requirements for the degree of Master of Science, with a major in Civil Engineering.

Dr. Richard Bennett, Major Professor

We have read this thesis
and recommend its acceptance:

Accepted for the Council:

Associate Vice Chancellor
and Dean of The Graduate School

STRUCTURAL BEHAVIOR AND DAMAGE ASSESSMENT OF RESIDENTIAL FOUNDATIONS SUBJECTED TO SUBSIDENCE

A Thesis

Presented for the

Master of Science

Degree

The University of Tennessee, Knoxville

David Charles Johnson

December 1992

ACKNOWLEDGMENT

I would like to express my respect and thanks to Dr. Richard Bennett for the opportunity to work with him on this project. His patience was tried at times and I deeply appreciate his assistance, leadership, and friendship during preparation of this document. Also deserving thanks are Dr. Eric Drumm and Dr. Edwin Burdette for taking the time to read this manuscript and sit on my defense committee. I highly respect them.

My wife, daughter, and parents provided the emotional support necessary to complete this document. My daughter Annie, was only one when I started graduate school. Most of my spare time for the last two years was spent on completion of this degree and a great sacrifice was made by her. My wife Stephanie, has provided constant support, and her sacrifices have been tremendous. I deeply appreciate her love and support. My parents, Irma and Les Johnson, have always provided unyielding support and the past two years have been no exception. I feel very fortunate to have them.

Funding of my participation in this project was provided by the Illinois Mine Subsidence Insurance Fund, National Science Foundation, U.S. Bureau of Mines Twin Cities Research Center, and Old Ben Coal Company. Thanks for providing this opportunity.

While a full-time employee of Tom Kesterson's Company, he provided financial support and allowed me a month off from work to complete this thesis. Thanks.

ABSTRACT

Coal mining in southern Illinois has resulted in many houses being exposed to subsidence damage. Insurance and coal companies compensate home owners for damage, and thus they are interested in ways to minimize losses. Damage mitigation techniques used in house foundations are effective in minimizing subsidence damage.

Various footing damage mitigation techniques were applied to twelve strip foundations constructed above an advancing long-wall mine. Post-tensioning, deformed bars, and steel fibers were used to reinforce three of the footings. Two of the footings were constructed with footing/soil interfaces and one used only plain concrete (control foundation). Construction of the foundations is described. The structural materials used in the foundations were tested to obtain parameters for analytic modeling. The behavior of the foundations was measured by using a tape extensometer. The measured behavior is compared with the costs of the various damage mitigation techniques to establish cost-benefit relationships.

The post-tensioned foundation had the least damage but was the most expensive. The deformed bar foundation performed well, but cost only slightly more than the control foundation. The footing/soil interfaces only slightly decreased damage over the control. A need for wall damage mitigation techniques was recognized.

TABLE OF CONTENTS

CHAPTER	PAGE

LIST OF TABLES

TABLE		PAGE

LIST OF FIGURES

FIGURE PAGE

FIGURE		PAGE

CHAPTER 1

INTRODUCTION

1.1 Statement of Problem

Illinois, the fifth largest producer of coal in the United States, produces approximately 60 million tons of coal from more than twenty-five underground and twelve surface mines. More than two thousand mines have been operated and abandoned since the mid 1800's. Until recently, coal was mined by extracting approximately 50% of the coal seam in a network of rooms and pillars. As years pass, the pillar support systems disintegrate from exposure to air or sink into the soft clay floor common to these mines. The result is an initiation of movement that propagates toward ground level, causing damage to homes and other structures. It is quite difficult to predict when, or at what rate this will occur.

A modern coal extraction method is long-wall mining. The coal is mined in panels several hundred feet wide and no pillars remain for roof support. The roof collapses immediately after removal of the coal and the ground surface subsides soon after. This method is efficient and ground movement occurs in a more controlled fashion.

On September 1, 1979, the Illinois General Assembly created the Illinois Mine Subsidence Insurance Fund. This fund requires insurance companies in Illinois to offer coverage against mine subsidence damage (usually from abandoned room and pillar mines) as part of their property insurance. Insurance companies are reimbursed from the insurance fund for these claims. The fund provides technical expertise to evaluate if claims are actually caused by mining subsidence or by other phenomena. They also are involved in research to suggest possible construction and repair techniques to minimize mining subsidence damage.

Old Ben Coal Company (now Zeigler Coal) uses long-wall mining to extract coal in southern Illinois. When they mine under an area, the property owners subjected to subsidence damage must be compensated. The company may purchase the property, provide pre-subsidence damage mitigation measures (e.g. set the house on jacks), or repair the damaged structure after subsidence. If the land is purchased, the coal company needs to know when and how a structure can be built to minimize company losses. Damage mitigation techniques used in house foundations may allow the land to be sold before the ground has completely stopped settling.

1.2 Purpose of Study

This thesis is based on information gained from a research project (Bennett and Drumm, 1992; Bennett et al., 1992) in which 12 foundations were constructed above an advancing long-wall mine in Franklin County, Illinois. Each foundation consisted of a strip footing and four course masonry wall loaded with soil bins spanning between adjacent foundations to simulate typical house loads. Partial funding of this research was provided by the Illinois Mine Subsidence Insurance Fund. Old Ben Coal provided the land where the foundations were constructed. They also mined under the site.

Prior to mining, six foundations were constructed above the centerline of the panel and six at the predicted zone of maximum tension. Six footing designs were used at each site to investigate their effectiveness on damage mitigation. In addition to a control foundation built according to conventional practice, several soil/footing interfaces and reinforcing methods were used in the footings. Finite element analysis was used to predict the behavior and select the proper reinforcing amounts used in the footings (Hudgings et al. 1990). The foundations were well instrumented and monitored closely during mining subsidence.

Foundation construction is described in this thesis. Structural material properties of the foundations were determined and are also included. These properties will be used in finite element analyses to develop models that better simulate measured behavior. Data obtained from a tape extensometer is used to show foundation behavior during subsidence. Also investigated in this thesis is the relative costs of using various damage mitigation techniques.

The purpose of this thesis is to document the construction and obtain material properties of the foundations. Using the tape extensometer and economic analysis, cost and benefit comparisons can be made between the expense and performance of the various damage mitigation techniques. This information is useful in selecting the proper foundation design for structures subjected to subsidence.

CHAPTER 2

FOUNDATION CONSTRUCTION

2.1 Foundations

2.1.1 General Description

The foundations were constructed to simulate typical residential house foundations. English units were used during construction, although values are reported herein in both SI and English units. Each foundation consists of a concrete strip footing, a four-course masonry wall, and a double sill plate. Typical house loads are simulated by wooden load bins that span between pairs of foundations.

2.1.2 Footing Types

One control footing and five different damage mitigation techniques were investigated on each test site. All of the construction methods used are considered practical and relatively economical for the geographical location. The footing dimensions are 40.0 feet (12.2 meters) long, 18 inches (460 mm) wide, and 10 inches (250 mm) deep, which is a typical size in residential construction. Three of the footing types are illustrated in Figure 2-1. The plain concrete footing is considered to be the most typical of existing construction in southern Illinois. It was constructed using only concrete placed in the footing trench. This footing served as the control footing in damage comparisons. The second footing was constructed using #4 A615 Grade 60

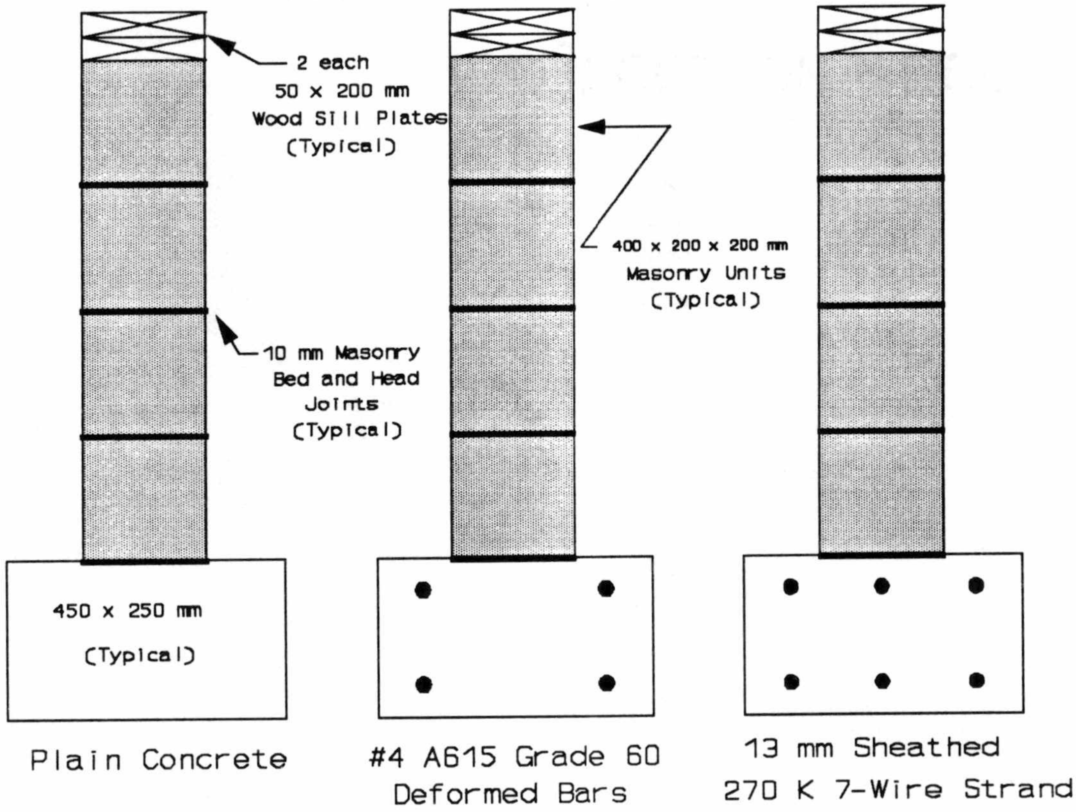

Figure 2-1 Plain Concrete, Deformed Bar, and Post-Tensioned Footings

deformed reinforcing bars. These bars are 0.5 inches (13 mm) in diameter and have a specified minimum yield stress of 60 ksi (414 MPa). There are two bars on the top and two on the bottom of the footing. A concrete cover of 2 inches (50 mm) was used on the top, bottom, and sides. The third footing is post-tensioned using 270K 7-wire strand which is greased and enclosed in a plastic sheath. The strand is 0.5 inches (13 mm) in diameter and has a specified guaranteed ultimate tensile strength of 270 ksi (1862 MPa). There are three strands evenly spaced at the top and the bottom of the footing with the same concrete cover as the deformed bars.

In Figure 2-2, the other three footings are illustrated. The first footing is a plain concrete footing cast on a 6 mil (0.15 mm) plastic interface that has a 6 inch (150 mm) layer of natural sand lining the trench bottom. Plastic surrounds the footing on the bottom and both sides. The second footing is a plain concrete footing completely surrounded by a 6 mil (0.15 mm) plastic interface directly in contact with the existing trench soil. The third footing has 1.0 inch (25 mm) steel fibers (trade name, "1 inch Anchorloc"; obtained from Mitchell Fibercon, Inc.) mixed in with the concrete. Steel fiber was added at a rate of 75.0 pounds per cubic yard (436 newtons per cubic meter) according to manufacturer's recommendations.

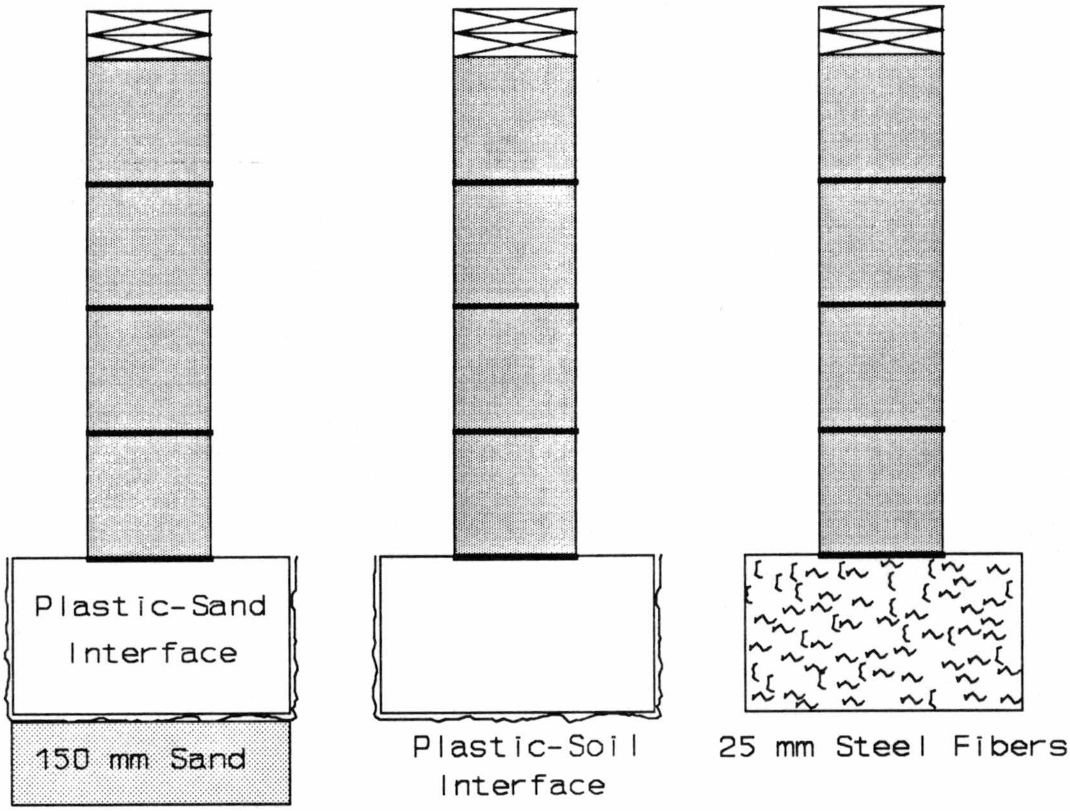

Figure 2-2 Plastic-on-Sand, Plastic-on-Soil, and Steel Fiber Footings

2.2 Site Layout

2.2.1 Choosing the Site

The site was chosen by Lindell Sneed, a representative of Old Ben Coal Company. Certain factors decided the location. First, the land chosen was above an advancing longwall panel and owned by Old Ben Coal Company. Second, the land had access for moving equipment in and out of the site.

The site was located approximately 4 miles (6 kilometers) east of Interstate 59 on Illinois State Route 149. Herron Road, a dead-end gravel road that ran perpendicular to the panel and came to within 45 feet (14 meters) of both sites, was used to access the sites. Both sites could be accessed from the gravel road with no obstructions. An abandoned house on the south side of the centerline footings was used to store inexpensive equipment and served as an occasional shelter from the rain.

2.2.2 Foundation Layout

The centerline and edge of panel were established from Old Ben Coal Company surveyors.

Through personal communications with Lindell Sneed of Old Ben Coal Company, it was determined the center of the tension zone foundations should be positioned 75 feet (23 meters) from the edge of the panel to be in the zone of maximum tension (as shown in Figure 2-3). Layout of the footings was accomplished by representatives of the research team in conjunction with a local contractor. The

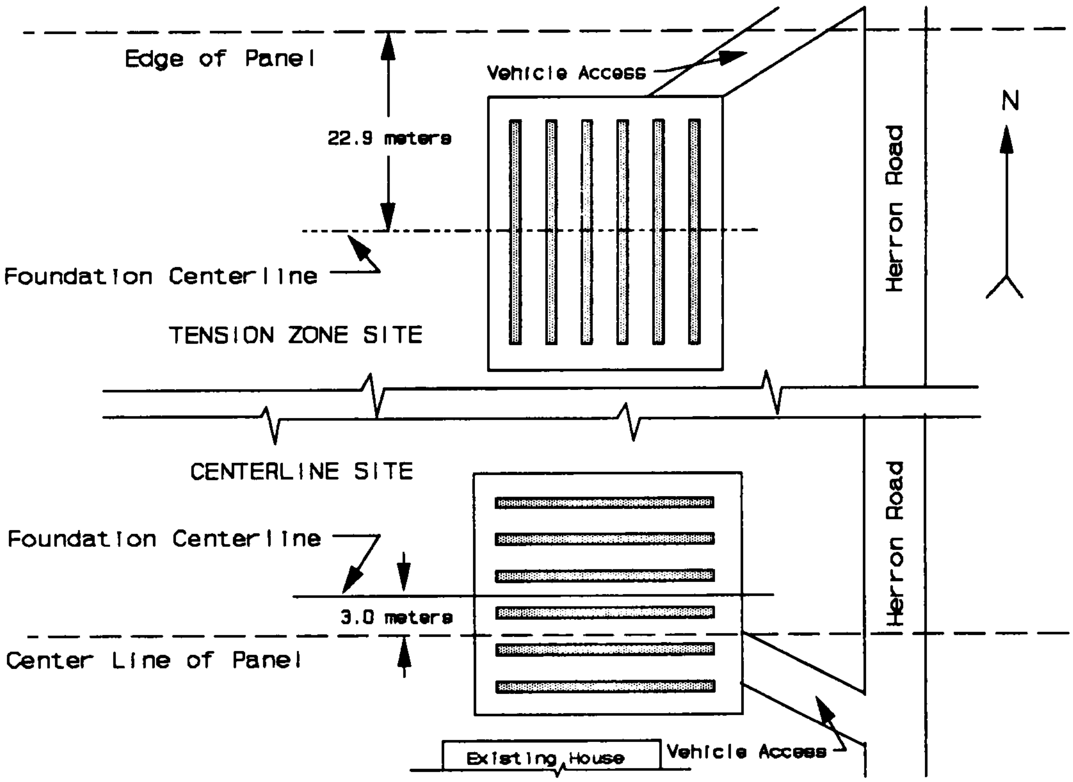

Figure 2-3 Tension Zone and Centerline Site Layout

centerline foundations were positioned parallel to and centered around a line 10 feet (3 meters) north of the panel centerline as illustrated in Figure 2-3. This provided clearance around the abandoned house and avoided an existing cistern. The only consideration to east-west positioning was to keep them as close as possible to the access road. The chosen foundation sites were within approximately 6 feet (2 meters) in elevation with respect to one another.

2.3 Excavation and Site Preparation

2.3.1 Initial Excavation

A local contractor, K. D. Crain and Sons, Inc., was hired to excavate the two test sites. The excavation took place during the second week of March, 1990, approximately one week before the concrete was placed. The sites had few trees or brush to clear, and there was complete access around the sites for excavation equipment.

A small bulldozer was used to strip and stockpile the top soil on each site. Using the bulldozer, the sites were fine-graded at a constant slope of two percent for drainage. The centerline site at finished grade was cut to approximately 2.5 feet (0.8 meters) below the original ground surface. The tension zone site, which was on an incline, required a cut of approximately 5 feet (1.5 meters) on the south end tapered to approximately 2 feet (0.6 meters) on the north end. A backhoe was used to excavate a sump (drainage ditch) along the length of the sites at a two percent slope for drainage. Figure 2-4 illustrates the original drainage scheme and the limits of excavation for the

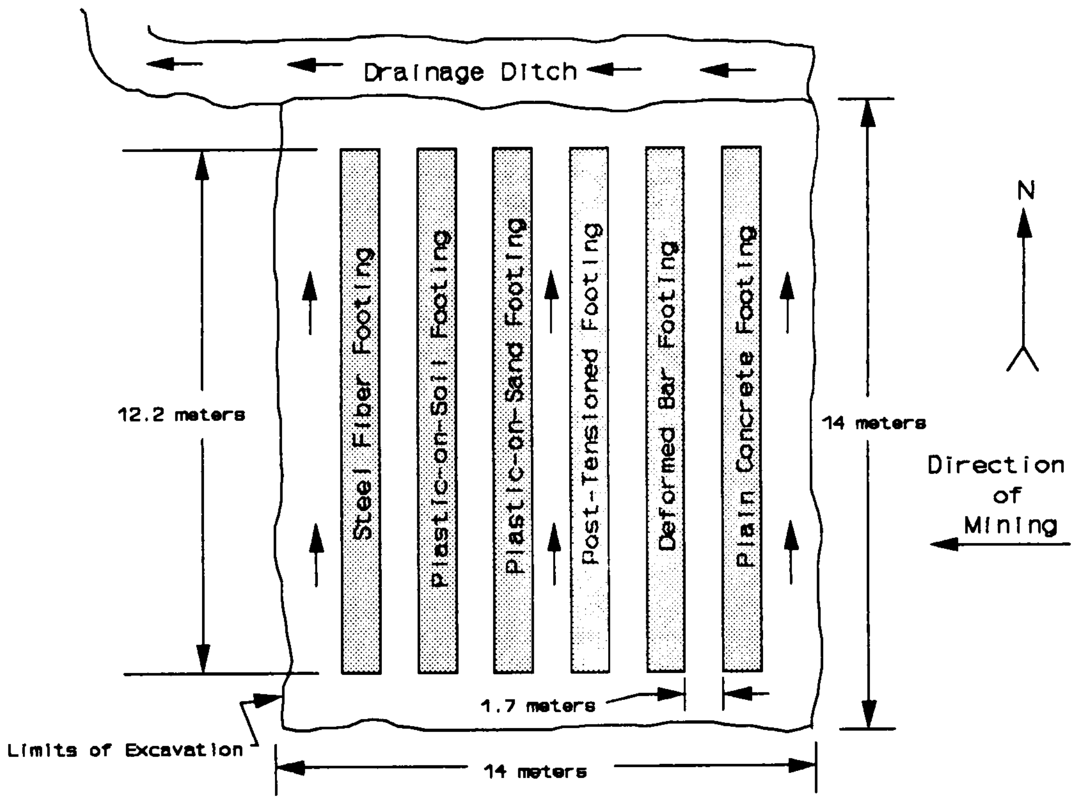

Figure 2-4 Tension Zone Site Drainage

tension zone site, which is typical of both sites. To minimize precipitation runoff on both sites, a water shed diverter was created by excavating a shallow trench around the uphill perimeter of the site.

Once the finished grade was established, a backhoe with an 18 inch (460 mm) bucket (the footing width) excavated trenches which served as forms for the footings. The trenches were excavated 40 feet (12.2 meters) long and 10 inches (250 mm) deep for all footings with two exceptions. The trenches excavated for the post-tensioned footings were constructed 44 feet (13.4 meters) long to leave 2 feet (0.6 meters) on either end for post-tensioning equipment. The trenches excavated for the plastic-on-sand interface were 16 inches (400 mm) deep to allow placement of 6 inches (150 mm) of sand.

2.3.2 Field Conditions

The research team arrived on March 17, 1990, to install the instrumentation and place the concrete in the footings. Heavy rains after the initial excavation caused the footing trenches to partially lose their shape. Both sites required trench repair and dewatering, but the centerline site demanded the most effort.

The tension zone trenches for the plain concrete and deformed bar footing (see Figure 2-4) were repaired and ready for instrumentation on March 17 after bailing and removal of approximately 1.5 inches (40 mm) of saturated soil from the trench bottoms. Adjacent pairs of trench bottoms were maintained at the same elevation where load bins span. The grade and strain gage stakes were placed and shot to grade using a survey level. The other tension zone trenches were bailed to help dry them out for the next day.

On March 18, the bottom layer of saturated soil was removed in the remaining tension zone trenches, and they were smoothed to final grade. The trench bottoms for the post-tensioned and plastic-on-sand footings and the trench bottoms for the plastic-on-soil and steel fiber footings (see Figure 2-4) were at the same elevation unique to each pair. The grade and strain gage stakes were set to the proper elevation.

On March 17, the research team started repair of the centerline footing trenches. The soil conditions were poor due to the rain received the previous week. The water table was located approximately 3 inches (70 mm) above the bottom of the footing trenches. Field problems were compounded due to the centerline site being located at the drainage outlet for the area water shed. Small trenches and sumps were excavated using hand tools to start dewatering the site.

On March 18, after completion of the tension zone footings, several members of the team began working on the centerline site. Several inches of saturated soil were removed from the footing trenches in an attempt to reach firm soil. Firm soil could not be obtained due to the high water table. To dewater the site a sump ditch at the same elevation as an existing culvert was excavated along the west, north, and east perimeters of the site as illustrated in Figure 2-5. This elevation was approximately 7 inches (180 mm) below the lowest trench bottom (the steel fiber and deformed bar footings).

At the end of the day on March 18, a light rain began to fall and both sites were covered with plastic. All strain gages were in place in the tension zone trenches. The

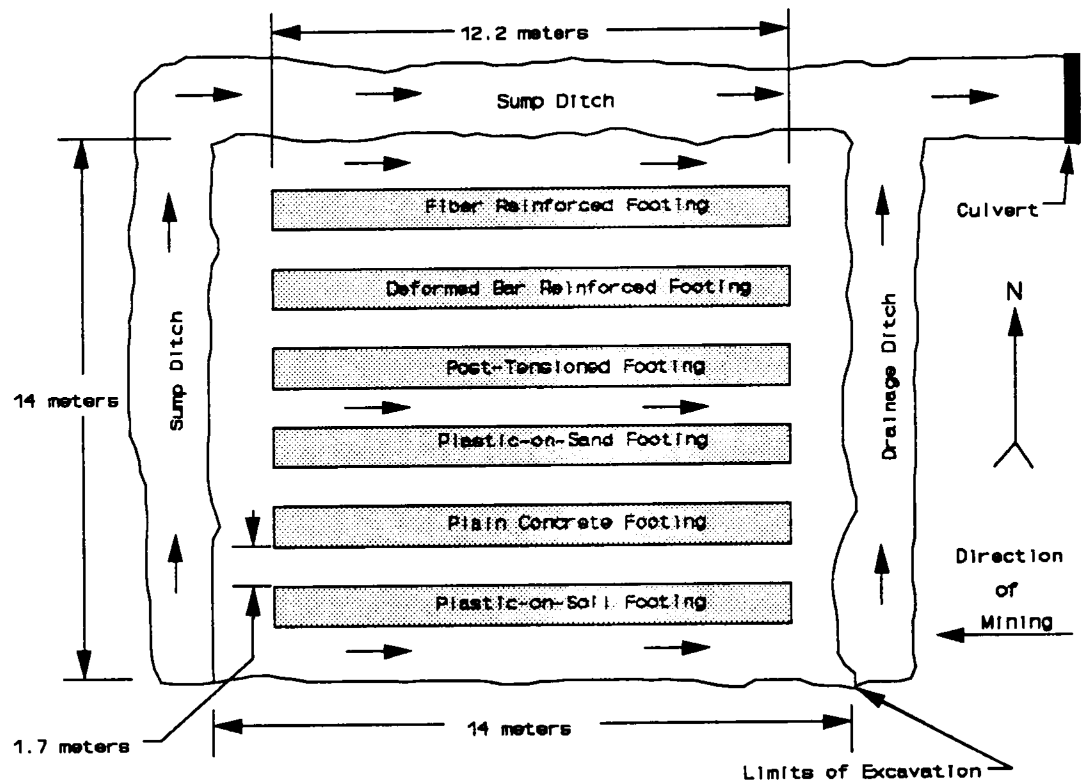

Figure 2-5 Centerline Site Drainage

plastic was allowed to sag in the trenches making it was necessary to place boards above each set of strain gages to keep the weight of the water collected on the plastic from affecting the completed work. The storm front produced wind and rain for several hours. A trip back to the site after dark verified the plastic was performing as expected.

On the morning of March 19, water bailing lines were formed to remove the water and ice that had collected on the plastic. The tension zone trenches were kept dry, and the centerline trenches had not been adversely affected from the rain.

All of the concrete had to be placed using wheelbarrows to avoid damage to the footing instrumentation. The site elevations were below the surrounding ground elevation; therefore, it was necessary to get a concrete truck in close enough for the truck chute to reach into the site. The ground conditions surrounding the tension zone site consisted of wet soft soil, incapable of vehicle traffic. Therefore, to facilitate concrete placement, a tandem truck load of 1 inch (25 mm) gravel was brought in. Using a small front-end loader, a vehicle access road as shown in Figure 2-3 was constructed to within 10 feet (3 meters) of the site.

On March 19, while concrete was being placed in the tension zone site, the centerline footing trenches were left to dewater. On the morning of March 20, all members of the research team worked to get the centerline footing trenches to grade and to set instrumentation. Due to the poor surrounding soil conditions, a tandem truck load of 3 inch (75 mm) aggregate was brought in to construct a vehicle access road (Figure 2-3). The reason for using the larger aggregate at the centerline site was due to the ground conditions being in even worse shape and the larger aggregate providing a better bearing surface.

The team concentrated their efforts on the plastic-on-soil, plain concrete, and the plastic-on-sand trenches (see Figure 2-5). The plastic-on-soil footing trench was in the worst condition and required the most work. The trench was wider in places than the original specified width of 18 inches (460 mm). The east end of these three trenches and the west end of the plastic-on-soil footing trench required forming due to the small drainage trenches that were excavated during dewatering.

Elevations of the trench bottoms had dropped considerably from the initial excavations. Extra work was required when the plastic-on-sand trench elevation had to be lowered. The existing sand placed by the contractor had to be removed and the trench bottom re-excavated to a lower elevation. Then the sand had to be replaced to the required 6 inches (150 mm) of thickness. The plastic-on-soil and the plain concrete trench bottoms were set at the same elevation. The plastic-on-sand footing trench bottom was set at an elevation to match the post-tensioned footing trench not to grade at this time. The strain gage and grade stakes were set in each trench. Additional instrumentation consisting of pressure meters and soil strain gages were added to the plain concrete footing.

After the concrete was placed in the first three footings, the team worked on the post-tensioned, deformed bar, and steel fiber footing trenches as seen in Figure 2-5. The steel fiber trench was in poor condition, and the trench walls on the north had to be partially formed from plywood. The east ends of these three footings also were formed with plywood. The deformed bar and the steel fiber trench bottoms were set at the same elevation. The post-tensioned trench should have been set at the same elevation as the plastic-on-sand trench but was set 0.8 inches (20 mm) too low. Therefore, instead of adding soil which would affect the undisturbed condition of the trench bottom, it was decided to pour as is and make up the difference in the masonry joints of the wall.

2.4 Concrete Placement

2.4.1 Tension Zone

On the morning of March 19, the concrete in the tension zone was scheduled to be placed. The footing trenches were ready except for the placement of reinforcing. The deformed bar reinforcing top bars were placed on 8 inch (20.3 cm) steel bolsters and the bottom bars on 2 inch (5.1 cm) steel bolsters both spaced at intervals of 8 feet (2.4 meters). The bars were lapped 12 inches (30 cm) and tied using standard tie wire. The reinforcing bars were tied to the bolsters using tie wire to prevent the bars from moving during placement of concrete.

The post-tensioned footing was prepared next. A form was built for each end of the footing trench. Six holes (three top and three bottom) were drilled in the form for the strand extensions. The holes were cut to an exact size for the post-tensioning anchor form to fit securely into the hole. The strand casing was stripped on the ends to fit through the anchors. Care was taken to ensure that the strand casing did not extend into the anchor. The anchors and plastic pocket formers were put on the strands and connected to the form. The above steps were performed for the other end of the footing until all six strands were in place. The strands were placed on 2 inch (50 mm) and 8 inch (200 mm) bolsters, as with the deformed bars above. The bolsters were spaced at intervals of 4 feet (1.2 meters).

A clear polyethylene 6 mil (0.15 mm) plastic was cut and laid in the plastic-on-soil and plastic-on-sand trenches. The sheet extended over the sides approximately 1 foot (300 mm) around the entire perimeter. No other preparation was necessary for these, the steel fiber, or the plain concrete footing trenches. Walk boards were laid over the drainage ditch between the gravel access road and the foundations for wheelbarrow running boards.

Concrete specifications called for a compressive strength of 3000 psi (21 newtons per square mm) at 28 days. The actual mix design used by the supplier was for 3500 psi (24 newtons per square mm) at 28 days. The mix design contained the proportions shown in Table 2-1.

The first concrete truck arrived with 6 cubic yards (4.6 cubic meters) of ready-mixed concrete to be used in the first three footings. A slump test measured 2.0 inches (50 mm). Approximately 5 gallons (19 liters) of water was added to the mix which increased the slump to 3 inches (76 mm). A 5% air content was determined using a pressure vessel device. Several representative test specimens were made from the mix. Six standard 6 inch (150 mm) diameter by 12 inch (300 mm) cylindrical specimens were cast for compression tests. Two 16 inch (406 mm) by 3 inch (76 mm) by 4 inch (102 mm) beams were cast for flexural testing.

The concrete was placed using various hand tools. The concrete was dumped

Table 2-1 Concrete Mix Proportions

Material	Quantity
Type I Portland Cement	517 pounds per cubic yard (3008 newtons per cubic meter)
Coarse Aggregate	1740 pounds per cubic yard (10122 newtons per cubic meter)
Fine Aggregate	1500 pounds per cubic yard (8726 newtons per cubic meter)
Water	26 gallons per cubic yard (128 liters per cubic meter)
Air Entrainment (Duravair)	3 ounces per cubic yard (116 ml per cubic meter)

into the trench from wheelbarrows at footing sections with no instrumentation. It was placed by hand and with shovels around the instrumentation. Great care was taken to ensure that no damage was done to the strain gages and that no voids were left in the concrete. Shovels and rakes served as manual vibrators to remove all voids. The footings were hand floated after obtaining proper grade to provide a smooth surface for laying masonry.

The second concrete truck arrived with 6 cubic yards of concrete to be used in the remaining three footings of the tension zone. The plastic-on-sand and the plastic-on-soil footings were to be placed next. After a slump test revealed a slump of 7.5 inches (190 mm), it was obvious that there was excess water in the mix. This high slump was a concern. However for the purposes of this research, it was important only that the strength be known, and thus the concrete was accepted. It was later learned that the excess water was due to the wash water from the first load being mistakenly left in the concrete truck when it was reloaded.

The air content was measured at 8% which is considered high, but this had probably come from the excess water in the mix. Four cylinders and two beams were cast to represent these two footings.

Concrete placement of the second batch was much easier due to the increased workability. After the plastic-on-sand and the plastic-on-soil footings were cast, there were approximately 2 cubic yards (1.5 cubic meters) of concrete remaining in the truck. According to manufacturer recommendations, 150 pounds (667 newtons) of steel fibers were added to the concrete truck. The truck mixed the fiber concrete for approximately five minutes and a slump was measured to be 4.5 inches (110 mm). This slump was considered acceptable, and the concrete was placed in the usual manner. The steel fibers made the concrete slightly harder to place and float. Four cylinders and three beams were cast from the fiber-reinforced concrete for testing.

Temperatures were predicted to drop well below freezing that night. As a precaution against freezing, the footings were covered with a layer of plastic. This was thought to be the only precaution necessary since the footings had protection from soil on three sides. The concrete cylinders and beams were not as well protected; therefore, they were covered with straw and plastic.

2.4.2 Centerline

On March 20, the centerline footings were scheduled to be placed. The plastic-on-sand, plain concrete, and plastic-on-soil footings were placed first. A walkboard was set-up to be used as a bridge across the drainage ditch to move the concrete from the truck to the footing trenches. The first concrete truck containing 6.0 cubic yards (4.6 cubic meters) of concrete arrived. The truck had to wait approximately 45 minutes while gravel was manually spread to access the site. This wait contributed to a low slump concrete and the need for additional water. After the gravel was placed, the truck was maneuvered to within 20 feet (6 meters) of the footings east end. The same mix design as the tension zone was used. The measured slump was 1 inch (25 mm); therefore, 7 gallons (26 liters) of water were added to increase the workability, changing the slump to 3.5 inches (90 mm). An acceptable air content of 6% was measured. Six cylinders and two beams were cast for testing. These footings were cast using the same construction methods as in the tension zone.

After placing the first three footings, the reinforcing in the deformed bar and post-tensioned footings was positioned. Considerable problems were experienced in setting the 8 inch (200 mm) bolsters due to the wet condition of the trench bottoms. The post-tensioned footing gave the most difficulty due to the soft ground and flexible strand, causing the bolsters to tip and move from their position.

The next concrete truck arrived with 6 cubic yards (4.6 cubic meters) of concrete and a slump was measured at 6.5 inches (160 mm). The air content was measured at 6%. This concrete was placed in the post-tensioned and the deformed bar trenches. Four cylinders and two beams were cast for testing.

After the post-tensioned and the deformed bar footings were cast, 150 pounds (667 newtons) of steel fiber were added to the remaining 2 cubic yards (1.5 cubic meters) of concrete in the truck. Slump was measured at 2 inches (50 mm); therefore, 0.7 gallons (2.5 liters) of a super-plasticizer supplied by Master Builders was added to the mix. This produced a slump of 4.5 inches (110 mm), which was considered workable. Four cylinders and three beams were cast.

The concrete test specimens were transported back to Knoxville, Tennessee, that night. All the test specimen forms were stripped on March 22 and placed in a moist curing room until testing.

2.4.3 Post Tensioning

When the concrete was 40-days old (April 28), the tension zone footing was post-tensioned. Due to rain, the ends of the footing trenches were filled with water and had to be bailed. The wood formwork and plastic pocket formers were removed from the tension zone footing ends. Some concrete had to be chiseled from around the anchor ends, but overall the plastic pocket formers performed well. Two cone-shaped wedges were placed at each end of a strand and driven into place using a special tool. Using a gas powered electric generator and a calibrated hydraulic tensioning device, each strand was tensioned to 23 kips (102 kN). Problems were encountered when tensioning the top right (facing south) tendon. The anchor did not have sufficient cover, and a shear failure occurred in the concrete around the anchor at 20 kips (89 kN). Full tension was obtained in the strand by placing an anchor over the original anchor and turning it in such a way as to obtain bearing. All six of the strands were tensioned to put the footing in compression.

On April 29, the post-tensioned footing at the centerline was compressed using the same approach. Problems were encountered when tensioning the bottom right (facing west) tendon. Due to improper consolidation of the concrete around the anchor (honeycomb), the tendon could not be tensioned. Only five of the six tendons were tensioned, and an eccentricity existed in the footing.

2.5 Masonry Walls

The masonry walls were constructed during the last two weeks of April by a local mason. The walls were laid using unreinforced masonry construction and standard two-core masonry units 15 5/8 inches (397 mm) long, 7 5/8 inches (194 mm) wide, and 7 5/8 high as illustrated in Figure 2-6. The walls were constructed 40 feet (12.2 meters) long and 32 inches (0.8 meters) high using a running bond wall pattern as shown in Figure 2-7. The block voids were not filled with materials or attached to the concrete footing in any way other than through the bed joint bond.

The mortar used was a standard mix consisting of Type N masonry cement and natural sand. All masonry joints (head and bed) are the standard 3/8 inches (10 mm) in thickness, which is based on the English system of units to make each masonry unit equal to 16 inches by 8 inches by 8 inches in place. The starter course of masonry used full mortar bedding between the footing and the block. This is where all the unit's webs and face shells are bedded in mortar as illustrated in Figure 2-8. The next three courses used face shell mortar bedding where only the face shells are bedded. The head joints use face shell mortar for all courses. Tooling was not used on mortar joints on either face.

Once the walls were complete, 1/2 inch (13 mm) all-thread bolts were placed in the top block void of every fourth block, for a total of seven bolts per wall (Figure 2-7). These bolts are for attachment of the double sill plates which lie on top of the walls. The bolts were placed by filling the top block void with mortar around the bolt. The wooden (pine) sill plates as shown in Figure 2-1 were nominally 8 inches (200 mm)

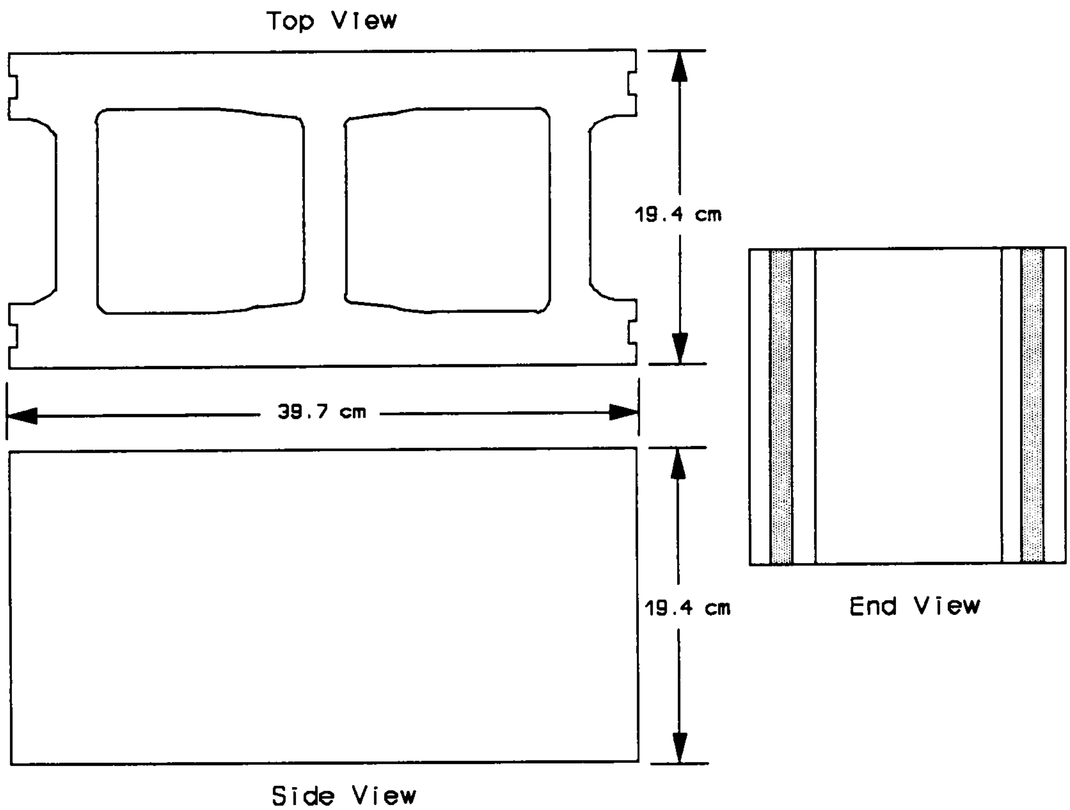

Figure 2-6 Standard Two-Core Masonry Unit

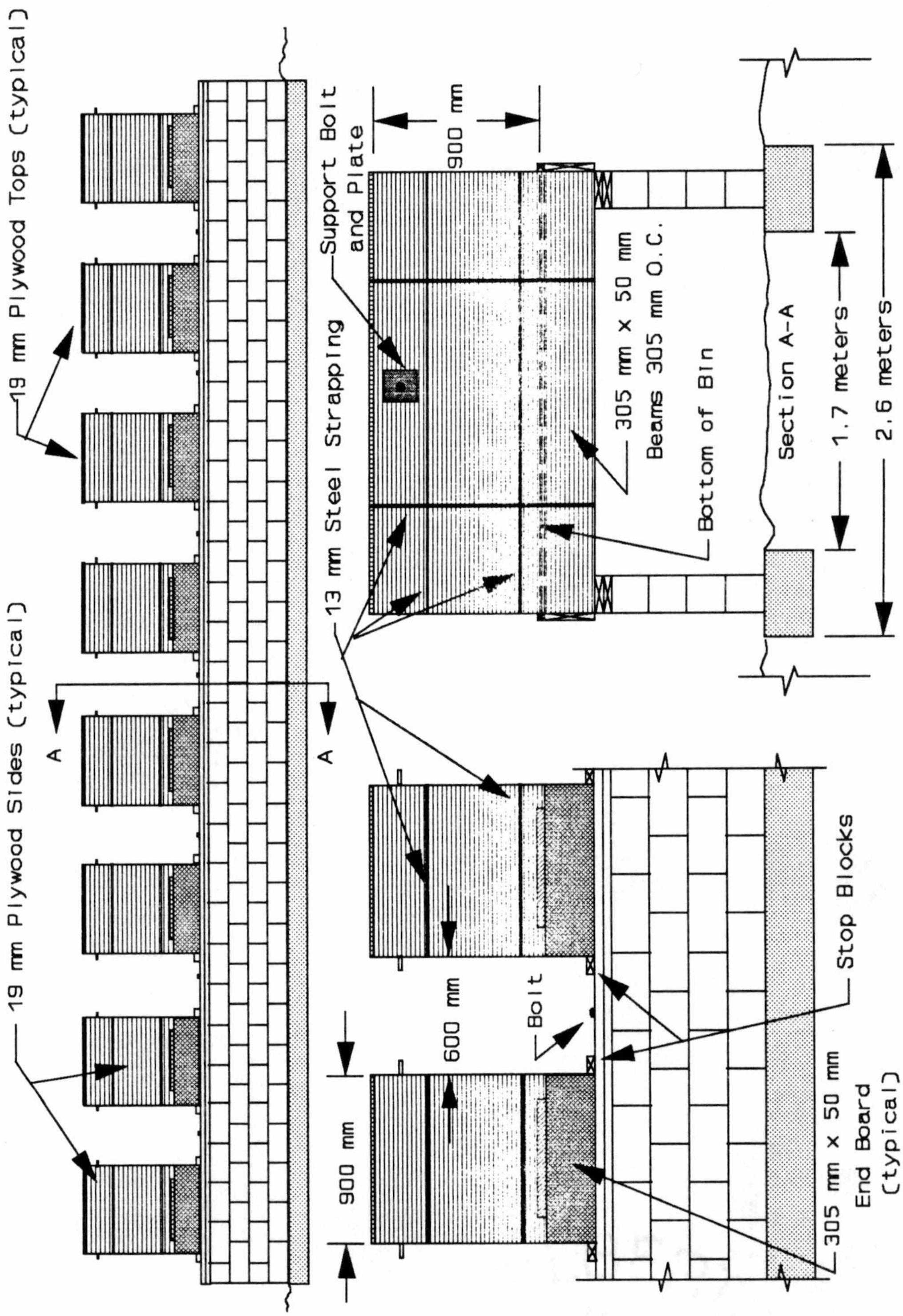

Figure 2-7 Wall and Load Bin Elevation

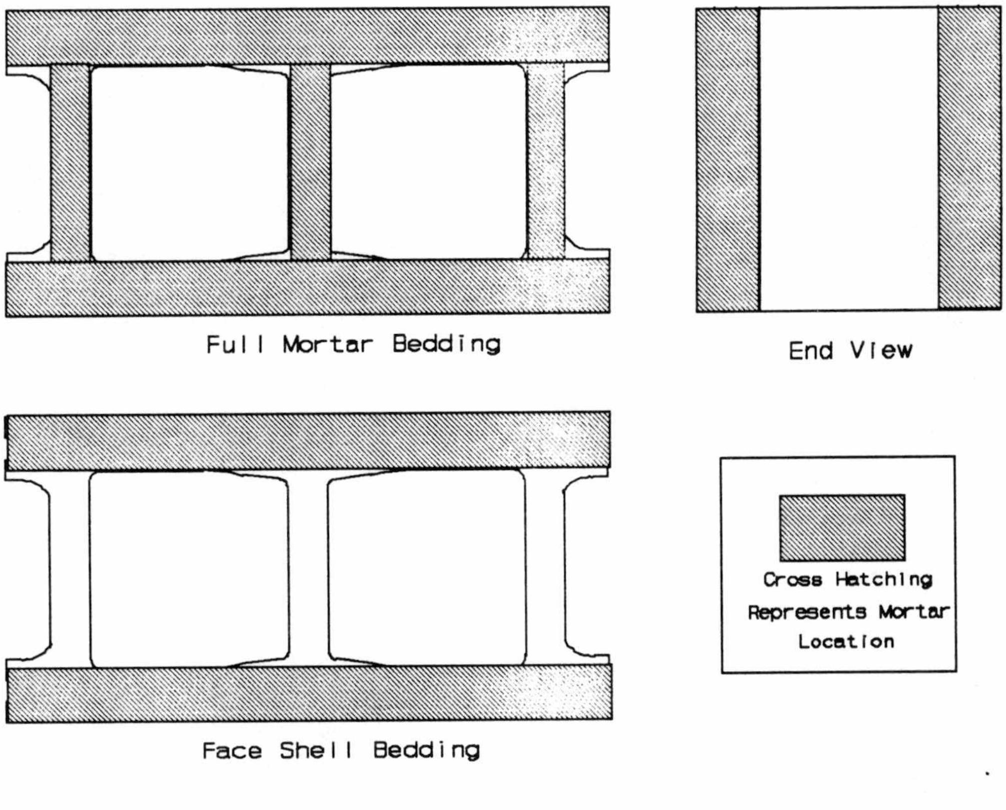

Figure 2-8 Mortar Bedding

wide by 2 inches (50 mm) thick. Holes were drilled through the sill plates the same diameter as the bolts to provide a tight fit around the bolt shaft. A nut was tightened over each bolt to hold the sill plates in place.

2.6 Load Bins

2.6.1 Constructing Load Bins

Soil-filled load bins were used to simulate a typical residential load. The bins were constructed by K. D. Crain and Sons. After constructing the bins, a trackhoe set eight bins on each adjacent pair of foundations. As illustrated in Figure 2-7, stop blocks were nailed to the sill plate on either side of the bins to keep them in place during subsidence. Plastic was used to line the inside of the bins for the purpose of maintaining a constant moisture content (a constant "residential" load) within the bin. Using the trackhoe, the bins were filled with soil stockpiled from the original excavations and sealed.

As illustrated in Figure 2-7, the soil bins span between two adjacent foundations and are supported by 8 foot (2.44 meters) by nominal 12 inch (305 mm) by 2 inch (50 mm) wooden (pine) beams at 12 inches (305 mm) on center. Buckling of the beams was prevented by using lateral bracing at 24 inches (600 mm) on center, perpendicular to the beam span. The shell of the bin is constructed from 3/4 inch (19 mm) thick plywood. The bin inside dimensions are 8 feet (2.44 meters) long by 3 feet (910 mm) wide by 3 feet deep and were filled to a depth of approximately 27 inches (685 mm).

To add lateral strength, steel strapping was bound around the bins and a support bolt was used at the top. The support bolt also served as a lifting point for the trackhoe when placing the bins. To keep moisture out of the bins, a plywood top was placed on each load bin.

2.6.2 Load Applied to Foundations

The load applied to the footings was determined to be heavier in the centerline than the tension zone site due to the soil in the bins having a higher moisture content at the centerline. The load applied to the footing is assumed to be uniform and comes from the weight of the masonry, sill plates, load bins, and soil in the load bins. The centerline site has a uniform load of 861 pounds per foot (12.6 kN/meter) applied to the footing (top surface of footing) and a soil contact pressure of 4.9 psi (0.030 N/mm^2). The tension zone site has a uniform load of 731 pounds per foot (10.7 kN/meter) applied to the footing and a soil contact pressure of 4.3 psi (0.034 N/mm^2).

CHAPTER 3

STRUCTURAL MATERIALS

3.1 Concrete in Compression

3.1.1 Field Sampling

Two concrete trucks delivered concrete to the tension zone site and two to the centerline site. Six separate batches of concrete were placed in the footing trenches at the two sites. The second truck at each site had steel fibers added immediately before placing the fiber reinforced footings. Table 3-1 summarizes the slump measured from each batch of concrete using ASTM C 143. All concrete batches had the same proportions of cement, coarse aggregate, and fine aggregate. The second truck of the centerline had 2/3 gallons of super-plasticizer added for workability. The measured slumps indicate that the water content varied between the trucks.

Twenty eight cylinders 12 inches high and 6 inches in diameter were tested in compression. The cylinders were transported to the lab and placed in a steam room for curing. The industry standard 7, 14, and 28 day breaks were not made because the properties were needed for the footings during subsidence. The cylinders were cast on March 19th and 20th, 1990 as the concrete was being placed. Appreciable subsidence began occurring on May 22, 1990 when the tension zone and centerline concrete was 64 and 65 days old respectfully. Testing took place during the week of June 19th, 1990 when the concrete was approximately 95 days old.

Table 3-1 Measured Slumps and Batch Information

Concrete Batch	Footings Composed of Batch	Measured Slump (in)
Truck 1 Tension Zone	Control, Deformed Bar, Post-Tensioned	3.0
Truck 2 Tension Zone	Plastic-on-Grade, Plastic-on-Sand	7.5
Fiber Added Tension Zone	Fiber	4.5
Truck 1 Centerline	Plastic-on-Grade, Control, Plastic-on-Sand	3.5
Truck 2 Centerline	Post-Tensioned, Deformed Bar	6.5
Fiber Added Centerline	Fiber with Super-Plasticizer Added	4.5

Although not accounted for in the tests, a slight increase in compressive strength and modulus of elasticity occurs with time (Mehta, 1986). Therefore the test results produced values slightly higher than the actual properties during subsidence. With all other factors equal, the compressive strength could have increased 1 to 2%. The modulus of elasticity increase should be slightly higher due to it's tendency to increase with time more than compressive strength (Mehta, 1986).

The field curing conditions were not the same as laboratory conditions. The cylinders were placed in the moist room on March 21. Moisture cured samples tend to have more complete hydration and are higher in later age strength (Mehta, 1986). The footings were surrounded by moist soil on three sides, but the top surface was not. Surface drying would have the worst effect on the footing top fibers.

The footings and cylinders were subjected to the same temperature conditions during initial set. Unlike the cylinders, the footings were subjected to freezing temperatures that occur during early spring. This is known to have detrimental effects on concrete strength at later ages (Fintel, 1985; Mehta, 1986).

Considering the above mentioned factors, values obtained from tests for ultimate compressive strength and modulus of elasticity are within acceptable ranges and are taken as exact.

3.1.2 Tests Procedures

The cylinders were initially loaded to approximately 40% of ultimate, unloaded completely, and then reloaded to failure in a separate testing machine. Longitudinal strain during uniaxial compression tests was measured using a compressometer with an attached dial gage that measured to 0.0001 inches. The gage length used was 8 inches. The cylinders were measured, weighed, and tested per ASTM C 39.

The reason for unloading and then reloading stemmed from several factors. To adequately define the concrete's behavior at low stresses, closely spaced readings were taken at the beginning of the tests. These readings were useful in determining the initial tangent modulus and the ASTM chord modulus. The cylinders were loaded initially in 2000 pound increments and readings taken up to 20,000 pounds. Then the increments were increased to 5000 pounds. To obtain readings at 2000 pound increments, the testing machine was set on a range with a capacity limit of 55,000 pounds (approximately 40% of ultimate). When the capacity was reached, the cylinder was slowly unloaded and measurements taken at 5000 pound increments.

Set on the highest range, the testing machine was capable of loading a cylinder to a stress of approximately 4,200 psi. To insure ultimate load was reached, the cylinders were moved to a testing machine with more capacity. The cylinders were loaded and deformations recorded at 5000 pound increments up to ultimate. The ultimate load and corresponding deformation was also recorded.

3.1.3 Discussion of Results

A typical stress-strain curve obtained from the compression tests is illustrated in Figure 3-1. Initial loading is the top line which starts at the origin and goes to approximately 1945 psi. The closeness of the first ten data points is evident. Typical

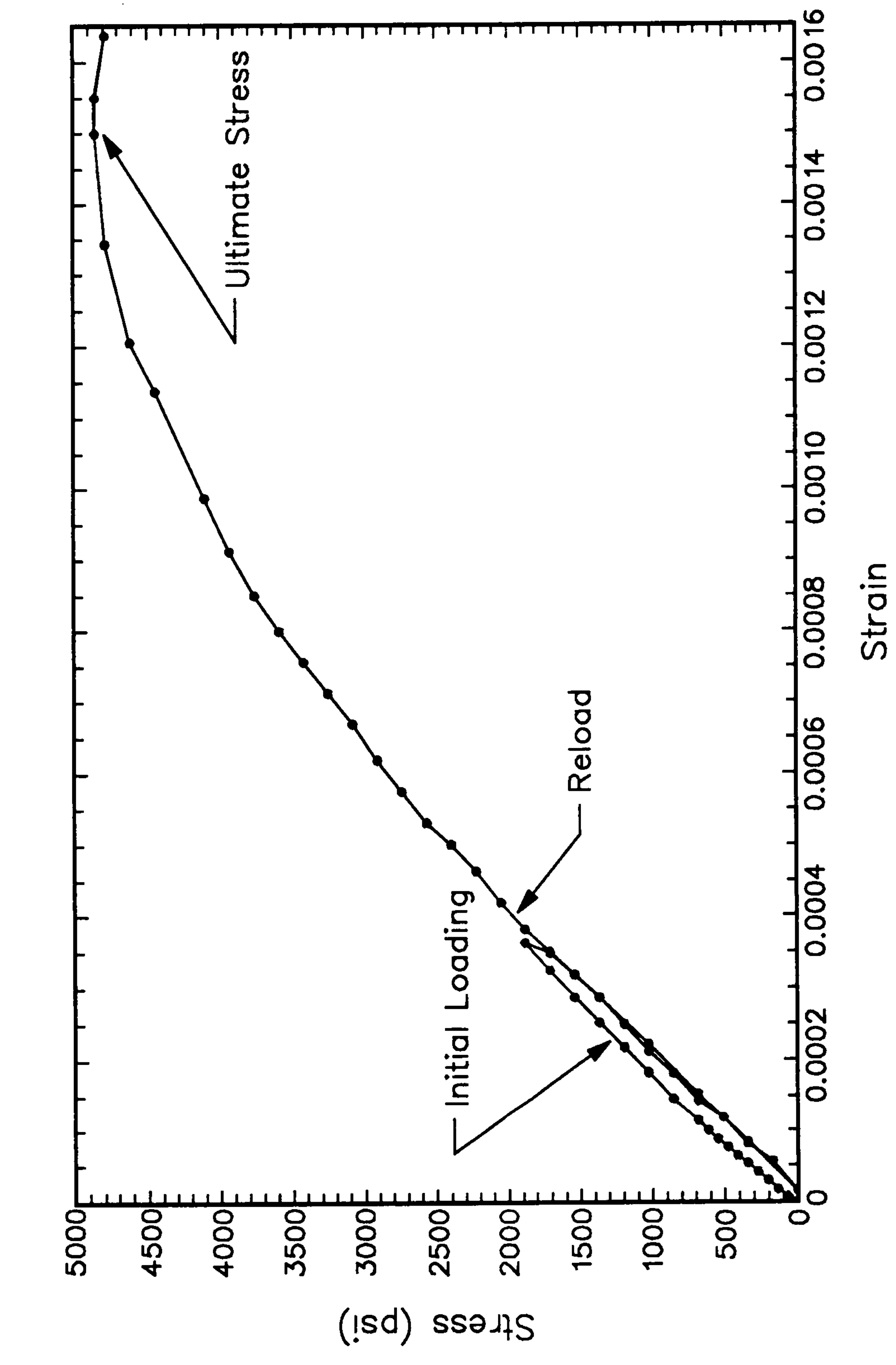

Figure 3-1 Typical Stress-Strain Curve from Concrete Compression Tests

of all stress-strain curves is the manner in which the unload portion of the graph follows the reload portion. All unload and reload graph sections were approximately linear.

There is a break in the curve where the cylinder was unloaded. By projecting the initial load curve upward toward the reload curve, the full stress-strain behavior can be defined. These curve portions should join because the initial load (approximately 40% of ultimate) is not high enough to cause major micro cracking in the concrete. All stress-strain curves obtained from the cylinders support this.

The ultimate strength, ultimate strain, unit weight, and modulus of elasticity are given in Tables 3-2 through 3-7 for each batch of concrete. The slump, which is a measure of workability and consistency of wet concrete, is tabulated for each batch in Table 3-1. The mixtures with a higher slump show a lower ultimate strength and modulus of elasticity. All concrete mixtures were equal except for water content. This demonstrates the detrimental effects of excessive water in concrete.

Table 3-4 and 3-7 show the effect on the compression behavior of adding steel fibers to concrete. The concrete mixture in Tables 3-3 and 3-4 are identical except for the addition of steel fibers in Table 3-4. Tables 3-6 and 3-7 represent the same batch except for the addition of fibers and approximately 2/3 of a gallon super-plasticizer in Table 3-7. In general, the concrete with steel fibers was slightly stronger, heavier, and had a higher ultimate strength, ultimate strain, and elastic modulus.

Table 3-2 Properties of Tension Zone: Control, Deformed Bar, and Post-Tensioned

Unit Weight (lbs)	Ultimate Compressive		Modulus of Elasticity (ksi)						
	Strength (ksi)	Strain	ACI	ASTM	Initial Tangent	Reload	40% Secant	50% Secant	60% Secant
146.4	5570	0.0019	4362	4990	5700	5354	5195	4917	4743
145.2	5182	0.0016	4157	4796	5779	5261	5012	4811	4660
146.4	5323	0.0012	4264	5286	6055	5727	5546	5265	5099
144.2	5113	0.0015	4084	4795	5784	4989	5056	4825	4603
144.4	5165	0.0017	4117	4857	5588	4988	4976	4701	4524
146.2	5112	0.0016	4170	5025	5947	5193	5284	4987	4758
145.5	*5244*	*0.0016*	*4192*	*4958*	*5809*	*5252*	*5178*	*4918*	*4731*

Table 3-3 Properties of Tension Zone: Plastic-on-Soil and Plastic-on-Sand

Unit Weight (lbs)	Ultimate Compressive		Modulus of Elasticity (ksi)						
	Strength (ksi)	Strain	ACI	ASTM	Initial Tangent	Reload	40% Secant	50% Secant	60% Secant
142.0	4725	0.0015	3838	4511	5420	4798	4730	4507	4357
143.6	4653	0.0015	3874	4886	5386	5147	5070	4851	4707
142.5	4272	0.0015	3669	4586	4947	4825	4745	4573	4415
140.9	4517	0.0016	3708	4558	5144	4635	4767	4478	4262
142.2	*4542*	*0.0015*	*3772*	*4635*	*5224*	*4851*	*4828*	*4602*	*4435*

Table 3-4 Properties of Tension Zone: Steel Fibers

Unit Weight (lbs)	Ultimate Compressive		Modulus of Elasticity (ksi)						
	Strength (ksi)	Strain	ACI	ASTM	Initial Tangent	Reload	40% Secant	50% Secant	60% Secant
144.9	4832	0.0016	4002	4894	5575	5105	5047	4830	4663
145.9	5078	0.0017	4145	4932	5846	5174	5120	4845	4613
144.9	5165	0.0017	4138	4900	5688	5138	5091	4841	4621
146.7	5340	0.0017	4284	4891	6187	5401	5181	4890	4674
145.6	***5104***	***0.0017***	***4142***	***4904***	***5824***	***5205***	***5110***	***4851***	***4643***

Table 3-5 Properties of Centerline: Control, Plastic-on-Sand, Plastic-on-Soil

Unit Weight (lbs)	Ultimate Compressive		Modulus of Elasticity (ksi)						
	Strength (ksi)	Strain	ACI	ASTM	Initial Tangent	Reload	40% Secant	50% Secant	60% Secant
148.6	5586	-	4469	5377	6489	6012	5634	5423	5233
146.7	5583	0.0015	4380	5359	6209	5822	5569	5365	5239
147.6	5708	0.0016	4473	5144	6424	5625	5414	5201	5057
148.6	5479	0.0016	4425	5260	6673	5742	5523	5332	5155
149.3	5585	0.0018	4500	5289	6397	5656	5557	5276	5066
148.2	***5588***	***0.0016***	***4449***	***5286***	***6439***	***5771***	***5539***	***5319***	***5150***

Table 3-6 Properties of Centerline: Deformed Bar, Post-Tensioned

Unit Weight (lbs)	Ultimate Compressive		Modulus of Elasticity (ksi)						
	Strength (ksi)	Strain	ACI	ASTM	Initial Tangent	Reload	40% Secant	50% Secant	60% Secant
144.9	4850	0.0017	4010	4796	5839	5071	5128	4923	4753
147.1	5463	0.0017	4351	4894	6007	5280	5104	4909	4741
144.7	5060	0.0015	4087	5139	6218	5486	5457	5147	4921
144.9	4956	0.0016	4054	5030	5936	5244	5239	4969	4790
145.4	***5082***	***0.0016***	***4125***	***4965***	***6000***	***5270***	***5232***	***4987***	***4801***

Table 3-7 Properties of Centerline: Steel Fiber

Unit Weight (lbs)	Ultimate Compressive		Modulus of Elasticity (ksi)						
	Strength (ksi)	Strain	ACI	ASTM	Initial Tangent	Reload	40% Secant	50% Secant	60% Secant
148.8	5428	0.0018	4415	5146	6073	5546	5331	5188	4951
147.4	4954	0.0018	4155	5047	5706	5382	5215	5027	4881
148.1	5603	-	4453	-	5451	-	-	-	-
147.9	5042	0.0016	4213	5243	6046	5538	5473	5196	4978
148.0	***5257***	***0.0017***	***4309***	***5145***	***5819***	***5489***	***5340***	***5137***	***4937***

3.1.4 Modulus of Elasticity

The modulus of elasticity is a property used to describe the linear relationship between stress and strain for linear elastic materials. It is the slope of the linear-elastic portion of a stress-strain curve. The stress-strain relationship of steel is well defined by using this property, but it's application to concrete is not as clear. Concrete does not show a linear relationship between stress and strain (Figure 3-1), nor is it completely elastic.

The assumption of linear behavior is commonly used to simplify analysis of concrete. At stresses below 30 to 40% of ultimate, the slope of the stress-strain curve is reasonably constant and this assumption is good (MacGregor, 1988). Micro cracking throughout the concrete paste-aggregate matrix causes the curve to become increasingly non-linear with additional load. When the load is approximately 70 to 80% of ultimate, the strain increases at a high rate and the linear assumption becomes unsuitable (Hognestad et al., 1955; MacGregor, 1988). The concrete becomes less stiff (lower modulus) as ultimate load is approached. This is evident in Figure 3-1.

Subsidence produces axial and flexural loads in tension and/or compression depending on the structures orientation with respect to the wave. The stress-strain curve used to determine the elastic modulus in this research comes from cylinder compression tests. Research has shown (Hognestad et al., 1955) that the shape of the stress-strain curve obtained from uniaxial compression tests shows a striking resemblance to the curve obtained from flexural compression tests. Therefore general characteristics of stress-strain relationships obtained from uniaxial compression tests are applicable for compression behavior in flexure.

Limited research has been done that relates stress-strain behavior of concrete in compression with it's behavior in tension. The research done indicates that the compression modulus of elasticity is slightly higher than the modulus in tension for loads up to approximately 75% of ultimate (Mirza et al., 1979; Johnson, 1928). At 75% of ultimate the compression modulus drops rapidly. The ultimate strength in tension is approximately 10% of the compression ultimate strength. Therefore the modulus comparisons are made based on stresses and strains an order of magnitude larger in compression than tension.

For symmetrical, homogeneous beams subjected to pure flexure, the neutral axis of bending occurs at mid-height. Half of the cross section is in compression and half in tension. Assuming a linear strain distribution, the maximum stress in both tension and compression occurs at the extreme fibers. These stresses are equal in magnitude. In the case of the plain concrete footing in pure flexure, failure occurs when the extreme tension fiber reaches the ultimate tensile strength. When the extreme tensile fiber reaches 50% of ultimate, the extreme compression fiber will be at approximately 5% of ultimate. Since the modulii are approximately equal with respect to their ultimate load, the compression side of the beam is stiffer than the tension side. This difference in stiffness would be considerable as the tension side reaches ultimate and the compression side is at approximately 10 to 15% of ultimate. To maintain equilibrium, the neutral axis shifts toward the compression side.

The modulus of elasticity is tabulated in Tables 3-2 to 3-7 using various recognized procedures. These values which are useful in linear-elastic analyses, give the analyst many choices. A modulus is selected based on the level of stress expected. For very low stresses, the initial tangent might be appropriate. For higher stresses, a secant modulus might be more appropriate.

Modulii obtained in Tables 3-2 to 3-7 are determined as follows. The ACI modulus is obtained by using the equation of section 8.5.1 of the *ACI 318-89 Code*

$$E = w_c^{1.5}\, 33 \sqrt{f'_c} \tag{3.1}$$

in which E is the modulus of elasticity (psi), w_c is the unit weight of the concrete (lbs/cf), and f'_c is the uniaxial compressive strength (psi). The unit weight used in equation 3.1 is tabulated in Tables 3-2 to 3-7. The ASTM modulus is a chord modulus described in ASTM C 469. It is measured as the slope of a line drawn between points on the stress-strain curve corresponding to a strain of 50 micro strain and a stress of 40% of ultimate. The initial tangent modulus was obtained for all cylinders by using a linear regression on six data points from 4000 pounds to 12000 pounds. These points were on the beginning of the curve and were arbitrarily selected to represent behavior at low loads. The regression started at 4000 pounds because the test specimens do not give adequate results until they are seated under loads. The reload modulus was obtained by calculating a linear regression on the reload portion from 5,000 to 55,000 pounds. The 40% secant modulus was found by determining the stress corresponding to 40% of ultimate stress. The modulus is the slope of a line from the origin to 40%

of ultimate. The 50 and 60% modulus were found in the same manner. Comparison of the various secant methods shows the effect of stress level on modulus.

To demonstrate the stress-strain behavior represented by these elastic modulii, several have been overlaid on the stress-strain curve used for Figure 3-1 in Figure 3-2. Not shown on the figure is the chord and the reload modulus. The chord modulus is approximately equal to the 50% secant modulus. The reload modulus is not shown for clarity.

3.2 Concrete in Tension and Flexure

3.2.1 Modulus of Rupture

The tensile strength of concrete varies from 8 to 15% of the compressive strength (MacGregor, 1988). The value obtained strongly depends on the procedure used to obtain it. For unreinforced concrete subjected to bending and/or axial tension, the tensile strength is the controlling parameter. For reinforced concrete under similar loads, the tensile capacity is also of great importance due to the stiffness reduction which takes place after cracking. For subsidence analysis, the tensile capacity is as important as the modulus of elasticity.

There are three standard testing procedures for determining the tensile strength of concrete: 1) direct tensile test; 2) split cylinder test; 3) modulus of rupture test. The direct tensile test grips a specimen (usually bone shaped) at both ends and pulls it until failure. The split cylinder test (ASTM C496) takes a cylindrical specimen and lays it

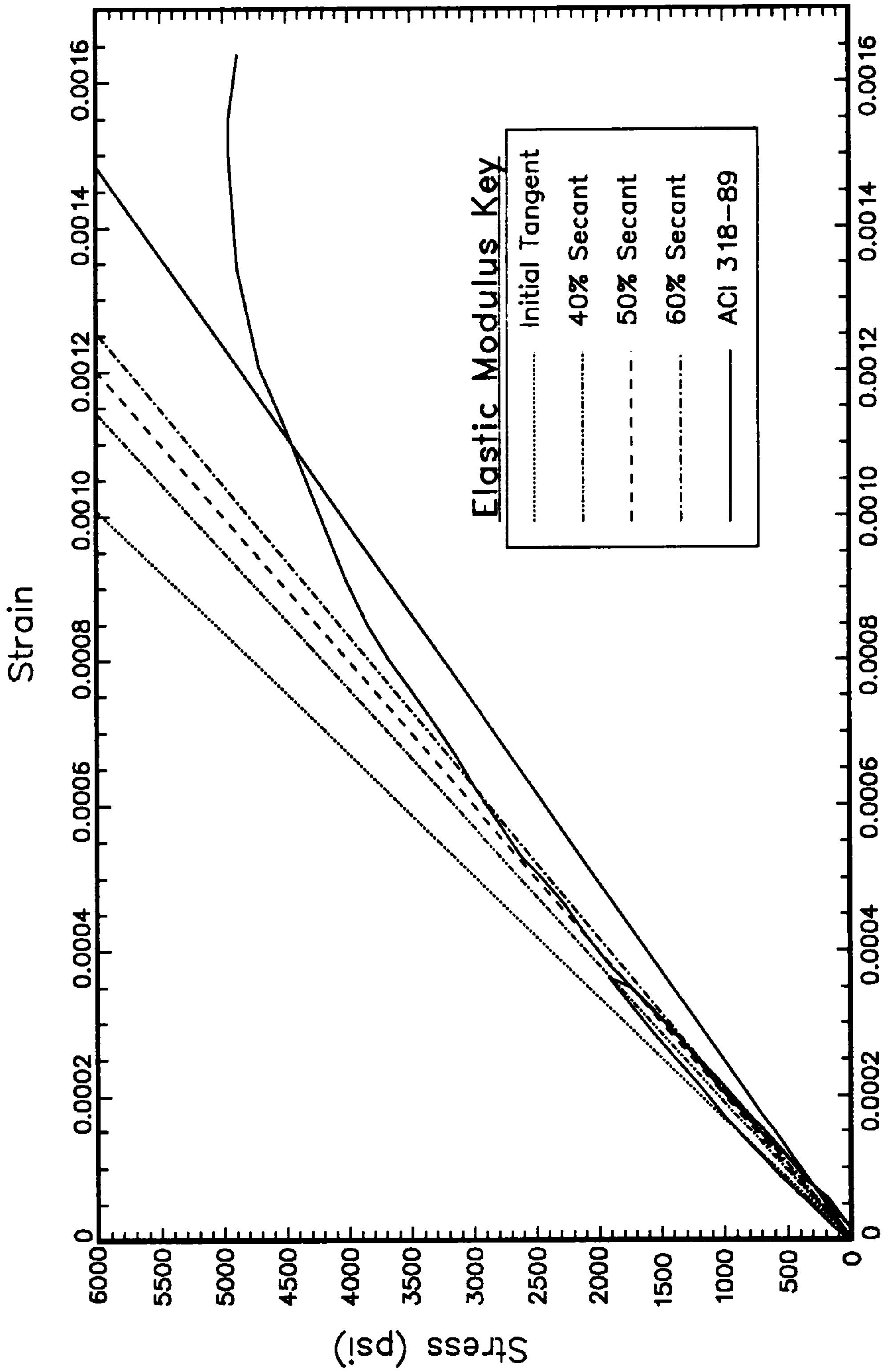

Figure 3-2 Comparisons Between Modulus of Elasticity Methods

on its side. The cylinder is loaded to failure with a compressive line load. This causes a tensile plane to develop across the diameter. The third procedure is the modulus of rupture test (ASTM C78 or C293). A rectangular beam is loaded at the center or third points in flexure until failure. This test was chosen for reasons explained below.

Results from the three previously mentioned testing procedures are not equal. The direct tension and split cylinder tests give approximately equal results, with the split cylinder slightly higher (MacGregor, 1988). The modulus of rupture test gives results that are 30 to 50% higher than the other tensile tests (Raphael, 1984).

The modulus of rupture is calculated using an equation derived from elastic theory. This equation assumes elastic behavior of concrete to the point of failure. Tests have shown that the stress-strain behavior for tensile specimens above approximately 50% of ultimate is marked by gradually increasing rates of deformation until failure (Raphael, 1984). Therefore the actual stress in the concrete at the same strain is lower than predicted by elastic theory. The stress distribution in the compression region of the beam is approximately linear due to the concrete stressed to a fraction of its compressive strength. The stress distribution in the tension region of the beam becomes very non-linear as the tensile strength is reached (Raphael, 1984). This would indicate a shift in the neutral axis toward the compression region as mentioned in 3.1.4.

The appropriate value to use for tensile strength in an analysis depends on the analysis method being used. The actual tensile strength instead of the modulus of rupture should be used in a finite element model that accounts for the nonlinear tensile behavior. An approximation of the tensile strength can be obtained from the modulus of rupture for rectangular cross sections by multiplying the modulus by 3/4 (Rapheal, 1984). For a linear-elastic model, the modulus of rupture gives the correct value (Raphael, 1984).

3.2.2 Field Sampling

Fourteen beams 16 by 3 by 4 inches were cast from the concrete used in the footings. Casting of the beams was per ASTM C31. Half were cast on March 19, 1990 (tension zone) and the other half on March 20, 1990 (centerline). The beam forms were made from steel plates that had a thin coating of oil applied to ease form removal. The beams were removed from their forms and placed in a moist room for curing on March 22, 1990.

The beams were tested on June 28 and 29, 1990 when the concrete was approximately 100 days old. Using the same reasoning as in 3.1.1, it is believed that the properties obtained are representative of subsidence conditions.

3.2.3 Test Procedures

The beams were tested as a simple beam using third-point loading as per ASTM C78. The span length was 12 inches. All beams were loaded to failure and the ultimate load recorded. The modulus of rupture can be calculated from:

$$f_r = \frac{Pl}{bh^2} \tag{3.2}$$

where P is the total load
l is the span length
b is the width
h is the height

Units of the modulus of rupture are force per area, or stress.

3.2.4 Steel Fiber Reinforced Concrete

The plain concrete beams instantly failed losing all load carrying capabilities when ultimate load was reached. Steel fibers in concrete should add to the post-cracking ductility and strength of beams in tension and flexure. There were three beams with steel fibers cast from each site for a total of six beams. These beams reached ultimate load and failed suddenly, but they would not lose all load carrying capability. These beams exhibited some post-cracking strength in the range of 1/4 to 1/3 of ultimate. They also had enhanced ductility over the plain concrete beams.

The beams with steel fibers were examined after each modulus of rupture test. It was observed that very few steel fibers had oriented themselves in the direction of the longitudinal dimension of the beam. In most cases, only 4 to 10 fibers had contributed to the post-cracking behavior in the tension region of the beams. Previous investigations (Shah and Rangan, 1971) show that the percentage of fiber content has a major influence on the strength and toughness of concrete beams. The toughness of a beam is related to the area under the load-deflection curve. High fiber content beams had almost double the strength of low fiber content beams, while the increase in toughness was as much as twenty times over small fiber contents. This was also the trend for tests. Others (Ramakrishnan et al., 1981) have also observed the increase of toughness with increasing fiber content. Other factors that influence the behavior are fiber orientation, aspect ratio, and fiber stress-strain behavior (Shah and Rangan, 1971).

Subsidence caused considerable bending in the footings. The fiber content used in the footings was close to manufacturers recommendations. It appears however that there were not enough fibers to give considerable increase in toughness or strength. The curvature in the footings has been measured to be fairly close to the cracking curvature. Therefore it is believed that larger quantities of steel fibers could minimize damage by minimizing crack propagation and increasing the post-cracking strength.

Steel fibers have been shown to effect the modulus of elasticity. In uncracked fiber reinforced concrete, the modulus increases approximately 3.3% over unreinforced concrete for every 1.0% increase in fiber content by volume (Patton and Whittaker, 1983). This trend can be seen by comparing Tables 3-3 and 3-4 and also Tables 3-6 and 3-7.

3.2.5 Discussion of Results

Several equations have been proposed that relate the tensile strength of concrete to the compressive strength (Mirza et al.,1979; Raphael, 1984; ACI 318-89). One equation (Mirza et al., 1979) for the mean modulus of rupture is:

$$f_r = 8.3 \sqrt{f'_c} \qquad (3.3)$$

in which f_r is the modulus of rupture. There is significant scatter when compared to measured modulii of rupture. Another slightly more conservative approximation given by ACI 318-89 is:

$$f_r = 7.5 \sqrt{f'_c} \tag{3.4}$$

Experimental values are tabulated in Table 3-8. Average results, and the modulus of rupture predicted from Equations 3.3 and 3.4 are given in Table 3-9. Since the averages are obtained from only two to three samples, there is the potential for statistical uncertainty. This is evident in that the low failure stress of "beam 11" significantly affects the results. The effects of steel fibers on tensile strength are observed in Table 3-9. Identical concrete, except for the addition of fibers in the tension zone, resulted in a tensile strength of 20.0 % higher.

3.3 Deformed Steel Reinforcing

3.3.1 Description of Test

The tension zone and centerline site each had a deformed bar reinforced footing. Standard ASTM A 615 Grade 60 deformed reinforcing steel with bar designation number 4 were used. There were two top bars and two bottom bars in each footing.

A 5 foot bar was taken to the lab for testing. The bar was cut in half so that two tests could be performed. Both bars were tested in tension by using a Tinus-Olsen

Table 3-8 Experimental Modulus of Rupture Values

Beam Number	Modulus of Rupture (psi)	Batch
1	632.1	Tension Zone: Control, Deformed Bar, and Post-Tensioned Footings
2	646.0	
3	513.0	Tension Zone: Plastic-on-Grade and Plastic-on-Sand Footings
6	555.1	
4	657.5	Tension Zone: Steel Fiber Footing
5	643.7	
7	615.0	
9	616.4	Centerline: Post-Tensioned and Deformed Bar Footings
12	617.5	
10	671.4	Centerline: Plastic-on-Grade, Plastic-on-Sand, and Control Footings
11	521.6	
8	643.5	Centerline: Steel Fiber Footing
13	703.5	
14	650.4	

Table 3-9 Comparisons of Modulus of Rupture Values

Batch	Average Compressive Strength (psi)	Modulus of Rupture (psi)		
		Experimental Average	Equation 3.3	Equation 3.4
Tension Zone: Control, Deformed Bar, and Post-Tensioned Footings	5244	639	601	543
Tension Zone: Plastic-on-Grade and Plastic-on-Sand Footings	4542	534	559	506
Tension Zone: Steel Fiber Footing	5104	639	593	536
Centerline: Post-Tensioned and Deformed Bar Footings	5082	617	592	535
Centerline: Plastic-on-Grade, Plastic-on-Sand, and Control Footings	5588	597	621	561
Centerline: Steel Fiber Footing	5257	666	602	544

testing machine and a electronic extensometer with a gage length of 10 inches. An X-Y plotter was used to obtain a continuous load-deflection curve. The extensometer was removed at an elongation of approximately 0.65 inches (strain of 0.065) to avoid damage to the extensometer. The bar was then loaded to ultimate with no strain data. The area used for stress determinations was 0.20 inches.

3.3.2 Results of Test

The stress-strain curves for both specimens were almost identical. Two views of the same stress-strain curve obtained from a specimen are shown in Figures 3-3 and 3-4. Figure 3-3 shows the entire stress-strain history up to where the measuring device was removed. The ultimate stress for this bar was 123.8 ksi and the other test resulted in an ultimate stress of 124.5 ksi. The yield point as seen in Figure 3-4 is 67.5 ksi; the other test resulted in a yield stress of 67.3 ksi. The minimum allowable ultimate and yield stress according to ASTM A 615 are 90.0 and 60.0 ksi respectfully. The results obtained met and exceeded the ASTM specification requirements.

The standard procedure in reinforced concrete design is to design the concrete based on the reinforcing steel never adding more strength than its yield strength. Actual ultimate tensile strength measured was approximately 106% greater than the allowable standard. This additional strength comes from strain hardening of the steel. The strain that corresponds with the onset of appreciable strain hardening is shown in Figure 3-4.

Young's Modulus of the reinforcing can be taken as 29,000 ksi. Measurements

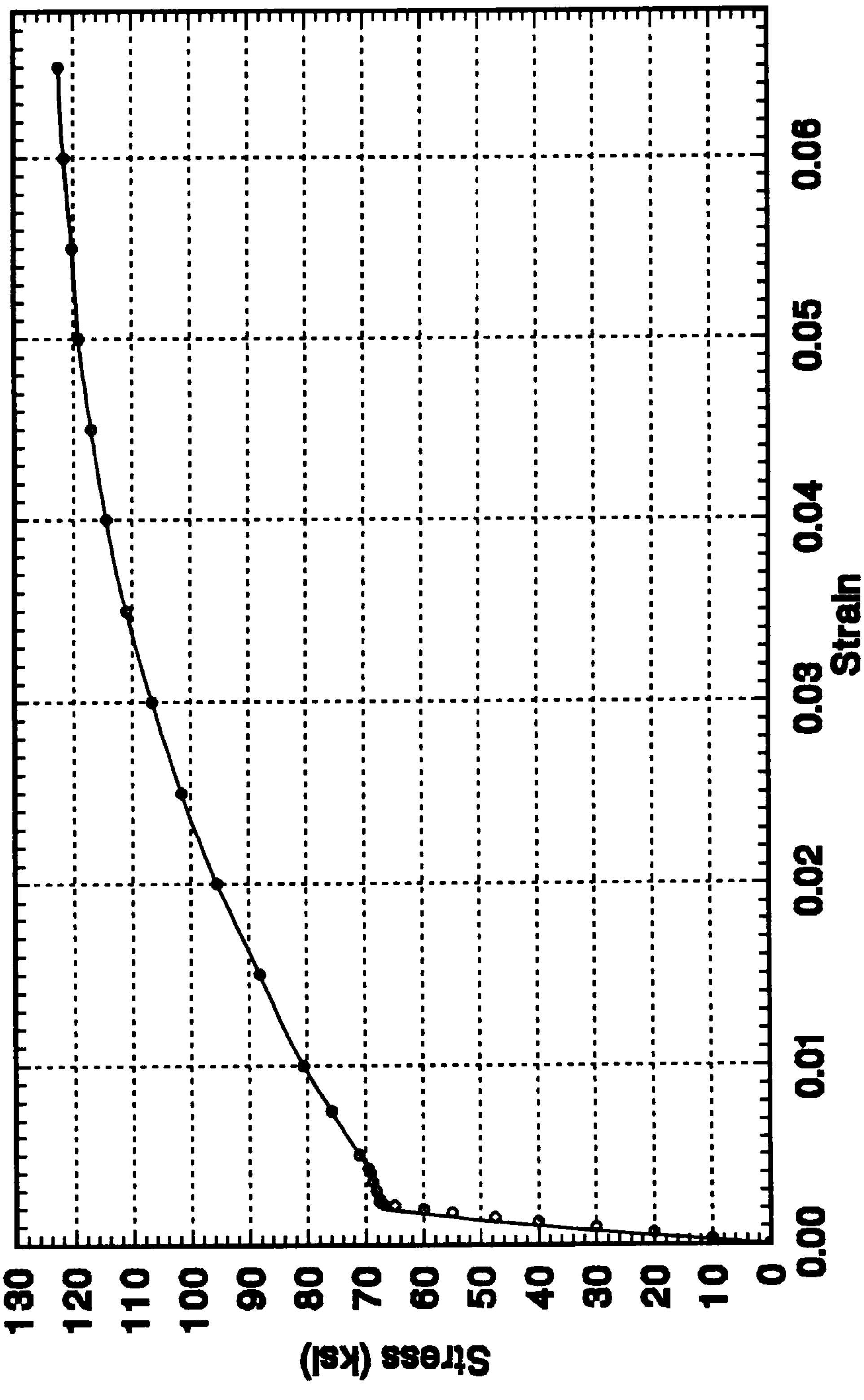

Figure 3-3 Deformed Reinforcing Bar Stress-Strain Curve

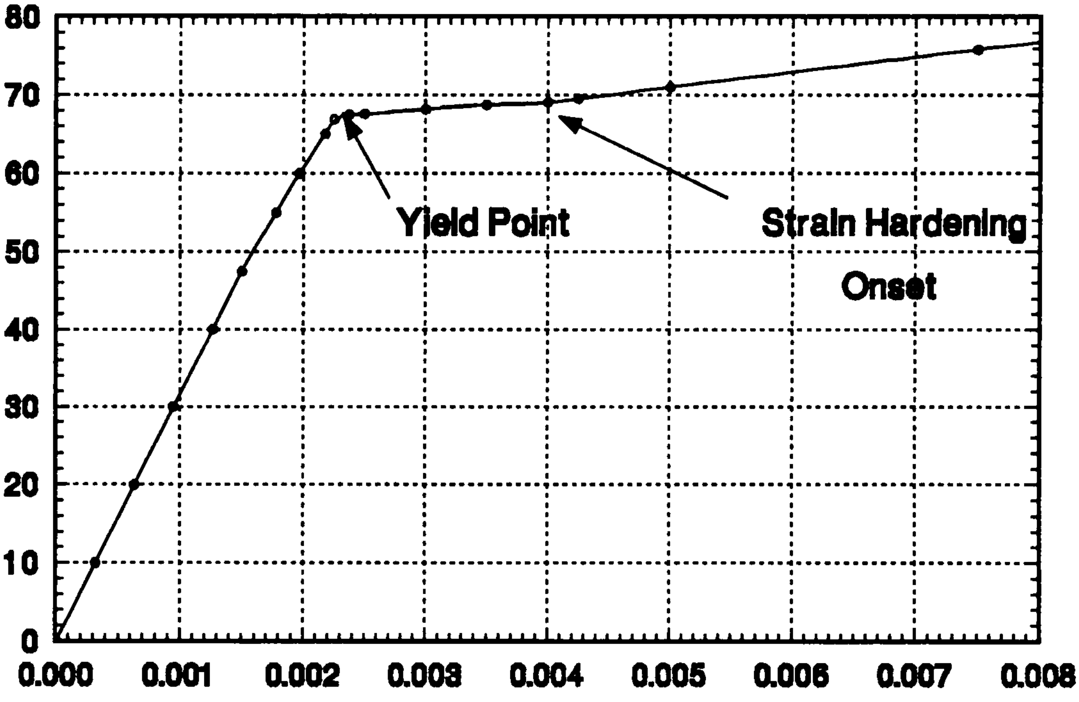

Figure 3-4 Lower Portion of Deformed Bar Stress-Strain Curve

from both test sets gave various values depending on how it was obtained. The "linear portion" of the curve (up to yield) has a slight concavity. Since 29,000 ksi was a frequent measurement and the industry standard, it was chosen as Young's Modulus for the reinforcing.

3.4 Steel Post-Tensioning Strand

3.4.1 Description of Test

The tension zone and centerline site each had an unbonded post-tensioned footing. Low relaxation ASTM A 416, 1/2 inch seven wire strand Grade 270 were used. There were three strands top and three strands bottom in each footing. The strands were encased in a greased flexible duct.

The manufacturer of the strand was Shinko Wire America, Inc., Houston, Texas. A mill report was obtained with all the required properties. The mill report gave the area of strand as 0.153 square inches, which is typical for 1/2 inch diameter seven-wire strand. The ultimate strength and yield strength were 278 ksi and 258 ksi respectively. Yield strength was measured as the load at 1% elongation divided by the area. Modulus of elasticity was given as 28,000 ksi. Also on the mill report was a load-elongation curve that went up to just past yield. All tests were performed per ASTM A 416.

3.5 Masonry Samples Used for Testing

3.5.1 Field Sampling

Three two block high masonry specimens were made as the wall was constructed using the same mortar and block used in the foundation walls. After being transported, only two of the three specimens were intact.

After subsidence had occurred, several specimens were cut from the deformed bar and steel fiber reinforced foundation wall on the centerline. All specimens were cut on one end of the wall where no cracks were visible. During subsidence, the wall ends were not stressed to high levels (particularly reinforced foundations) and it was believed that these samples adequately represented the before subsidence wall strength. Several three and two block high specimens were cut, banded, and transported to the lab for testing.

3.5.2 Masonry Unit Specifics

Single blocks from the original group of samples were used to determine block dimensions, weights, and absorption quantities (ASTM C 140). These quantities are useful for comparisons with other block and in determining strength characteristics. Table 3-10 shows the results of measurements taken on two individual blocks. These values are considered typical and are used in determination of values throughout this chapter.

Gross specific weight is the oven dry weight divided by the gross volume. This

Table 3-10 General Information of Masonry Units

Measured Quantity	Block #1	Block #2	Average
Length (in)	15.703	15.656	**15.680**
Width (in)	7.656	7.656	**7.656**
Height (in)	7.609	7.625	**7.617**
Minimum Face Shell (in)	1.331	1.328	**1.330**
Minimum Web Thickness (in)	1.040	1.035	**1.038**
Equivalent Web Thickness (in)	2.434	2.483	**2.459**
Submerged Weight (lbs)	21.79	22.05	**21.92**
Towel Dry Weight (lbs)	39.74	40.01	**39.88**
Oven Dry Weight (lbs)	37.90	38.08	**37.99**
Gross Volume (cf)	0.529	0.529	**0.529**
Net Volume (cf)	0.288	0.288	**0.288**
Net Area (Percent of Gross)	54.44	54.44	**54.44**
Gross Specific Weight (lbs/cf)	71.65	71.99	**71.82**
Net Specific Weight (lbs/cf)	131.61	132.24	**131.92**
Absorption (lbs/cf)	6.40	6.70	**6.55**
Absorption (Percent)	4.86	5.06	**4.96**

quantity, not specified by ASTM C 140, was added since the wall may be modeled as an equivalent solid section. All other values were obtained as in ASTM C 140.

3.5.3 Mortar Bond Measurements

The second group of samples taken from the site were subjected to various tests that involved breaking the mortar bond. To determine actual (net) stresses on the mortar, the mortar area which adhered to the block was measured to the nearest hundredth of an inch and recorded. These measurements were used in calculations for specific tests and were also considered generically. A need was recognized for obtaining an average area of mortar bond in the head and bed joints for use in certain strength calculations.

Tables 3-11 and 3-12 summarize the measurements taken from the bed and head joints respectively. There is a major difference in the two tables. In Table 3-11, the areas represent the total bond area of **both** faces of a nominal 8 inch unit's **bed** joint. The length refers to the average length of both faces of the mortar joint in the direction of the wall. Also tabulated is the area of both mortar joints per unit length in the direction of the wall. In Table 3-12, the areas represent **one** face of a nominal 8 inch unit's **head** joint. Therefore this value will have to be multiplied by two for comparison with Table 3-11. This is done under the heading "Double Area". The length refers to the actual length of the head joint in the vertical direction. The area per unit length will also need to be multiplied by two for comparison with Table 3-11. This is done under the heading "Double Area/Length". As can be seen in Table 3-11 and 3-12, the head

Table 3-11 Bed Joint Bond Dimensions

Joint Number	Area (sqi)	Length (in)	Area/Length (sqi/in)
1	27.02	7.84	3.45
2	28.23	7.92	3.56
3	25.98	7.69	3.38
4	23.81	7.92	3.01
5	23.82	7.74	3.08
6	23.83	7.81	3.05
7	24.61	7.90	3.12
8	27.78	7.63	3.64
9	24.40	7.77	3.14
10	26.30	7.36	3.57
11	28.06	8.01	3.50
12	27.84	7.93	3.51
13	28.10	7.71	3.64
14	26.96	7.53	3.58
15	25.47	7.66	3.33
16	27.20	7.77	3.50
17	27.08	7.46	3.63
18	23.25	7.46	3.12
19	27.53	8.15	3.38
20	28.67	8.12	3.53
Average	**26.30**	**7.77**	**3.39**

Table 3-12 Head Joint Bond Dimensions

Joint Number	Area (sqi)	Double Area (sqi)	Length (in)	Area/Length (sqi/in)	Double Area/Length (sqi/in)
1	13.29	26.58	7.57	1.76	3.52
2	10.65	21.30	7.84	1.36	2.72
3	14.95	29.90	7.81	1.91	3.82
4	11.44	22.88	7.79	1.47	2.94
5	13.96	27.92	7.63	1.83	3.66
6	10.21	20.42	8.15	1.25	2.50
7	12.93	25.86	8.55	1.51	3.02
8	11.93	23.86	7.55	1.58	3.16
9	13.91	27.82	7.97	1.75	3.50
10	13.52	27.04	7.97	1.70	3.40
11	12.28	24.56	7.85	1.56	3.12
Average	**12.64**	**25.28**	**7.88**	**1.61**	**3.22**

and bed joint areas per length are approximately equal. This suggests that the use of an average area would be adequate.

3.6 Masonry in Compression

3.6.1 Masonry Units Compressive Strength

Two individual masonry units were tested for determination of the block compressive strength per ASTM C 140. These were single block units that were capped with a gypsum plaster called "Hydrocal White". The results are shown in Table 3-13.

3.6.2 Young's Modulus

Also tested in compression were two sets of two block high masonry prisms obtained from the first group of field samples. The tests were modeled after ASTM E 447 with slight differences. The prisms tested were built from two complete masonry units with a single mortar joint between them. The prisms were capped using "Hydrocal White" as in the individual units.

A stress-strain curve for the prisms was obtained using a "Demac" gage to measure change in length. Two "Demac" points were attached along a vertical line centered above and below the bed joint on the horizontal center of the prism face. A pair of points were attached on both sides of the prism at the same relative location. Readings were taken on both sides of the prism at 5000 pound intervals. Due to laboratory problems, only one prism sample produced reasonable results.

Table 3-13 Masonry Unit Compressive Strength

Specimen	Load (kips)	Gross Area (sqi)	Net Area (sqi)	Gross Ultimate Strength (psi)	Net Ultimate Strength (psi)
Block #1	207.0	120.05	65.35	1724.3	3167.6
Block #2	254.0	120.05	65.35	2115.8	3886.8
Average	**230.5**	**120.05**	**65.35**	**1920.0**	**3527.2**

Instead of using ASTM E 111 for obtaining the secant modulus, a chord approach was taken. Two points along the curve were chosen arbitrarily as shown in Figure 3-5. Two values of Young's Modulus were chosen to represent the stress-strain behavior at different stress levels. Since the stress level of the masonry in compression is relatively low during subsidence, the higher numerical value of 1443.0 ksi seems more appropriate for analysis.

The ultimate strength of the prisms were 850 psi and 1074 psi (corresponds with above modulus) on the gross area for an average of 962 psi. The average net ultimate strength was 1767 psi.

3.7 Masonry in Tension

3.7.1 Masonry Unit Tensile Strength

Tensile strength of the masonry units was determined by using ASTM C 1006. A single masonry unit was cut in half along the center web to produce two specimens. Round steel bars are centered on the top and bottom of the specimen perpendicular to the face. The steel bars were held in place with "Hydrocal White" and placed in the testing machine. The specimen was loaded and a tensile failure developed between the two bars. The gross tensile stress is calculated as:

$$\textit{Gross Tensile Stress} = \frac{(2\,(\textit{split-load}))}{(\pi\,(\textit{gross area}))} \tag{3.5}$$

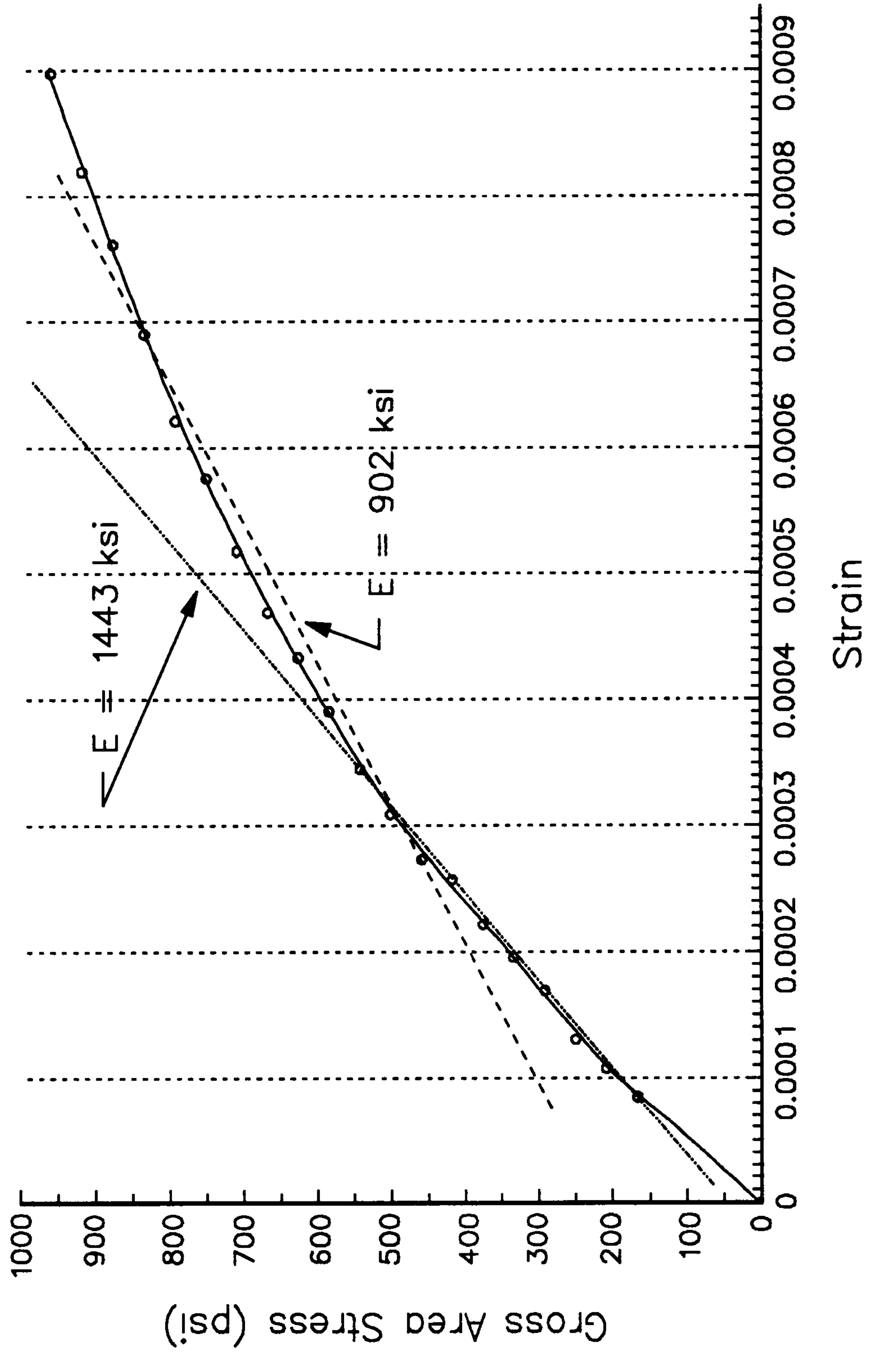

Figure 3-5 Stress-Strain Relationship of Masonry Prism

The gross area is calculated using an average block width of 7 21/32 inches. The net tensile stress is found by replacing the gross area with the net area in equation 3.5. The results of these tests are summarized in Table 3-14

3.6.2 Mortar Tensile Bond Strength

During subsidence every wall crack, with few exceptions, occurred at the head and bed joints of the blocks. The head joint undergoes a tensile failure and the bed joint a shear failure. In general the cracks did not go through the masonry units, but around them at the bonding surface of the mortar. This suggests that the controlling factor is the mortar bond strength in tension and shear.

Seven tests for mortar tensile strength were performed from the second group of samples. No standard test procedures were found for the field specimens. Since the specimens had to be cut from sections of the wall, the tests had to be developed around the samples shape.

To gather specimens, the wall was cut vertically approximately 16 inches on center aligned on the alternating head joints. Samples were two to three blocks high, and were banded before transport. In the lab, specimens were banded further to accommodate additional cuts for the appropriate tests. Again, the samples were cut vertically (in the direction of voids) with an end result of a nominal 8 inch by 8 inch bonded bed joint left undisturbed for testing. A hole was drilled through the center of each unit. A steel plate with a hole was inserted in each void. A rod was inserted through the hole in the unit and the steel plate. The plate was gripped in the jaws of

Table 3-14 Tensile Strength of Masonry Units

Sample	Height (in)	Net Thickness (in)	Gross Area (sqi)	Net Area (sqi)	Split Load (lbs)	Gross Tensile Stress (psi)	Net Tensile Stress (psi)
Block #1	7.612	2.784	58.28	21.19	10280	112.3	308.8
Block #2	7.630	2.789	58.42	21.28	10270	111.9	307.2
Block #3	7.648	2.768	58.56	21.17	10280	111.8	309.1
Block #4	7.625	2.794	58.38	21.30	10110	110.2	302.1
Average	**7.629**	**2.784**	**58.41**	**21.24**	**10235.0**	**111.6**	**306.8**

a universal tension testing machine for testing the tensile mortar bond.

The tensile bond mode of failure during subsidence is at the head joint. All the samples tested the bed joint tensile bond strength. The ultimate load obtained from bed joint tests would be higher than the load obtained from head joint tests due to the mortar bond contact area difference. This assumes the mechanics of the bond are equal in each, and area difference is the only variable. From Tables 3-11 and 3-12, the bed joint area is on the average approximately 4% larger than the head joint area. This difference is influenced by the block dimensions, mason's method of construction, and position in wall. Table 3-15 summarizes the test results of the tensile capacity of the mortar bond.

The net tensile stress is obtained as:

$$\textit{Net Tensile Stress} = \frac{\textit{Ultimate Load Bed Joint}}{\textit{Bed Joint Area}} \tag{3.6}$$

Assuming the only important variable between head and bed joint bond surface is the area difference, the net tensile stress is unaffected by its location as head or bed joint.

The "Approximate Ultimate Load Head Joint" is found by using a ratio of areas as:

$$\textit{Approximate Ultimate Load HJ} = (\textit{Ultimate Load BJ})\,\frac{\textit{Average HJ Area}}{\textit{Actual BJ Area}} \tag{3.7}$$

where HJ and BJ are the head and bed joints respectfully. The average head joint area is 25.28 square inches. The "Approximate Gross Tensile Stress" is found by using the average measured width and length of the head joint from Tables 3-10 and 3-12 of

Table 3-15 Mortar Bond Tensile Strength

Sample	Bed Joint Area (sqi)	Ultimate Load Bed Joint (lbs)	Approximate Ultimate Load Head Joint (lbs)	Net Tensile Stress (psi)	Approximate Gross Tensile Stress Head Joint (psi)
1	27.02	229.1	214.3	8.5	3.6
2	28.23	277.4	248.4	9.8	4.1
3	25.98	50.7	49.3	2.0	0.8
4	31.38	59.4	47.9	1.9	0.8
5	30.97	72.6	59.3	2.3	1.0
6	24.61	537.8	552.4	21.9	9.2
7	27.78	338.2	307.8	12.2	5.1
Average	**28.00**	**223.6**	**211.3**	**8.4**	**3.5**

7.656 and 7.88 inches respectfully as:

$$\textit{Approximate Gross Tensile Stress} = \frac{\textit{Approximate HJ Load}}{(\textit{Average Width})(\textit{Average Length HJ})} \tag{3.8}$$

3.8 Masonry in Shear

3.8.1 Mortar Shear Strength

Mortar bond shear and tensile strength are of equal importance when determining failure stresses of masonry walls during subsidence. Both mechanisms appear to occur simultaneously. Wall cracks observed during subsidence involved both shear and tensile bond failures along the bed and head joints respectfully. After the head and bed joints fail, the wall still offers resistance to loads through residual shear. The wall cracks continue to open after initial failure by sliding of the blocks on the bed joints.

To obtain the mortar bond shear strength parameters, a test was developed that could be used on the samples cut from the wall. Three block high nominal 16 inch long specimens were banded and cut in half. This left a specimen with nominal dimensions of 8 by 8 by 24 inches composed of three half blocks. Three plates were machined to 7 5/8 inches square from 3/8 inch plate. Two of the plates were placed on the base of the testing machine spaced 8.5 inches apart (block height plus two mortar joints and 1/8 inch). The specimen, Figure 3-6, was placed on its side onto the plates with gypsum ("Hydrocal White") spread on the plates upper surface. The specimen was leveled using a four foot carpenter's level in all directions. Gypsum was put on top of the center

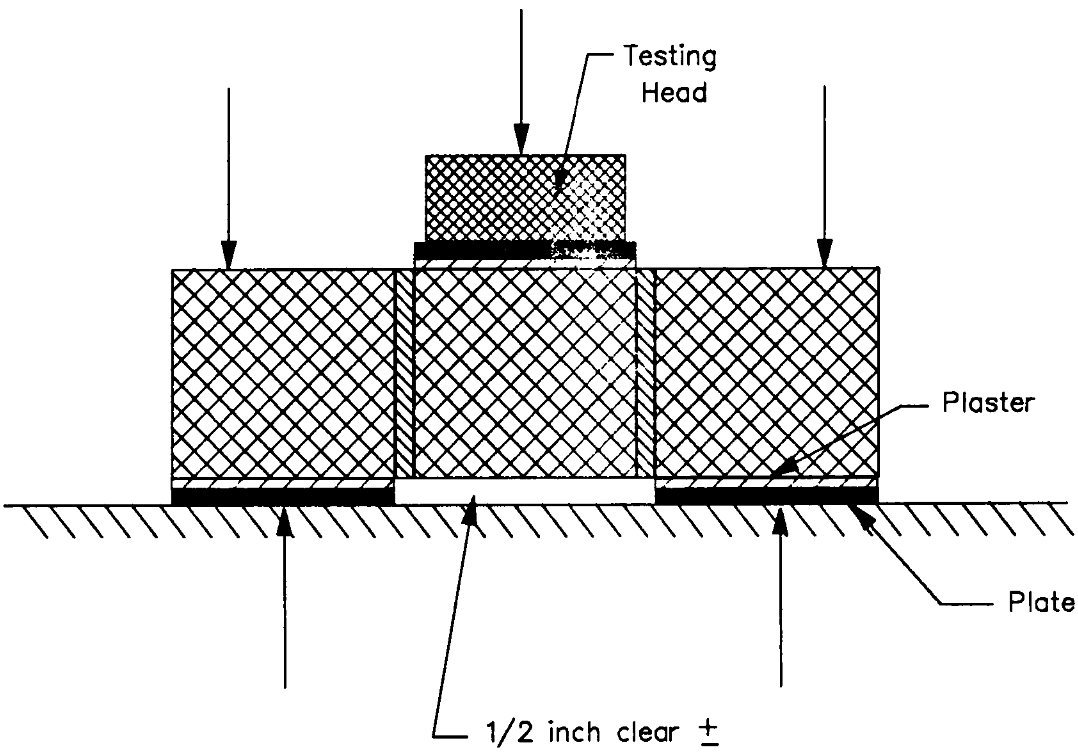

Figure 3-6 Shear Bond Testing Apparatus

block and the third plate was placed and leveled. To force a failure through both mortar joints and approach pure shear, the outer two blocks were rigidly clamped to the testing machine base. The center block was then loaded and pushed through the outer two blocks shearing the bed joint. The specimen was loaded slowly until failure and the ultimate load recorded. After failure, the specimen continued to be loaded at the same strain rate. After 3 to 4 minutes, the load dropped and became approximately constant. This load is recorded as the residual load. The residual load normally occurred at a displacement of approximately 1/16 inch.

Six specimens were tested and the results are tabulated in Table 3-16. The "Length of Bed Joint" refers to the average taken from the four bed joint bonded shear areas. The "Gross Shear Area" is obtained using the average width (7.656 inches) from Table 3-10 as:

$$\textit{Gross Shear Area} = (\textit{Length Bed Joint})(\textit{Average Width})(2) \qquad (3.9)$$

The "Net Shear Area" is the actual measured bond area. The ultimate and residual shear stresses are obtained by dividing the ultimate or residual load by the gross or net area as applicable.

Table 3-16 Mortar Bond Shear Strength

	Test Number						
	1	2	3	4	5	6	**Average**
Length of Bed Joint (in)	7.56	7.97	7.62	7.72	7.46	8.13	**7.74**
Gross Shear Area (sqi)	115.8	122.0	116.7	118.2	114.2	124.5	**118.6**
Net Shear Area (sqi)	50.7	55.9	55.1	52.7	50.3	56.2	**53.5**
Ultimate Load (lbs)	2468.	2298.	6176.	4555.	3203.	1328.	**3338.**
Gross Ultimate Shear Stress (psi)	21.3	18.8	52.9	38.5	28.0	10.7	**28.4**
Net Ultimate Shear Stress (psi)	48.7	41.1	112.2	86.5	63.6	23.6	**62.6**
Residual Load (lbs)	1027.	1128.	2026.	1225.	1073.	858.	**1222.8**
Gross Residual Shear Stress (psi)	8.9	9.2	17.4	10.4	9.4	6.9	**10.4**
Net Residual Shear Stress (psi)	20.3	20.2	36.8	23.3	21.3	15.3	**22.8**

CHAPTER 4

TAPE EXTENSOMETER

4.1 Tape Extensometer Description

4.1.1 Purpose of Tape Extensometer

Structures within the influence zone of subsidence are subjected to axial and bending stresses. These stresses stem from changes in length of the structure which induce strain. The effect on the structure is damage, visible from cracks and displacements. The severity of the damage is related to the resulting change in length of the structure.

The main goal of this research is to compare several damage mitigation techniques and determine which ones are suitable for subsidence prone areas. The tape extensometer provides a means to measure changes in length of the structures and compare the damage mitigation techniques used.

The results obtained are not as susceptible to varying local conditions as some of the other instruments used in this research. Measurements are taken over approximately 2.7 meter distances and visual inspection of the tape is easily made.

4.1.2 Components

The tape extensometer used was Model 518155 E/M manufactured by Slope Indicator Company, Seattle, Washington. The tape extensometer is a portable instrument which is hand-held while making readings. The overall length of the instrument housing and frame is 0.65 meters. It uses a 20 meter stainless steel engineer's tape coiled on a tape reel with holes punched at 50 mm intervals. A metal hook on the near side of the stainless steel extensometer frame is attached to a point and the tape extended for attachment to a second point. The tape has a snap hook fixed to its end. Slack is removed from the tape and it is locked into a locking pin on the opposite end of the frame at the nearest punched hole. Approximately 186 newtons of tension is applied to the tape from a screw collar on the aluminum housing that compresses a coiled spring. The proper tension is in the tape when scribed lines precisely align on the frame. A dial caliper inside the housing indicates the travel of the screw required to apply the proper tension on the tape. The dial reading is the increment of distance to be added to the tape reading. The caliper has a resolution of 0.05 mm and field readings were interpolated to the 0.01mm. The overall accuracy of the tape extensometer is +- 0.15 mm.

4.1.3 Reference Point Bolts

As mentioned previously, the tape extensometer measures the change in distance of two reference points. A reference point must be securely attached to the structure and have a place for attachment of the above mentioned hooks. These points were placed on the structure into two different types of material. A series of bottom bolts were connected to the concrete footing and top bolts connected to the concrete masonry wall. This necessitated the use of two different fastening anchors.

Several eye bolts were tested in the laboratory to predict their effectiveness in the field. A bolt and eye coupling combination manufactured by HILTI, Corporation were ultimately chosen. The bolt used for attachment to the concrete footings was an "Extra Thread Length Kwik Bolt II" 9.5 mm diameter by 178 mm wedge anchor. The bolt used for the masonry attachment was a "Hex Head HX" 7.9 mm diameter by 76.2 mm sleeve anchor. Attached to each bolt was a "Eye Coupling EC-3/8" for attachment of the extensometer hooks.

4.2 Bolt Locations and Subsidence Measurement

4.2.1 Location of Bolts and Original Measurements

The footing and wall were each measured in four segments for a total of eight measurements per foundation. The holes for the bolts were drilled using a hammer drill. The location of the footing bolts from the wall were determined by the amount of clearance necessary to operate the extensometer. The bolts in the wall were positioned as close to the top as could be achieved without splitting the block (approximately 60 mm). The first and last bolt were positioned longitudinally approximately 0.40 meters from each end of the foundation. The other bolts were positioned to obtain approximately four even segments. There was no attempt made to exactly duplicate or evenly space bolts along the foundations. Figure 4-1 and Tables 4-1 through 4-4 show the locations of the reference points (extensometer bolts) before subsidence. The total column does not add exactly to 12.19 meters (40 feet - 0 inches as constructed) because

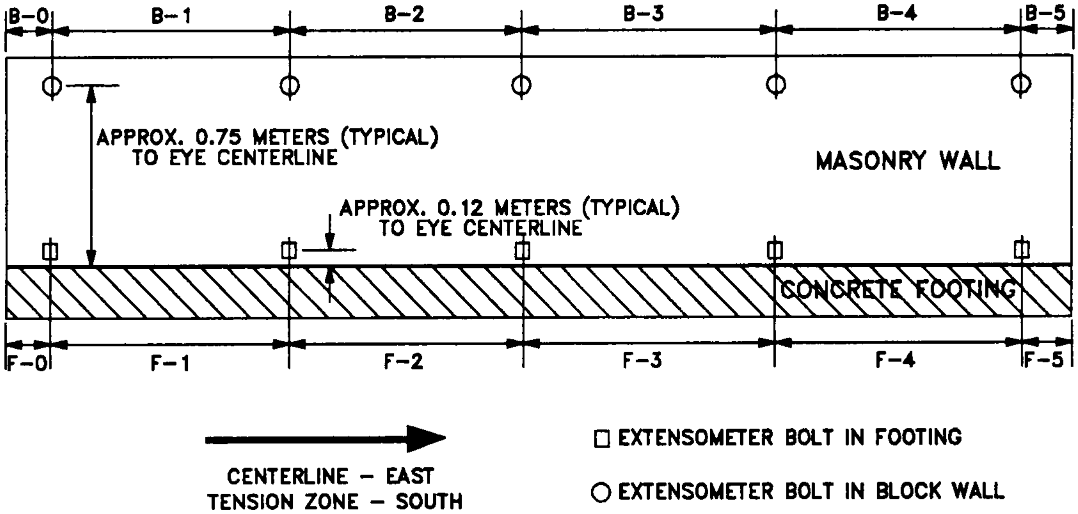

Figure 4-1 Extensometer Bolt Locations and Key to Tables 4-1 to 4-4

Table 4-1 Centerline Footing Extensometer Bolt Locations

Footing Description	F-0 (meters)	F-1 (meters)	F-2 (meters)	F-3 (meters)	F-4 (meters)	F-5 (meters)	TOTAL (meters)
Plastic-Soil	0.387	2.804	2.831	2.846	2.933	0.349	12.152
Plain	0.457	2.844	2.884	2.747	2.898	0.311	12.142
Plastic-Sand	0.432	2.505	2.949	3.005	2.861	0.400	12.153
Post-Tensioned	0.406	2.971	2.846	2.267	3.252	0.406	12.149
Deformed Bar	0.419	2.768	2.683	3.044	2.775	0.464	12.153
Steel Fiber	0.432	2.881	2.664	2.939	2.837	0.394	12.146

Table 4-2 Centerline Wall Extensometer Bolt Locations

Footing Description	B-0 (meters)	B-1 (meters)	B-2 (meters)	B-3 (meters)	B-4 (meters)	B-5 (meters)	TOTAL (meters)
Plastic-Soil	0.416	2.850	2.838	2.830	2.836	0.397	12.168
Plain	0.400	2.834	2.844	2.845	2.828	0.406	12.157
Plastic-Sand	0.416	2.827	2.838	2.854	2.834	0.384	12.152
Post-Tensioned	0.410	2.835	2.835	2.416	3.254	0.406	12.156
Deformed Bar	0.403	2.843	2.837	2.838	2.844	0.397	12.163
Steel Fiber	0.400	2.831	2.832	2.839	2.837	0.400	12.140

Table 4-3 Tension Zone Footing Extensometer Bolt Locations

Footing Description	F-0 (meters)	F-1 (meters)	F-2 (meters)	F-3 (meters)	F-4 (meters)	F-5 (meters)	TOTAL (meters)
Plain	0.540	2.599	2.698	3.025	2.705	0.565	12.132
Deformed Bar	0.413	2.700	3.210	2.584	2.893	0.330	12.130
Post-Tensioned	0.381	2.846	2.599	3.099	2.858	0.368	12.152
Plastic-Sand	0.406	2.572	3.216	2.801	2.567	0.584	12.146
Plastic-Soil	0.400	2.867	2.748	3.010	2.801	0.311	12.137
Steel Fiber	0.444	2.763	2.946	2.750	2.858	0.368	12.130

Table 4-4 Tension Zone Wall Extensometer Bolt Locations

Footing Description	B-0 (meters)	B-1 (meters)	B-2 (meters)	B-3 (meters)	B-4 (meters)	B-5 (meters)	TOTAL (meters)
Plain	0.400	2.843	2.821	2.853	2.827	0.406	12.150
Deformed Bar	0.425	2.419	3.230	2.847	2.837	0.387	12.145
Post-Tensioned	0.400	2.423	3.246	2.833	2.836	0.419	12.157
Plastic-Sand	0.422	2.420	3.243	2.838	2.837	0.390	12.151
Plastic-Soil	0.400	2.839	2.825	2.840	2.835	0.422	12.162
Steel Fiber	0.406	2.824	2.838	2.835	2.833	0.406	12.143

the extensometer measurement does not include the five 9.5 mm diameter holes in the eye couplings, the end measurements (B-0,B-5,F-0,F-5) are approximate, and the constructed length of the foundations is not accurate to more than two decimal places.

4.2.2 Field Measurements

Extensometer data was obtained from May 16, to August 7, 1990. A single reading was made in a day, except during peak behavior two readings were obtained (i.e. day 12.5). All dates, times, and temperatures of available data are tabulated in Table 4-5 for both sites. The "Time" column has "NA" listed if a time was not documented. Each set of six foundations took approximately 1 1/2 hours to complete a data set.

4.2.3 Data Reduction

The tape extensometer does not directly read a distance. Instead, it is used to measure change in length. The manufacturer does not supply the exact length of the instrument. The measurement taken must have the length of the extensometer frame added to it to give the actual length. To determine this length, exact hand measurements were taken of an extensometer calibration frame. The tape extensometer was set in the frame and a reading taken. This reading was subtracted from the frame's length to obtain the length of the instrument. During field application, there is a minor difference in the readings at the footing compared to the wall. The extensometer hook bolt is threaded and therefore rotated out one quarter turn during wall readings to make the

Table 4-5 Available Extensometer Data Information

Date	Day	Centerline Foundations			Tension Zone Foundations		
		Data ?	Time	Temp (°C)	Data ?	Time	Temp (°C)
5-16-90	6	Yes	NA	22	Yes	NA	23
5-17-90	7	Yes	NA	19	Yes	NA	21
5-18-90	8	Yes	NA	19	Yes	NA	23
5-19-90	9	Yes	12:00 PM	21	Yes	10:00 AM	21
5-20-90	10	Yes	NA	24	Yes	NA	27
5-21-90	11	Yes	7:30 AM	18	Yes	10:00 AM	18
5-22-90	12	Yes	8:30 AM	18	Yes	12:00 PM	21
5-22-90	12.5	Yes	3:00 PM	21	No	-	-
5-23-90	13	Yes	8:00 AM	13	Yes	11:00 AM	17
5-23-90	13.5	Yes	4:00 PM	23	Yes	6:00 PM	20
5-24-90	14	Yes	9:00 AM	19	Yes	11:00 AM	24
5-24-90	14.5	Yes	5:00 PM	23	Yes	PM	23
5-25-90	15	No	-	-	Yes	7:00 AM	18
5-30-90	20	Yes	2:00 PM	19	Yes	10:00 AM	17
5-31-90	21	-	-	-	-	-	-
6-1-90	22	No	-	-	Yes	7:30 AM	15
6-27-90	48	Yes	9:30 AM	27	Yes	8:30 AM	27
8-7-90	89	Yes	2:00 PM	24	No	-	-

caliper visible. The wall reading is less than the footing. To determine the actual length of the measurements, add 0.4288 and 0.4293 meters to the footing and wall readings respectfully. Small error in hand measurement of the extensometer frame produces insignificant error in computation of strain when the above adjustments are used consistently.

A possible source of error comes from the hook on the instrument having the ability to screw out. Each complete turn of the hook produces an error of approximately 1.3 mm. This was observed to happen on May 31, 1990 (day 21) when the hook screwed out at least one turn. The misplaced hook was noticed toward the end of the day, and the extent of the error was not known. After the data was reduced, it was obvious that this day had to be excluded in data comparisons. Therefore no data is exhibited from May 31. Another source of error is obtained by improper reading of the instrument. The reading is a several step process which can lead to error. The most common mistake is a reading 5 mm too large or too small.

No data was obtained for the tension zone plain concrete footing segments F-3 and F-4 (see Figure 4-1) after May 25 (day 15). A subsidence crack developed directly through a common extensometer bolt. The wall readings at this location were unaffected.

Temperature changes effect the extensometer readings. The extensometer frame and tape are made of stainless steel with a coefficient of thermal expansion equal to 9.6 x 10^{-6}. Unlike the concrete footing and wall with a coefficient of approximately 4.3 x 10^{-6}, temperature has an immediate effect on the tape. The footing responds to thermal expansion the least due to it being protected from the elements on three sides resulting in slow temperature change internal to the member. Even though the wall is directly exposed to the elements, only the outside surface changes immediately. Temperature changes take several hours to be uniform throughout the thickness of the wall. With the above reasoning and the fact that the concrete coefficient of thermal expansion is considerably less than stainless steel, temperature changes of the concrete wall and footing were neglected. All readings were adjusted by the thermal expansions of the tape and frame only using the coefficient of thermal expansion of stainless steel.

4.3 General Behavior

4.3.1 Centerline General Behavior

Results obtained from the centerline foundations all follow the same basic trends. During the earliest stages of subsidence, the foundations were exposed to slight axial tension and bending. When considerable subsidence begins, negative bending (tension top fibers) dominates and generates high stresses in the upper portion of the foundations (above the neutral axis). As the wave passes, the foundation curvature reverses placing the wall in compression and the bottom of the footing in tension. The foundation relaxes after the wave has passed to a uniform elongated state that shows only slight bending.

Figure 4-2 shows the total elongation of the post-tensioned foundation wall segments (B-1 through B-4 added together) during subsidence. The elongation steadily

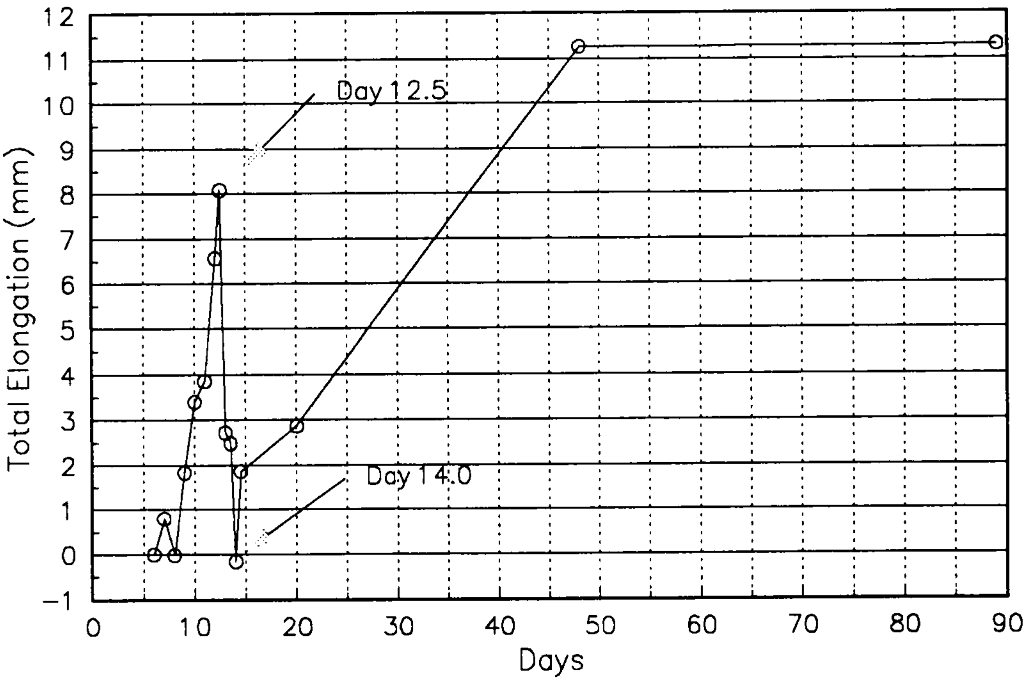

Figure 4-2 Total Elongation of Centerline Post-Tensioned Wall

increases from the initial reading (day 6) until day 11 for both the wall and the footing. Only the wall readings are shown here for clarity. The unusual reading of day 8 observed in several foundations appears to be in error because this trend was not consistent throughout. The first hairline block cracks and soil tension cracks were noticed at the centerline site before nightfall on day 11. Major subsidence began overnight. The first reading of day 12 shows significant extension in the wall. The foundations had visible cracks during this reading that enlarged as day 12 progressed. Seven hours later during the day 12.5 reading, the foundation cracks appeared to have doubled in size. This reading represents the approximate maximum extension observed during the day. The foundations' curvature reversed overnight, and thirteen hours later (day 13) the cracks were almost closed. Approximately nine hours after the day 13 reading (day 13.5) the foundation cracks had closed with the exception of a few hairline cracks. The morning of day 14, approximately sixteen hours later, no cracks were visible. The reading of day 14 captured the maximum compression in the wall. This behavior is typical in all of the foundation plots that show the day 14 reading as being slightly less than the day 14.5 reading recorded only eight hours later. The magnitude of compression in the wall is significant due to the reading of day 14 being shorter than the initial reading of day 6. This was observed to happen on a few other isolated cases. There was no data on day 15, but the foundations were showing no cracks therefore positive bending still existed. The next reading in the centerline was on day 20. Cracks on the foundations had reopened and in general were slightly less in size than during day 12.5. The foundations are in the relaxation phase. The magnitude of the post-tensioned elongation data of day 20 is not representative of all foundations. The plain concrete, plastic-on-soil, and the plastic-on-sand show day 20 at approximately the same elongation as day 12.5. The next two readings were taken on day 48 and 89. The cracks were visibly larger and in general less isolated than on day 12.5. This trend is consistent throughout the data.

4.3.2 Tension Zone General Behavior

Figure 4-3 shows the total elongation of the plastic-on-sand foundation wall in the tension zone during subsidence. The readings from day 9 to 12 show a lengthening of the foundation; however, there was no visible damage. On day 15, soil and head joint cracks were observed during the early morning reading. The next reading on day 20 shows large elongations which were accompanied by severe damage. The next reading on day 22 shows the elongation rate slowing. From day 22 to 48 the foundation wall and footing show a slight lengthening.

4.4 Stress/Strain Distribution

4.4.1 Centerline Stress/Strain Distribution

Figure 4-4 shows the location of wall damage recorded on day 90 with respect to the extensometer segments. There is a large concentration of damage in all of the foundations' segment B-2. Figure 4-5 shows a plot of strain vs. time for all four segments of the plastic-on-soil foundation wall, and the concentration of damage in

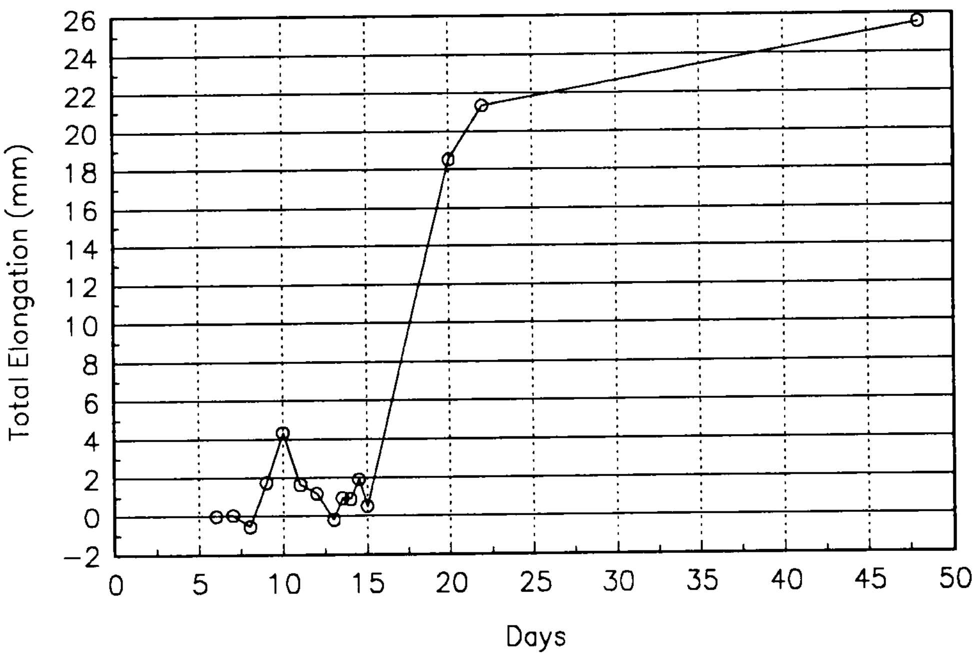

Figure 4-3 Total Elongation of Tension Zone Plastic-on-Sand Wall

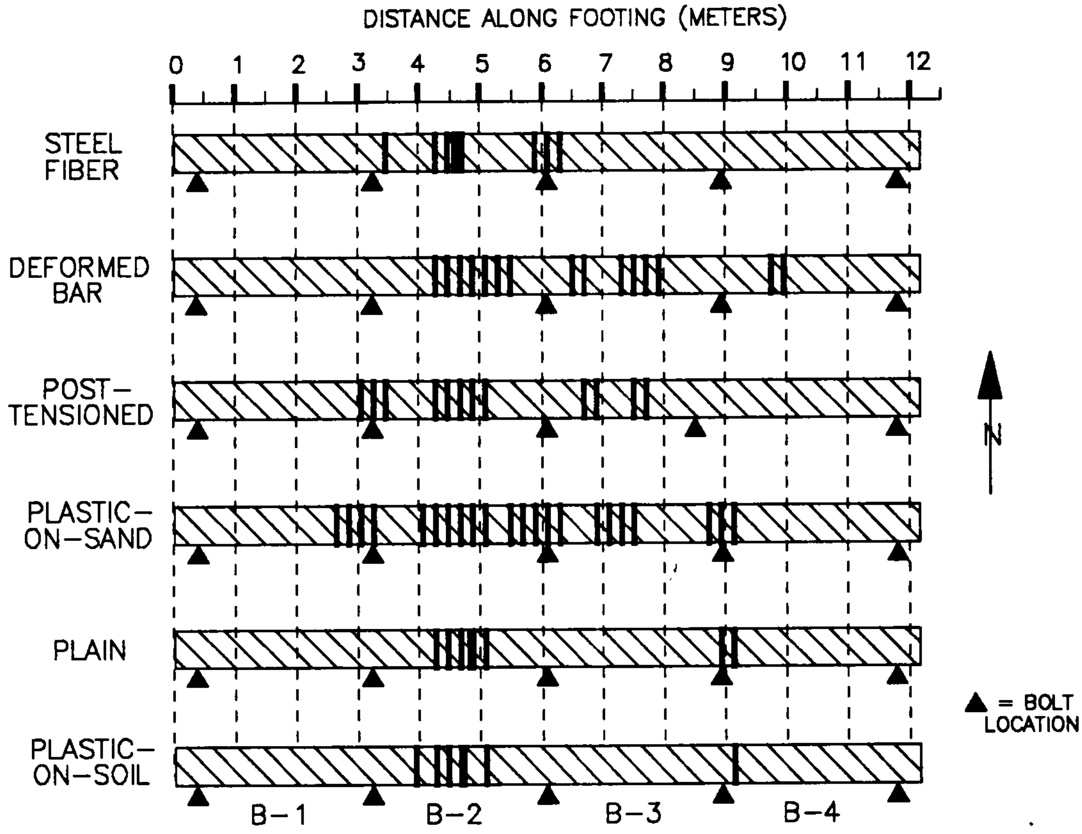

Figure 4-4 Day 90 Centerline Wall Crack - Extensometer Segment Location

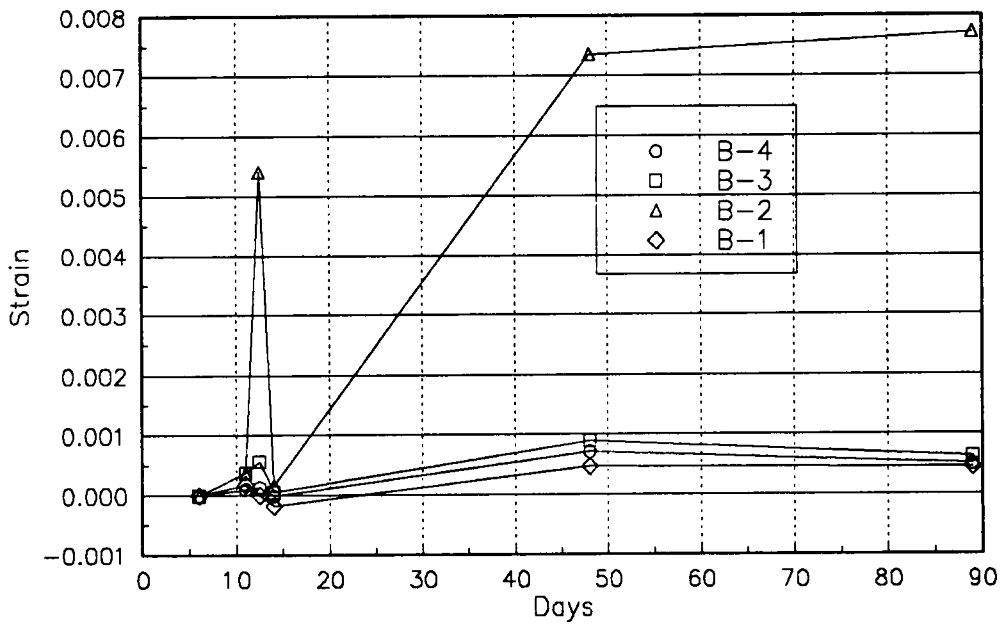

Figure 4-5 Strain in Wall Segments of Centerline Plastic-on-Soil

segment B-2. Segment B-2 has strains an order of magnitude greater than the other segments for both day 12.5 and day 48 through 89. Table 4-6 summarizes the segmental distribution of strain in the foundation walls. In addition to the main concentration of damage in segment B-2, the deformed bar and post-tensioned foundations have another concentration of cracks in segment B-3. The plastic-on-sand foundation has a concentration of cracks in segments B-2 and B-3. The segments where little or no cracking occurred have considerably less recorded strains. Segment B-1 has the smallest strains on day 48 (and little damage) in all foundation walls except the plastic-on-sand.

Figure 4-6 shows the location of footing damage with respect to the extensometer segments. Figure 4-7 shows the strain vs. time for the plastic-on-soil footing segments. Table 4-7 summarizes the segmental distribution of strain in the footings. The largest strains are in segment F-2 for all footings on day 12.5 and 48, with the exception of the plastic-on-sand. This corresponds with the main crack location. The plastic-on-sand footing had a second crack in segment F-3, where its largest strains are located.

4.4.2 Tension Zone Stress/Strain Distribution

Figure 4-8 shows the location of wall damage recorded on day 91 with respect to the wall extensometer segments. The cracks are more evenly distributed across the foundations than in the centerline, but in general the largest cracking occurred in segments B-2 and B-4. Figure 4-9 shows a plot of all four segments of the plastic-on-soil wall strain vs. time. Segments B-2 and B-4 have the largest strains due to the damage being concentrated in these segments. Table 4-8 summarizes the segmental

Table 4-6 Strain in Wall Segments of Centerline

Footing Type	Day	Wall Segment Strain				
		B-1	B-2	B-3	B-4	TOTAL
Plastic-Soil	12.5	.00000	.00541	.00056	.00013	.00152
	14	-.00018	.00017	.00005	-.00001	.00001
	48	.00047	.00736	.00089	.00071	.00235
Plain	12.5	.00031	.00237	.00050	.00057	.00094
	14	.00016	.00012	.00011	.00019	.00015
	48	.00089	.00572	.00093	.00119	.00218
Plastic-Sand	12.5	.00055	.00062	.00118	.00042	.00069
	14	.00003	-.00010	-.00010	.00015	-.00001
	48	.00109	.00124	.00201	.00105	.00135
Post-Tensioned	12.5	-.00006	.00189	.00070	.00037	.00071
	14	-.00015	.00007	-.00010	.00010	-.00001
	48	.00056	.00180	.00085	.00077	.00099
Rebar	12.5	.00056	.00166	.00063	.00038	.00081
	14	.00012	.00013	-.00001	.00024	.00012
	48	.00068	.00154	.00097	.00076	.00099
Fiber	12.5	.00025	.00250	.00046	-.00002	.00079
	14	.00005	.00007	.00002	.00002	.00004
	48	.00067	.00203	.00074	.00078	.00105

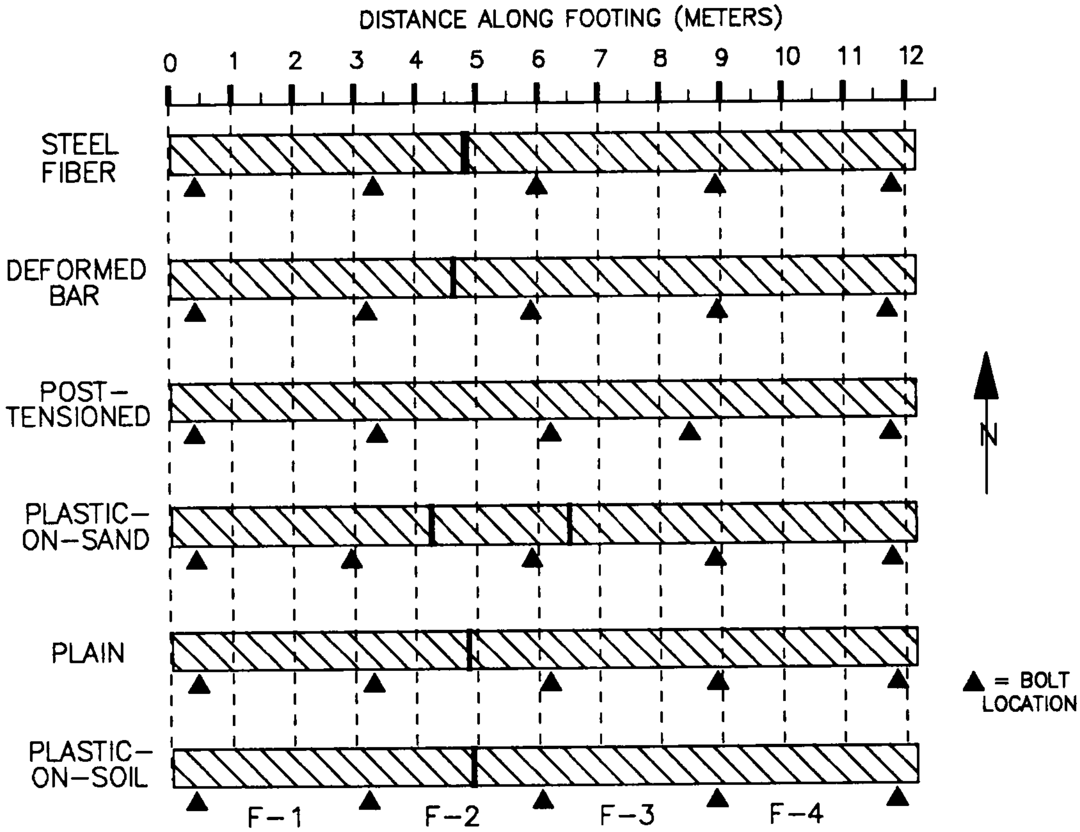

Figure 4-6 Day 90 Centerline Footing Crack - Extensometer Segment Location

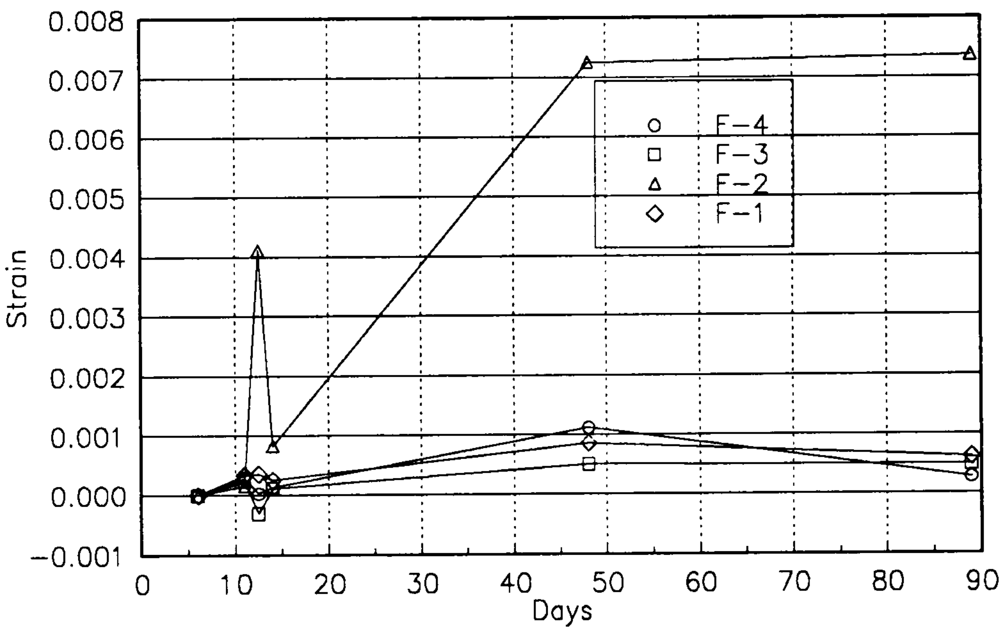

Figure 4-7 Strain in Footing Segments of Centerline Plastic-on-Soil Foundation

Table 4-7 Strain in Footing Segments of Centerline

Footing Type	Day	Footing Segment Strain				
		F-1	F-2	F-3	F-4	TOTAL
Plastic-Soil	12.5	.00036	.00411	-.00031	.00002	.00103
	14	.00025	.00083	.00011	.00013	.00033
	48	.00086	.00725	.00050	.00112	.00242
Plain	12.5	.00009	.00196	.00016	.00038	.00065
	14	.00022	.00097	.00000	.00011	.00033
	48	.00047	.00560	.00077	.00064	.00188
Plastic-Sand	12.5	.00024	.00028	.00031	-.00024	.00015
	14	.00014	.00016	.00029	.00010	.00017
	48	.00084	.00135	.00164	.00056	.00111
Post-Tensioned	12.5	-.00015	.00067	.00038	.00009	.00023
	14	.00015	.00009	.00000	.00020	.00012
	48	.00054	.00106	.00090	.00061	.00076
Rebar	12.5	.00029	.00047	-.00010	.00010	.00018
	14	.00019	.00024	-.00015	.00004	.00008
	48	.00064	.00168	.00053	.00091	.00092
Fiber	12.5	.00001	.00082	-.00020	.00018	.00019
	14	.00022	.00033	.00023	.00014	.00023
	48	.00046	.00187	.00059	.00086	.00093

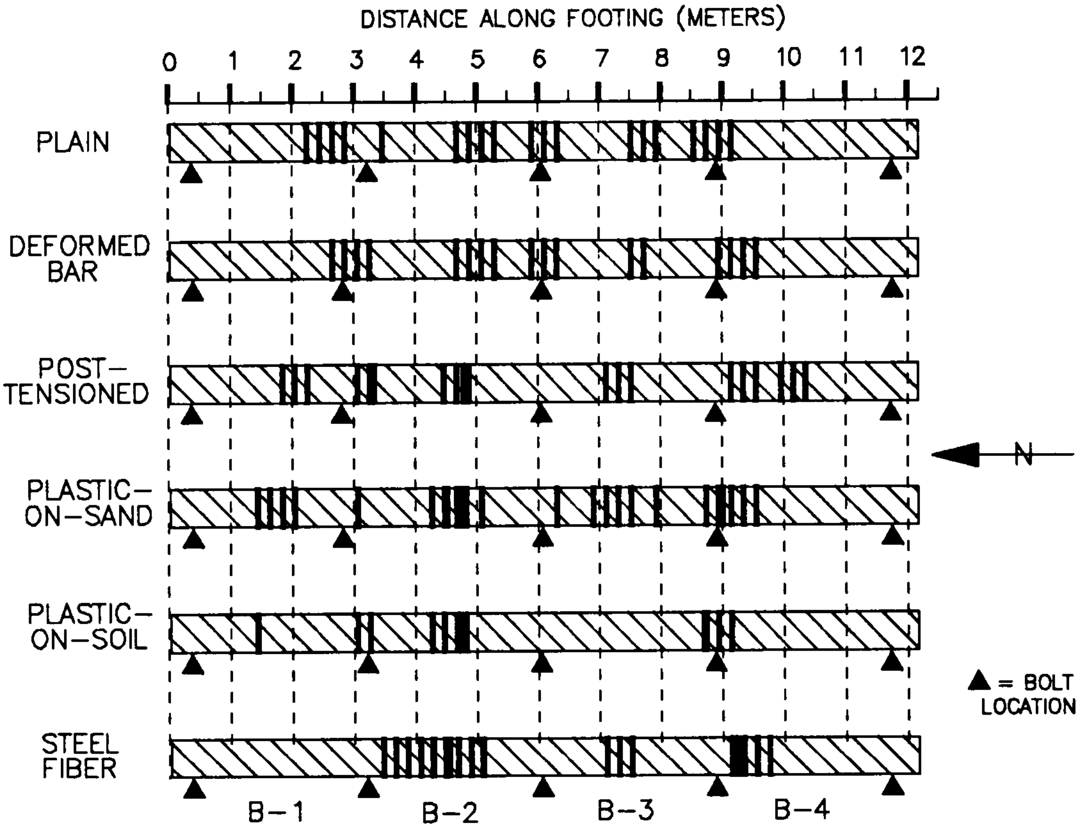

Figure 4-8 Day 91 Tension Zone Wall Crack - Extensometer Segment Location

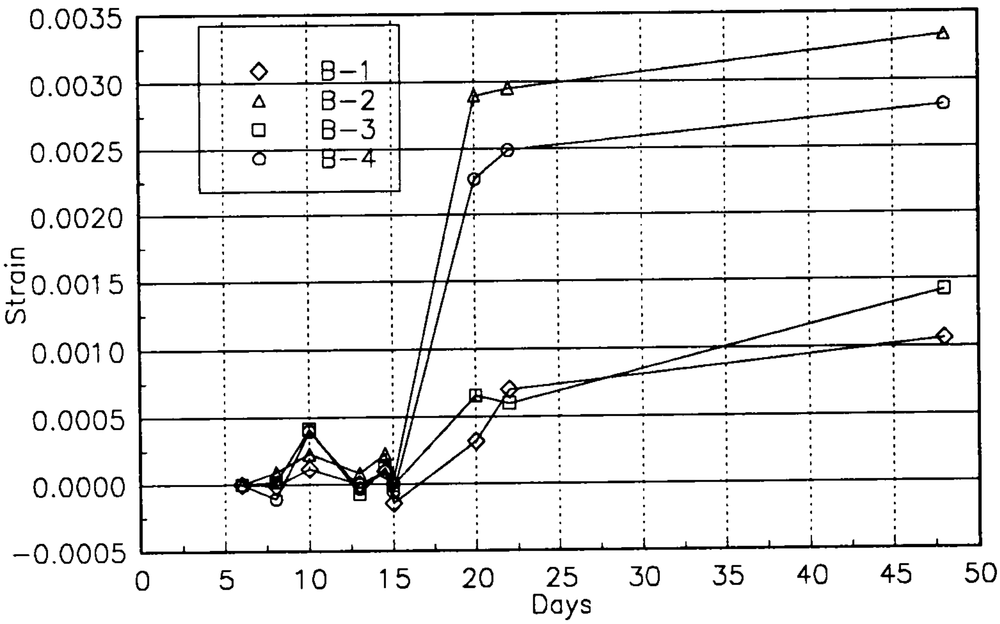

Figure 4-9 Strain in Wall Segments of Tension Zone Plastic-on-Soil

Table 4-8 Strain in Wall Segments of Tension Zone

Footing Type	Day	Wall Segment Strain				
		B-1	B-2	B-3	B-4	TOTAL
Plain	20 48	.00077 .00161	.00898 .00946	.00056 .00104	.00102 .00172	.00281 .00343
Rebar	20 48	.00045 .00125	.00175 .00228	.00066 .00102	.00110 .00178	.00103 .00162
Post-Tensioned	20 48	.00024 .00117	.00127 .00166	.00080 .00130	.00078 .00133	.00081 .00138
Plastic-Sand	20 48	.00031 .00096	.00308 .00376	.00052 .00111	.00222 .00279	.00163 .00225
Plastic-Soil	20 48	.00032 .00106	.00290 .00334	.00065 .00142	.00227 .00282	.00153 .00215
Fiber	20 48	-.00001 .00081	.00434 .00526	-.00008 .00050	.00287 .00315	.00178 .00243

distribution of strain in the foundation walls. Segment B-2 has the largest strains in all foundations and this is where the largest group of cracks were located. Segment B-4 has the second highest strains (except post-tensioned day 20) which are approximately 70% in magnitude to segment B-2. This segment had the second largest group of cracks. Segments B-1 and B-3 are approximately equal.

Figure 4-10 shows the location of footing damage recorded on day 91 with respect to the extensometer segments. A series of major cracks occurred in segment F-2 with another band of cracks between segments F-3 and F-4. This corresponds with Figure 4-8 except that as the cracks propagated down the head and bed joints of the wall, they ended up mainly in segment three of the footing. Figure 4-11, a plot of strain vs. time for the plastic-on-soil footing segments, graphically shows the strain distribution throughout the footing. The strain distribution in the footing is different than in the wall because of the location of the cracks. In the wall, segment four had the second highest strain, but since the crack occurred in segment three of the footing, segment F-3 is second in magnitude. The steel fiber footing, which had a crack in segment F-4, shows this segment as second in magnitude and thus a similarity to the wall results. Table 4-9 summarizes the segmental distribution of strain in the footings. The largest strains are in segment F-2 for all footings on day 20 and 48. The second largest strains are in segment F-3 for all foundations except the fiber reinforced. The data missing from the plain concrete footing is due to a missing extensometer bolt.

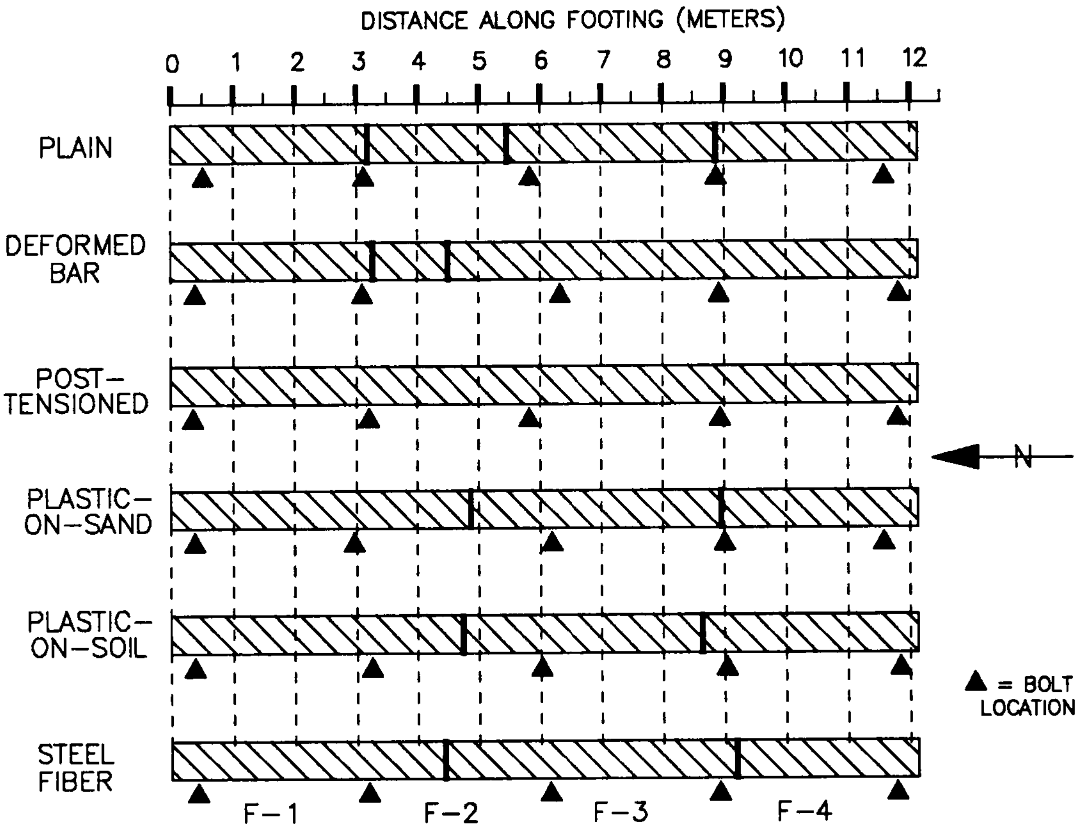

Figure 4-10 Day 91 Tension Zone Footing Crack - Extensometer Segment Location

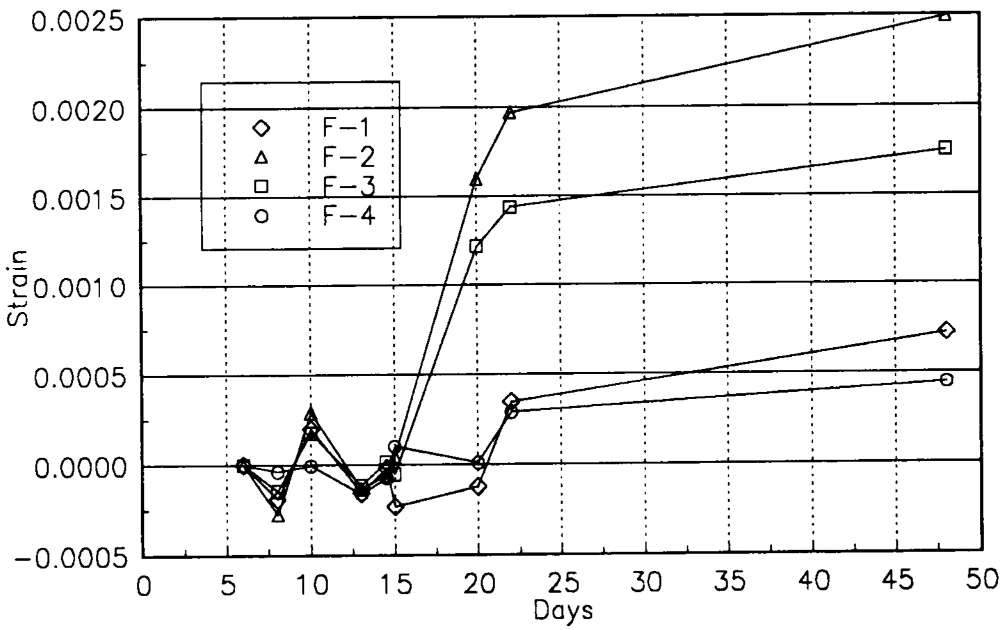

Figure 4-11 Strain in Footing Segments of Tension Zone Plastic-on-Soil

Table 4-9 Strain in Footing Segments of Tension Zone

Footing Type	Day	Footing Segment Strain				
		F-1	F-2	F-3	F-4	TOTAL
Plain	20 48	.00014 .00062	.00816 .00904	- -	- -	- -
Rebar	20 48	.00018 .00071	.00077 .00137	.00049 .00105	.00013 .00056	.00040 .00093
Post-Tensioned	20 48	.00020 .00087	.00052 .00110	.00022 .00085	.00016 .00088	.00027 .00092
Plastic-Sand	20 48	.00018 .00056	.00222 .00283	.00114 .00144	-.00053 .00039	.00085 .00139
Plastic-Soil	20 48	-.00012 .00072	.00160 .00250	.00122 .00175	.00001 .00044	.00067 .00135
Fiber	20 48	-.00009 .00088	.00282 .00358	.00027 .00086	.00155 .00185	.00117 .00182

4.4.3 Sill Plate Effect on Stress/Strain Distribution

Construction of the sill plate has been shown to have an effect on behavior (Bennett and Drumm, 1992). Figure 4-12 shows the orientation of the butt joints in the centerline. The plastic-on-soil, plain, and post-tensioned foundations in the centerline had a double butt joint that occurred within segment two. The remainder of the foundations in the centerline and tension zone had lapped sill plates. All of these lapped sill plates were oriented similarly (with respect to approaching wave) with the exception of the centerline plastic-on-sand.

The extensometer data shows that construction of the sill plate has an effect on the distribution of strains. The lapped sill reduces the amount of strain in a segment due to its composite effect with the wall and footing. Tables 4-8 and 4-9 show that the strain in each segment of the tension zone plastic-on-sand and plastic-on-soil foundations were approximately equal. The behavior of the plastic-on-soil and plastic-on-sand foundations in the centerline were quite different, Table 4-6 and 4-7. The plastic-on-soil in the centerline has a major concentration of strain in segment two, where the double butt joint in the sill plate is located. The centerline plastic-on-sand has a more even distribution of strain due to the composite effect of the lapped sill plate.

4.4.4 Reinforcing Effect on Elongation

Figure 4-13 shows a plot of strain vs. time for all four segments of the tension zone deformed bar footing. Comparison to the plastic-on-soil footing (Figure 4-11) shows that reinforcing allows the footing to maintain stiffness after cracking. The strain

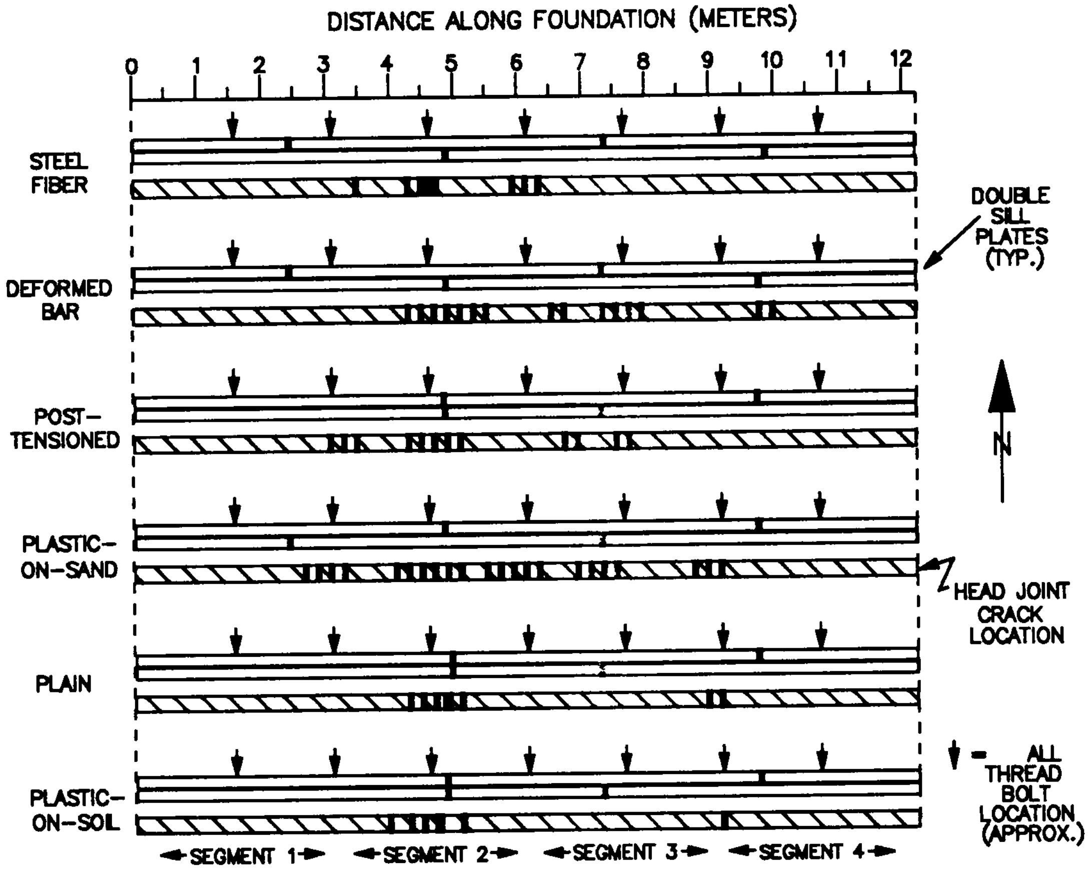

Figure 4-12 Centerline Sill Plate Orientation - Extensometer Segments

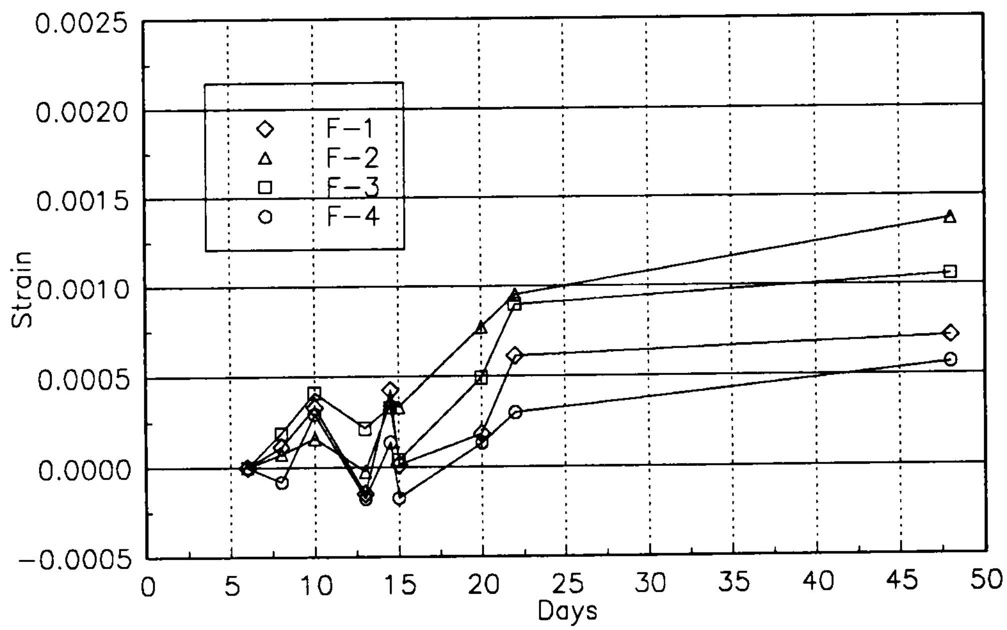

Figure 4-13 Strain in Footing Segments of Tension Zone Deformed Bar

in segment F-2 of the deformed bar footing is approximately 50% of the unreinforced footing. Table 4-8 shows a decrease in strain for the wall, indicating the stiffness increase of the footing increased the entire foundation stiffness.

4.5 Foundation Cross-Section Stress Distribution

4.5.1 General Considerations

The extensometer provided strain measurement at two places on the cross section. The distance between the upper and lower bolts provided a means to distinguish between axial and bending strains. Figure 4-14 shows a cross-section of the foundation and the possible stress conditions that may be present. The estimated neutral axis of 297 mm above the bottom of the footing is based on an uncracked section with a composite sill plate.

4.5.2 Centerline Stresses

Figure 4-15 shows the footing and wall strains for the centerline plastic-on-sand second and third segment. From day 11 to day 12, both segments show an increase in strain. The third segment shows an increase in axial stress because the footing and wall strain increased by the same amount. The second segment indicates that bending is also present since the wall strain increased more than the footing. By day 12.5 the third segment shows the wall strain increasing considerably and the footing strain decreasing. These strains closely match the case of pure negative bending shown in Figure 4-14

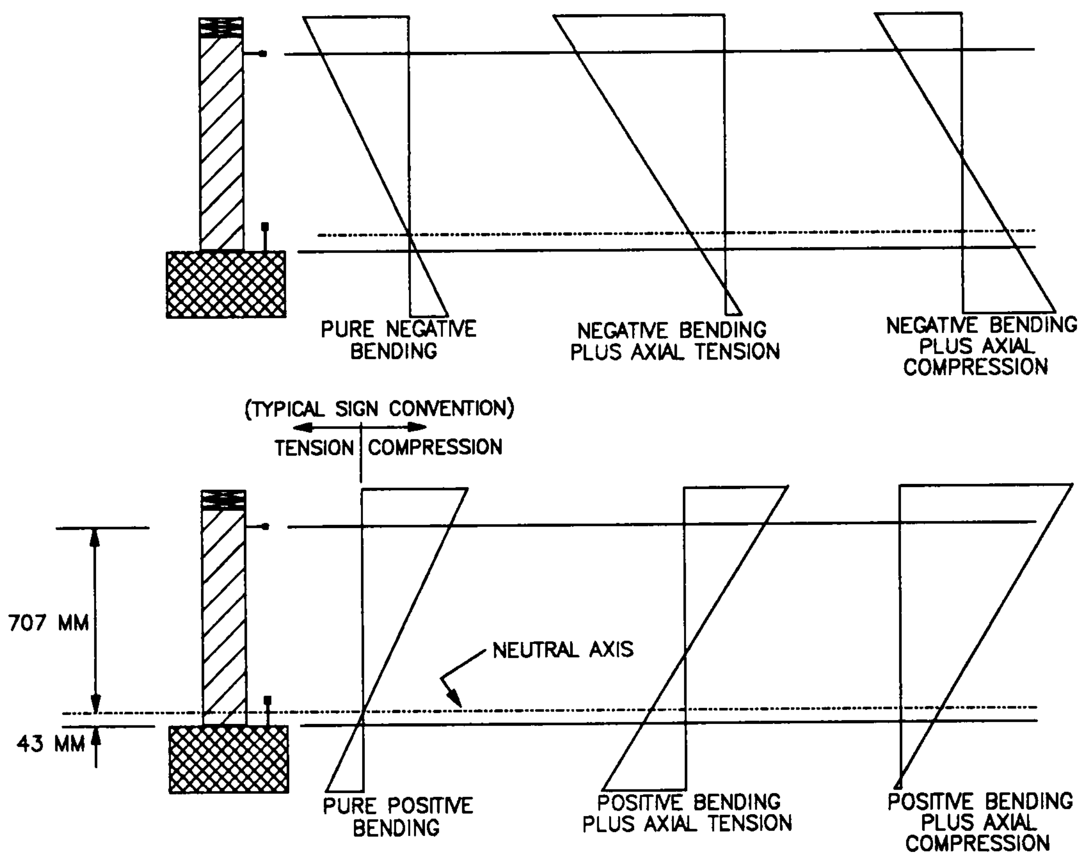

Figure 4-14 Cross Section Strain Distribution and Extensometer Reading Location

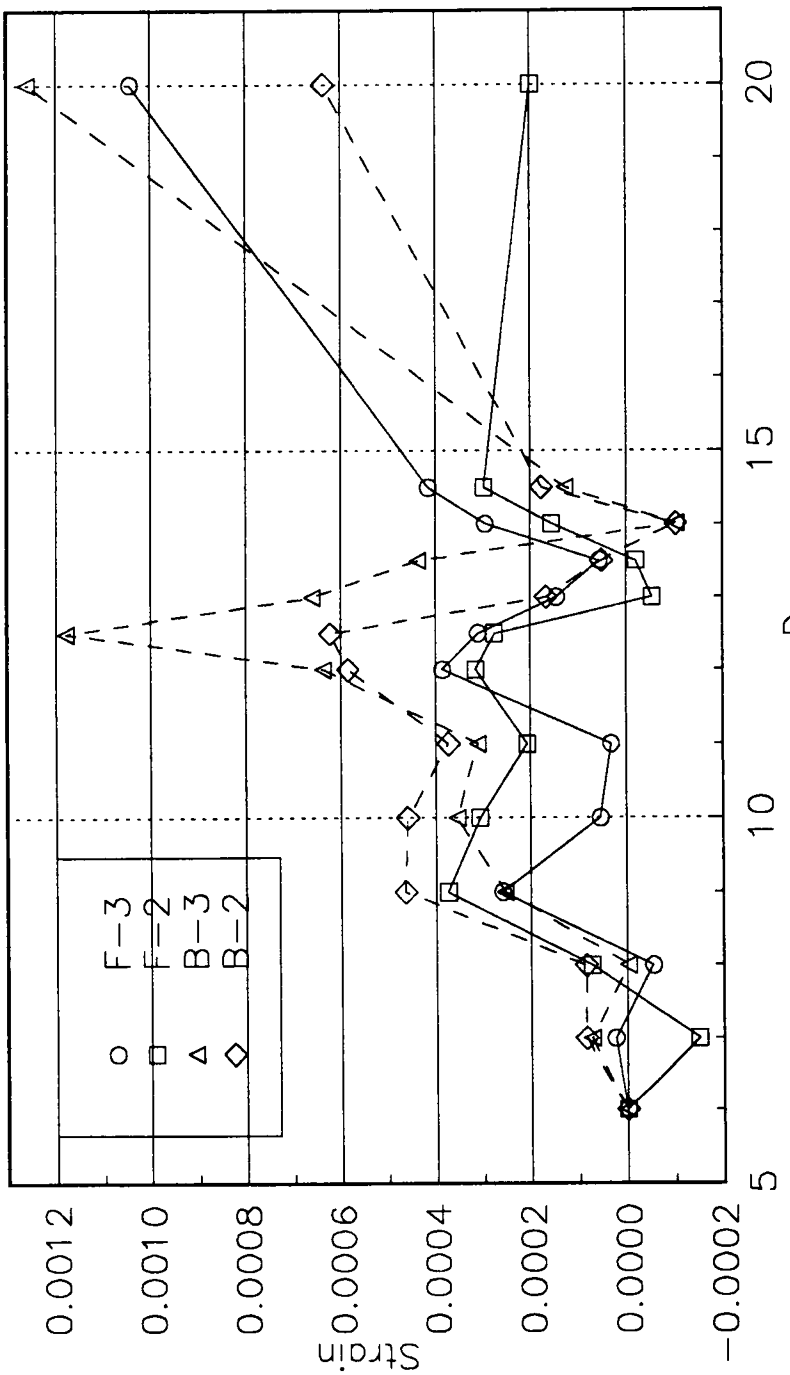

Figure 4-15 Strain in Centerline Plastic-on-Sand Footing and Wall Segments

and they indicate that the neutral axis is high in the cross-section. Only slight damage was observed during this phase and the foundation appears to have behaved much like an uncracked section.

The foundations were in the reverse curvature and compression phase from day 13 to 14. Segment three shows a decrease in curvature from day 12.5 to 13.5. Segment two shows a decrease in axial tension from day 12.5 to 13.0 and positive bending from day 13.0 to 13.5. From day 13.5 to 14.0 the footing strain increases and the wall strain continues to decline. Both segments show compression in the top of the wall and tension in the footing on day 14.0 indicating positive curvature. After day 14.0, there is an increase in axial tension and a return to negative bending.

Figure 4-16 shows the centerline deformed bar footing and wall strain and Figure 4-17 shows the post-tensioned footing and wall strain of the second segment. From day 14 to 20 the footing and wall show the same trend as the plastic-on-sand second segment indicating that the neutral axis is high in the cross-section. Figure 4-18 shows the centerline plastic-on-soil footing and wall strain of the second segment. By day 12.5, the footing had cracked and due to the sill plate butt joint there were two distinct segments of the footing. The only strength comes from friction at the bed joint mortar to block interface. The extensometer is primarily measuring the uniform opening and closing of the gap between the two footing segments.

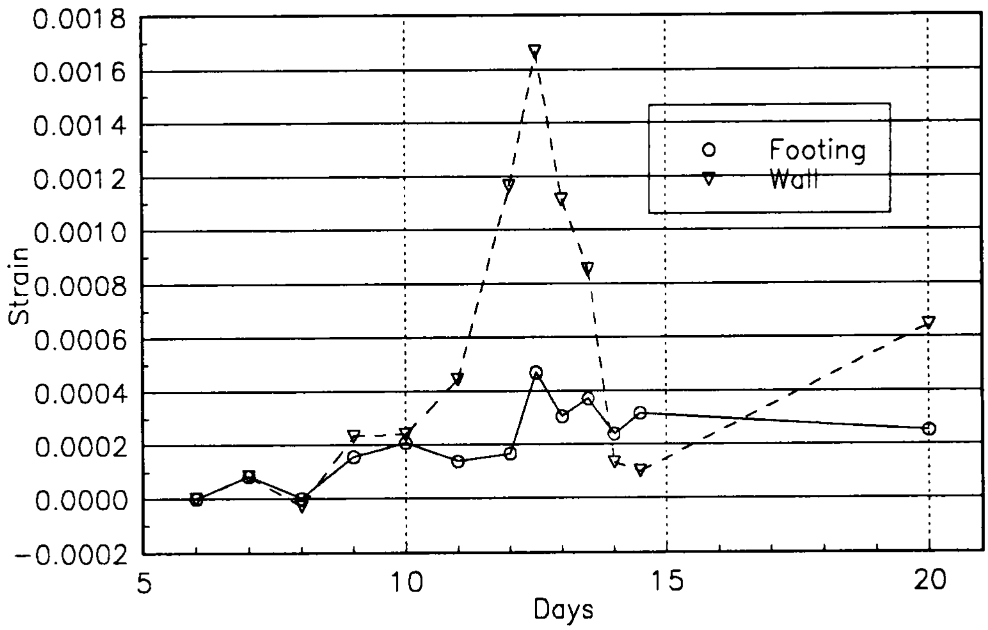

Figure 4-16 Strain in Centerline Deformed Bar Footing and Wall Segment Two

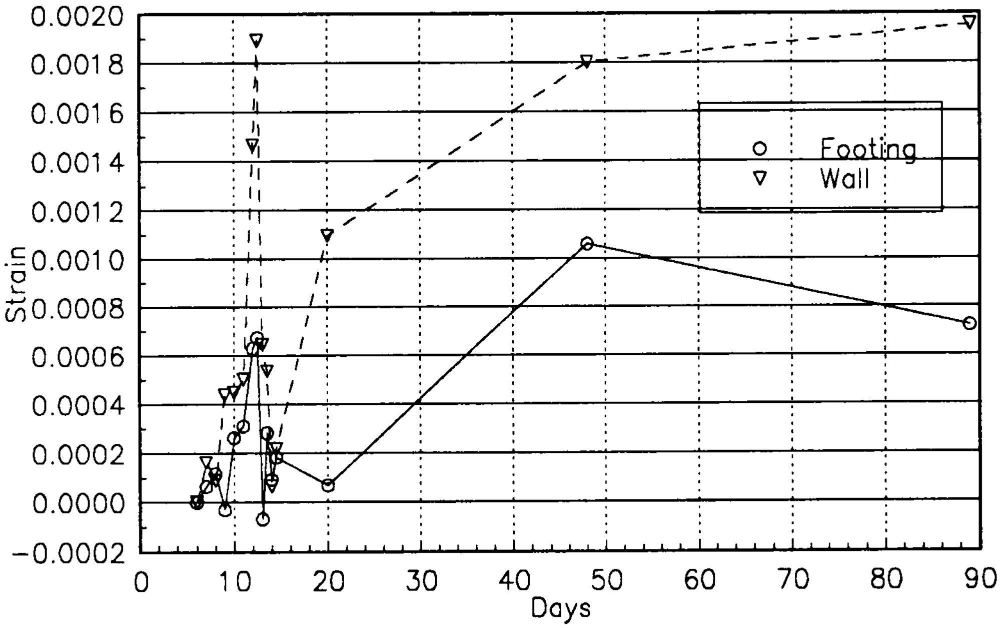

Figure 4-17 Strain in Centerline Post-Tensioned Footing and Wall Segment Two

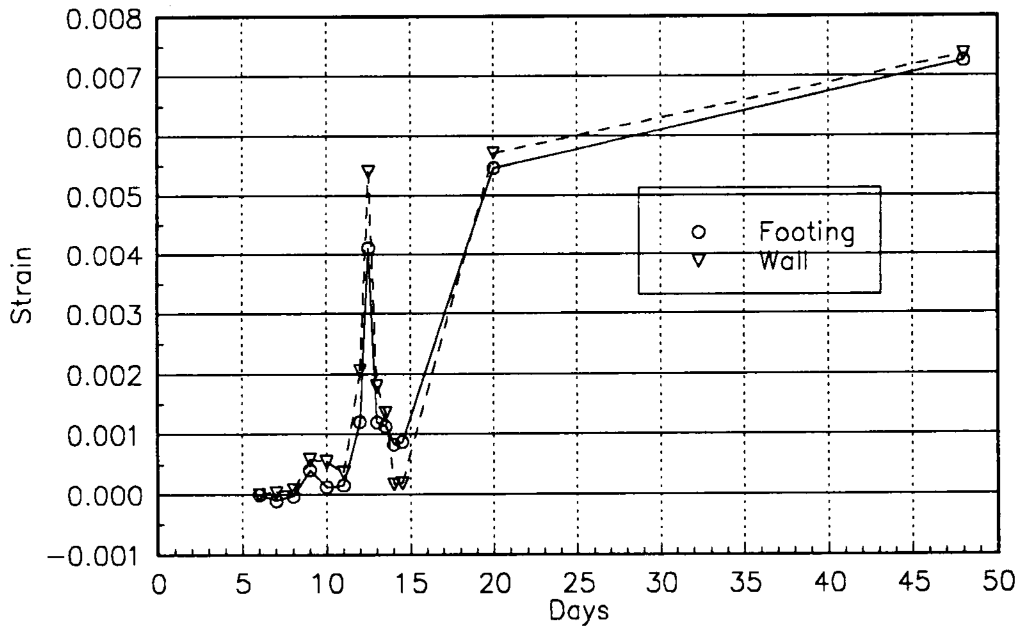

Figure 4-18 Strain in Centerline Plastic-on-Soil Footing and Wall Segment Two

4.5.3 Tension Zone Stresses

The tension zone is exposed to only axial tension and negative bending. This bending is greater in magnitude and more distributed than in the centerline. The result is that almost all of the segments received extensive damage.

The tension zone fiber reinforced foundation in Figure 4-19 shows significant elongation in the second segment of both the wall and footing. From day 15.0 to 20.0 all of the footing segments except segment four of the plastic-on-sand and plastic-on-soil and segment one of the fiber reinforced show an increase in strain. These segments all behave similar to the plastic-on-soil footing shown in Figure 4-20. The segments which show a decrease in footing strain are three of the least damaged.

4.6 Damage Comparisons

4.6.1 Centerline Damage Comparisons

Figure 4-21 and 4-22 show the total foundation elongations of all six of the centerline footings and walls respectfully. The post-tensioned foundation had the smallest elongation in both the footing and wall. This foundation would have even less elongation if it had lapped sill plates. Post-tensioning decreased elongations by approximately a factor of two in the wall and three in the footing compared to the other foundations without lapped sill plates (the plain, and plastic-on-sand). The plastic-on-soil foundation had the poorest performance by elongating more than even the control foundation (plain).

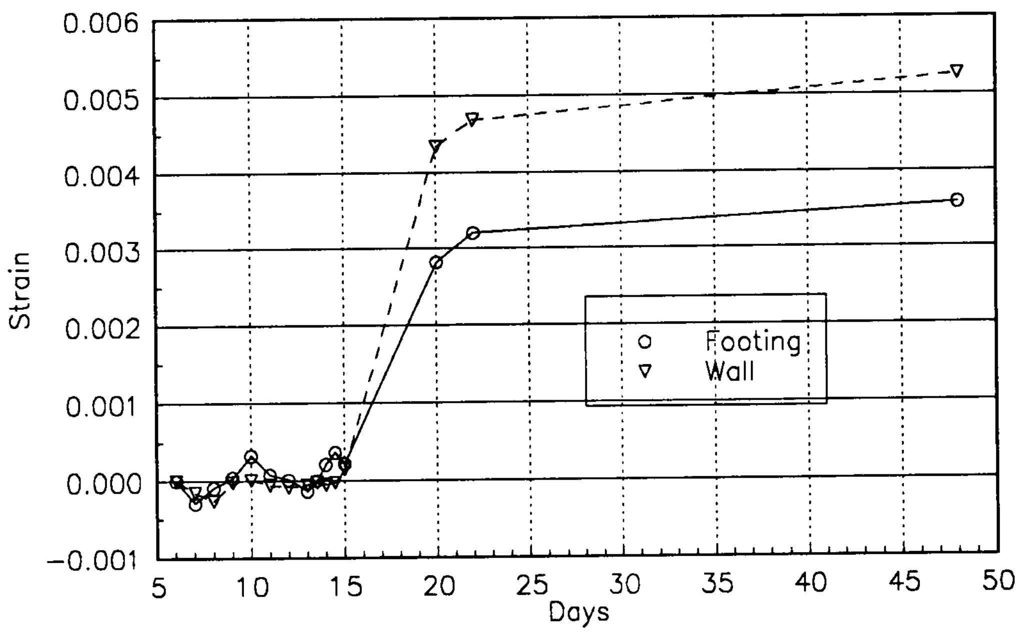

Figure 4-19 Strain in Tension Zone Fiber Footing and Wall Segment Two

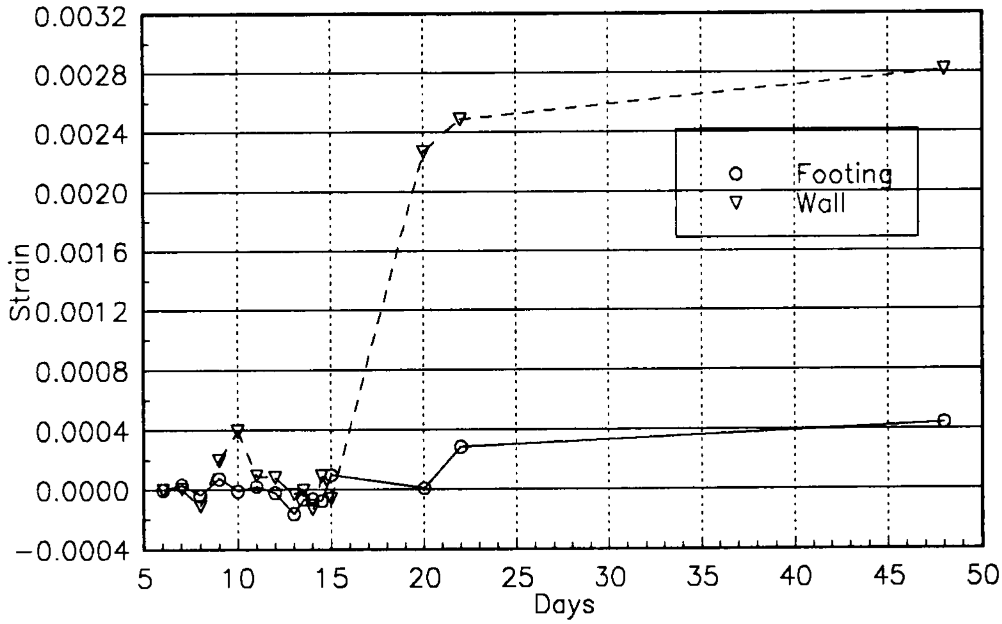

Figure 4-20 Strain in Tension Zone Plastic-on-Soil Footing and Wall Segment Four

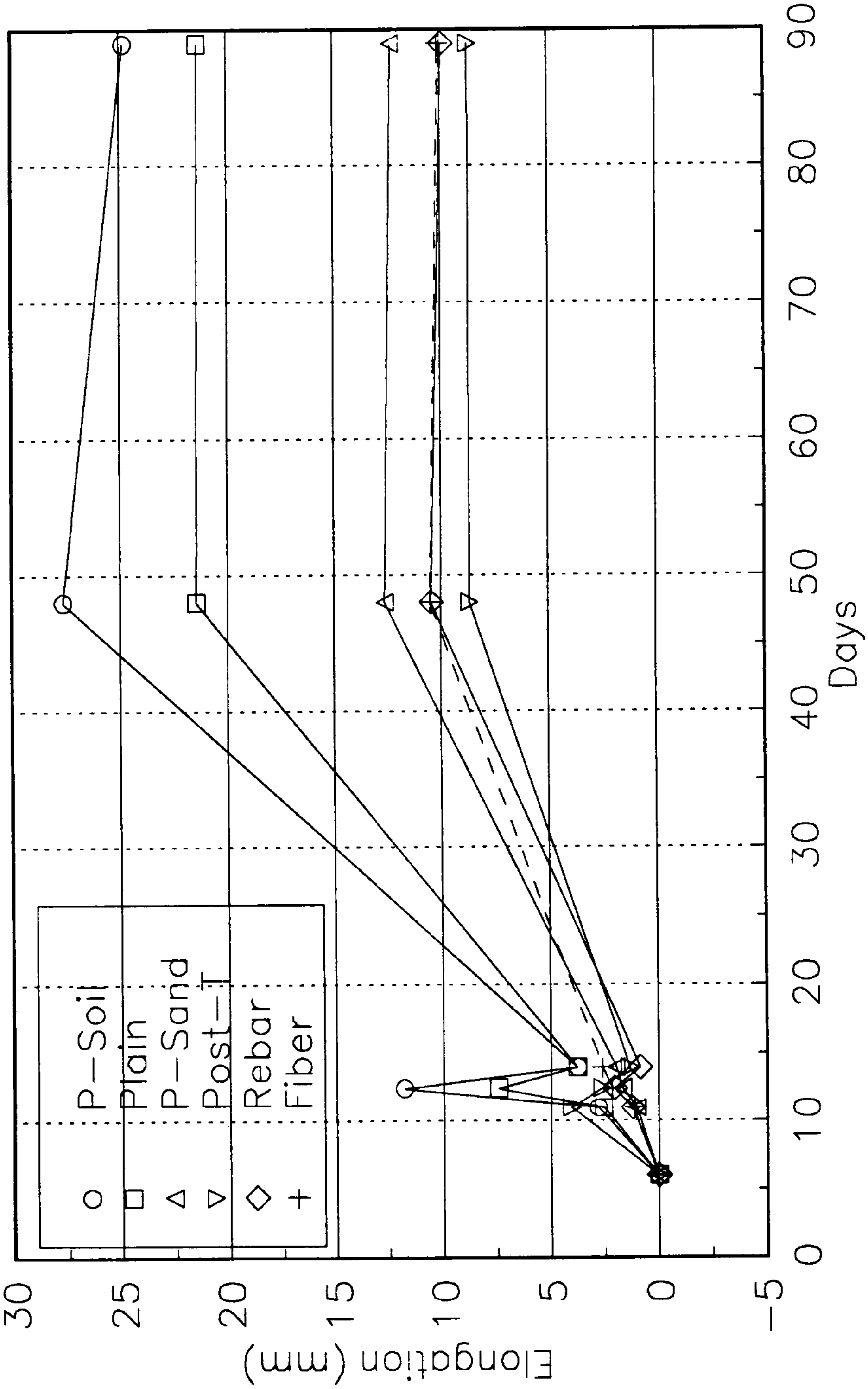

Figure 4-21 Centerline Footing Elongation Comparisons

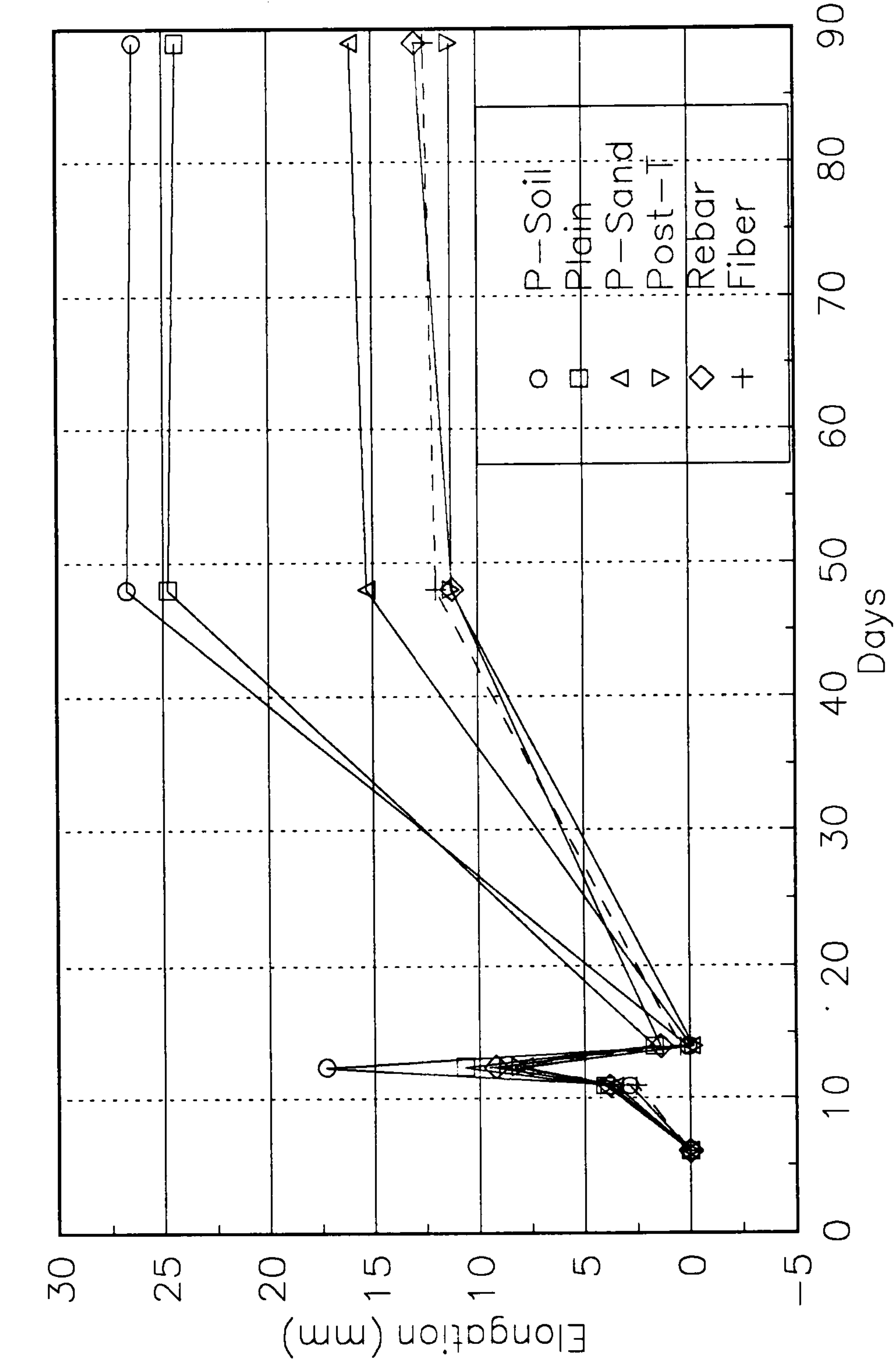

Figure 4-22 Centerline Wall Elongation Comparisons

The effect of the sill plate can be seen by how it reduced the elongation in the fiber reinforced and plastic-on-sand foundations to comparable levels of the post-tensioned foundation. The fiber reinforced foundation performed almost identically to the deformed foundation. This result is unexplained, but one possible reason could be that the fiber reinforced footing was built with irregular forms on one side and was therefore slightly larger than specified during construction.

4.6.2 Tension Zone Damage Comparisons

The tension zone data provides better information for damage comparisons than the centerline. The footing trenches were constructed to close tolerances and the soil had the proper moisture content during concrete placement. All of the sill plates were constructed in the same manner.

Figure 4-23 and 4-24 show the total elongation of all six of the tension zone footing and walls respectfully. Figure 4-23 does not show the plain concrete footing for the last days of subsidence due to the crack through the bolt. The plain concrete foundation had the largest elongations and the post-tensioned the least. The plastic-on-sand and plastic-on-soil foundations behaved approximately identically, with the plastic-on-soil interface having slightly smaller elongations. The deformed bar foundation had only slightly larger elongations than the post-tensioned foundation.

Figure 4-25 shows the wall strain in segment two, the dominating segment of all six foundations in the tension zone. The plot shows the same trend as the two previous figures, except the differences between mitigation techniques is more defined. This

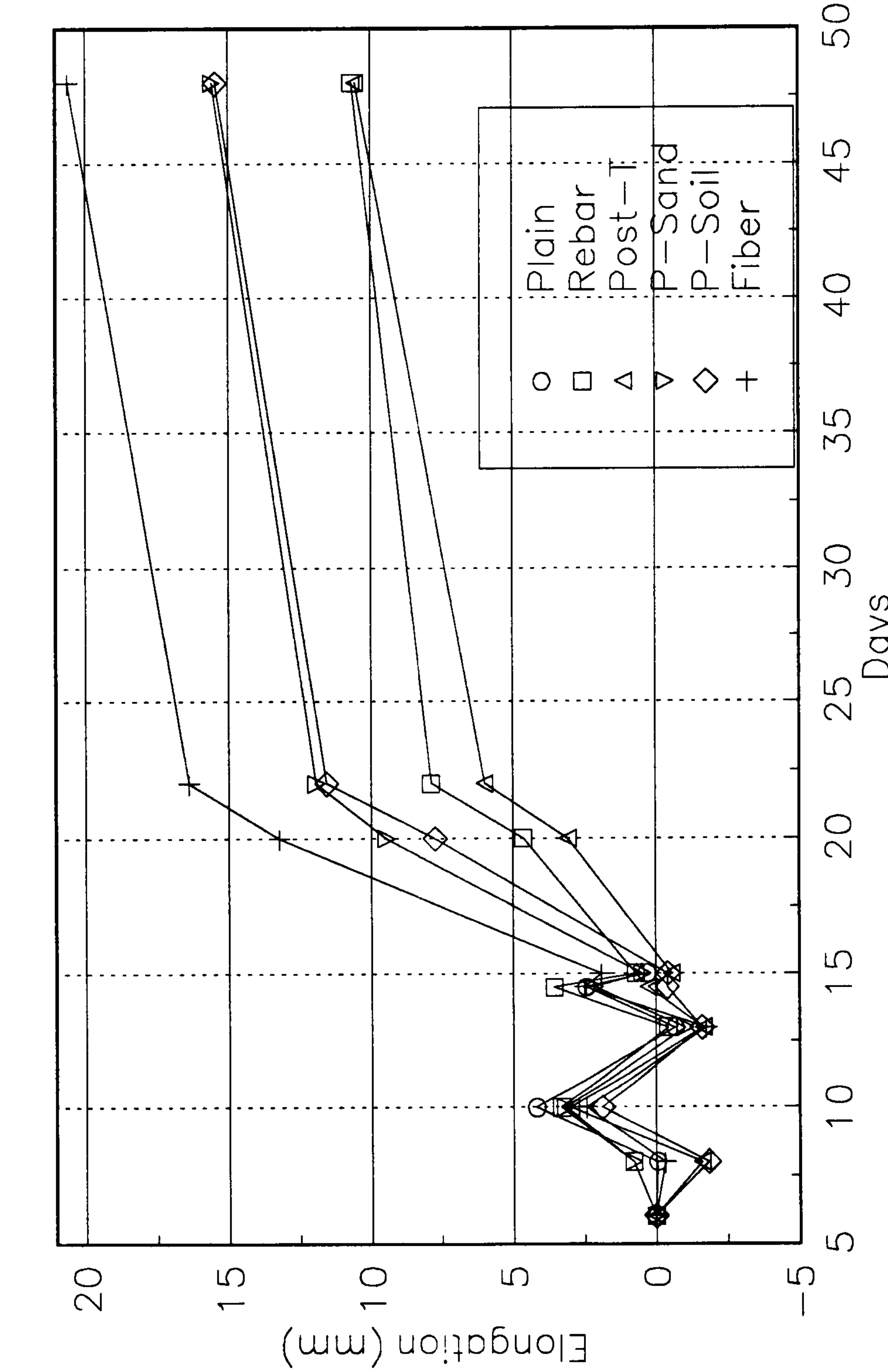

Figure 4-23 Tension Zone Footing Elongation Comparisons

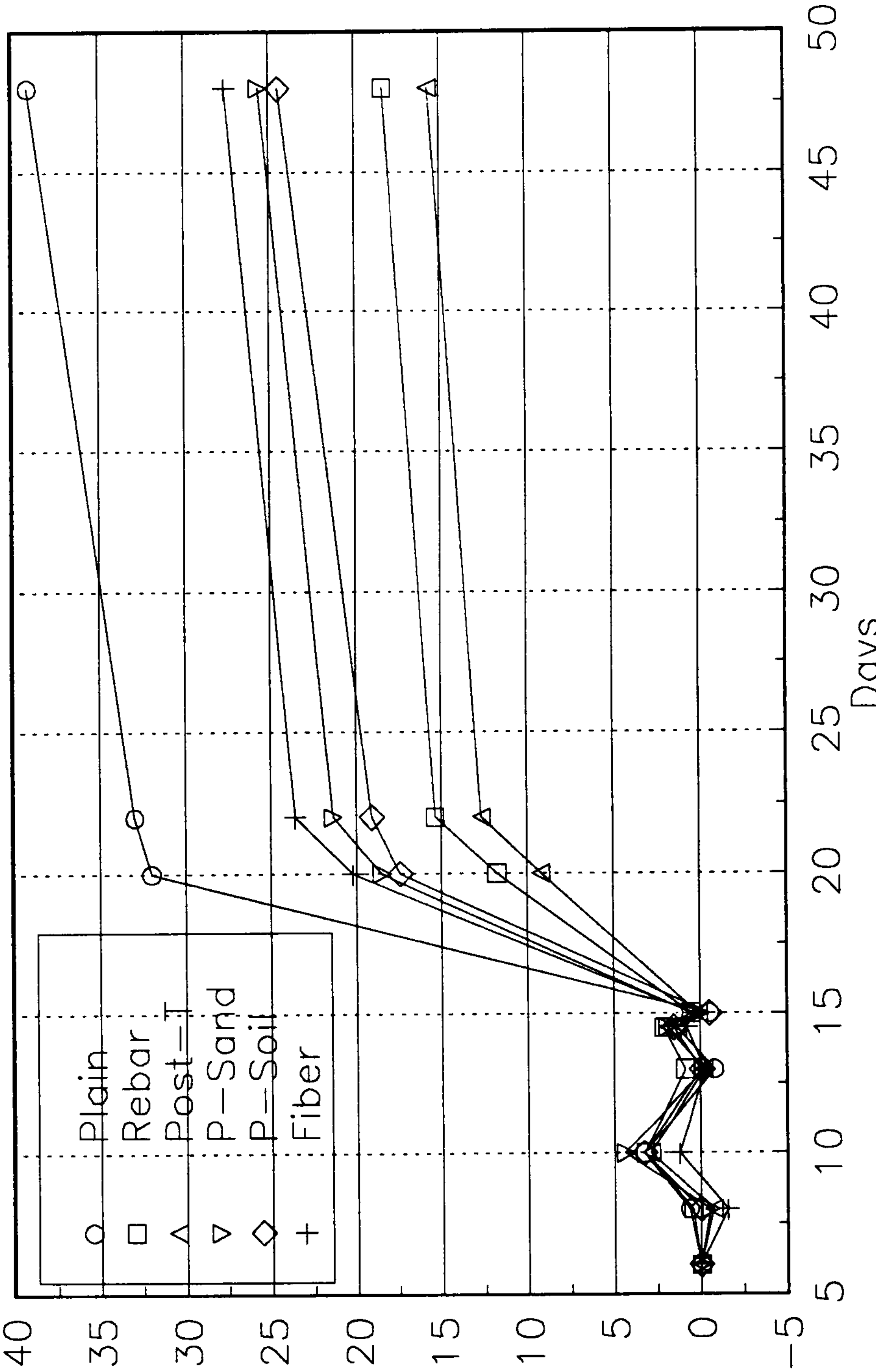

Figure 4-24 Tension Zone Wall Elongation Comparisons

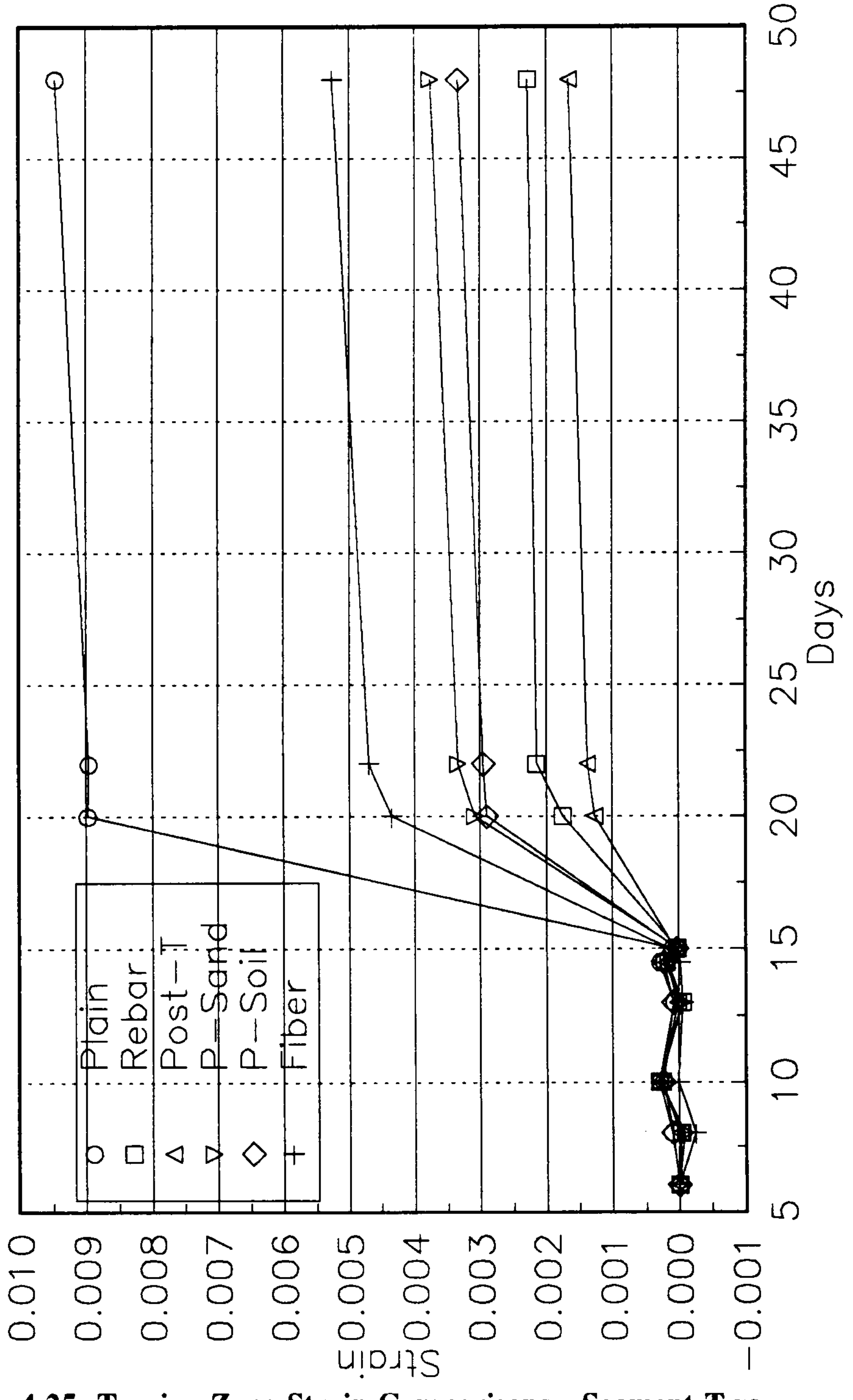

Figure 4-25 Tension Zone Strain Comparisons - Segment Two

figure gives a better comparison because it is not until after cracking that the individual mitigation techniques show a considerable difference; the plots of total elongation have an averaging effect on strain.

CHAPTER 5

ECONOMIC ANALYSIS

5.1 Costs Estimate Assumptions

5.1.1 Introduction

The impact of foundation damage mitigation techniques (DMT) on residential building costs is investigated. There are many possible house sizes, shapes, sites, geographical locations, and materials. Various foundations are better suited for certain type houses and geographical locations. This chapter is limited to the economic study of typical residential construction in southern Illinois.

The information obtained in this chapter is intended to show only approximate costs relationships between various construction methods; it is not intended as an estimating guide. Costs for a particular structure could vary from prices listed herein and would have to be determined on an individual basis. Total house, foundation, and mitigation costs were obtained using a national cost data standard (Means, 1992) and this author's judgment. The costs obtained from Means (1992) reflect good economic conditions. During times of economic depression, contractors will typically bid work with little or no profit to maintain cash flow. The values in this chapter reflect a 10% profit margin for the installing contractor. Depression could cause labor wages to drop considerably, and so would the cost of construction.

All houses compared are rectangular one-story homes that have a length to width ratio of two. There are four building classes considered to show that more expensive homes are proportionally less effected by foundation costs. Class definitions as given by Means are shown in Table 5-1. The impact of economy of scale is seen by comparing homes ranging from 800 square feet of living space to 3200 square feet. Wood siding and brick veneer exterior construction, both typical to the area, were considered since typically there is slight differences in foundation costs. However, brick veneer homes may require more extensive DMT to prevent noticeable damage from subsidence.

The geographical location of a house effects the type of foundation chosen. To avoid frost-heave and meet building codes, the foundation bottom needs to be below the frost-line. Typically houses in the south can achieve this by using a slab-on-grade with a perimeter turn down. In the northern states where the frost-line can be several feet deep, a common foundation would consist of a wall resting on a strip footing. The frost-line in Illinois varies from approximately 1 to 3 feet in depth and a foundation wall and footing is more often used. A typical house floor would either be a slab-on-grade (cast within the walls if used) or constructed from wood girders, joists, and sheathing. When a wood floor is used, the house will typically have a crawl space. The only foundation considered in this chapter is the strip footing and wall type that supports a house with a wood floor and crawl space.

Table 5-1 Description of Building Classes (Means, 1992)

Building Class	Description
Economy	An economy class residence is usually mass-produced from stock plans. The materials and workmanship are sufficient only to satisfy minimum building codes. Low construction cost is more important than distinctive features. Design is seldom other than square or rectangular.
Average	An average class residence is simple in design and is built from standard designer plans. Materials and workmanship are average, but often exceed the minimum building codes. There are frequently special features that give the residence some distinctive characteristics.
Custom	A custom class residence is usually built from a designer's plans which have been modified to give the building a distinction of design. Materials and workmanship are generally above average with obvious attention given to construction details. Construction normally exceeds building code requirements.
Luxury	A luxury class residence is built from an architect's plan for a specific owner. It is unique in design and workmanship. There are many special features, and construction usually exceeds all building codes. It is obvious that primary attention is placed on the owner's comfort and pleasure. Construction is supervised by an architect.

5.1.2 Base Foundation Assumptions

The "base foundations" shown in Figure 5-1 employ no mitigation techniques and have only the minimum necessities for a house foundation. The only difference in the two shown is the brick veneer foundation uses two courses of larger block filled with mortar to reduce the quantity of brick (and the costs) required on a house. This causes the cost of the brick veneer foundation to increase slightly. The five course wall comes from assuming a 24 inch frost-line and placing the house on a gently sloping lot that on average requires five courses. The exposed face of the foundation wall was assumed to be plastered for aesthetics in the custom and luxury building classes. The footing is cast-in-place (CIP) concrete.

5.1.3 Mitigation Assumptions

In later comparisons, the cost of DMT will be added to the "base foundation" costs. The Heron Road site was intended to investigate only footing DMT. A considerable improvement in damage mitigation was observed from the sill plate contribution. The costs of various common wall DMT are determined and further study needs to be done. The results indicate that the wall and footing should be constructed to behave compositely to fully utilize DMT.

The footing construction specifics used at the Heron Road site were modified in some of the foundations for the economic analysis. The changes shown in Table 5-2 were made either to better simulate the existing practices used in the residential construction industry, to meet code requirements, or to better the behavior of the

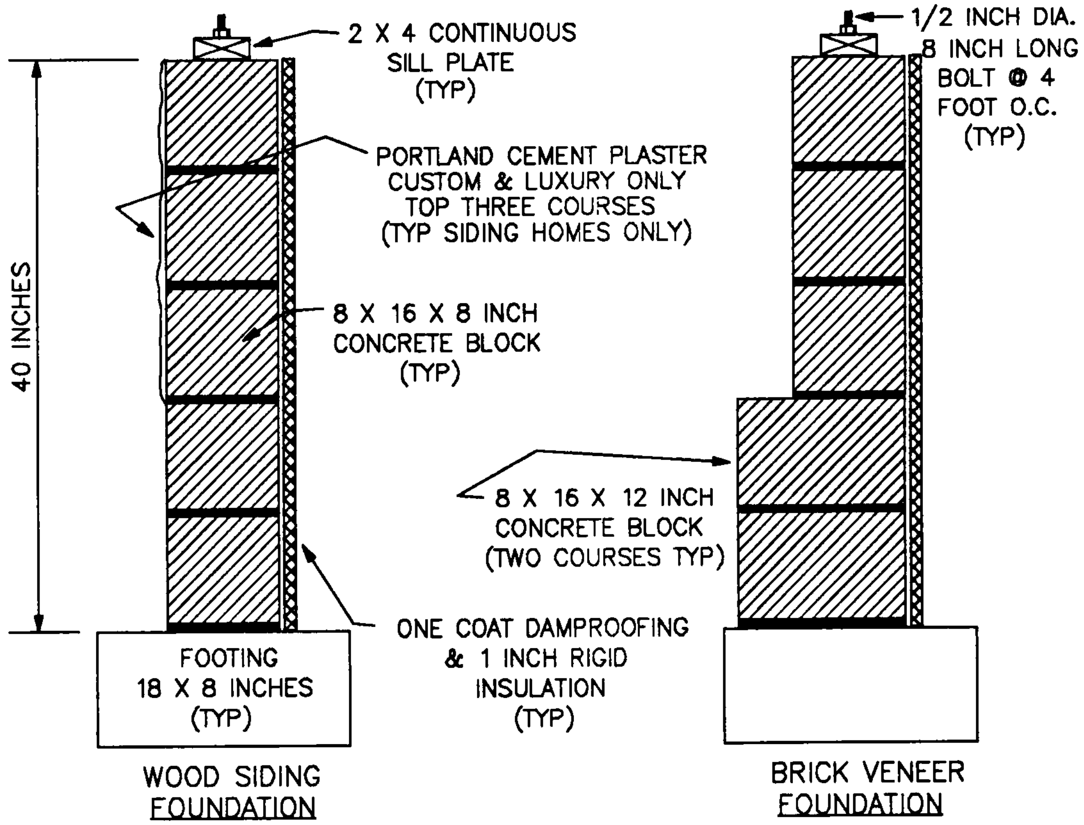

Figure 5-1 Base Foundations

Table 5-2 Specifics of Footing Construction Techniques - Economic Analysis

Footing Damage Mitigation Technique	Specifics/Changes Made Over Original Foundations
Plastic-Soil	Unchanged
Plastic-Sand	Unchanged
Steel Fiber	Dosage increased from 75 pounds per CY to 100
Deformed Bar	Only one layer of two #4 bars (1/2 inch) with 3 inches clear cover from bottom of footing trench. Meets ACI 318-89
Post-Tensioning	Only four strands - two top and two bottom. Load strands to higher stress

foundations. The steel fiber content was increased because lab tests indicated that the quantity used was insufficient to increase the tensile capacity. The deformed bar footing was changed because after meeting ACI cover requirements, the two layers of steel are close in proximity and improvements in behavior from the second layer are minimal. Another consideration is if the wall is constructed to act compositely with the footing, the footing bars need only act as tension steel for positive bending (i.e. compression phase in centerline). The post-tensioned footing eliminated two strands because the original six strands were not stressed to their full capacity (but they can be in the four strand case) and the cross-sectional area of the footing has been reduced.

Table 5-3 shows the specifics of the wall DMT which are evaluated for economy. These techniques can easily be applied in residential construction. The double sill plate method which has been investigated, requires excellent workmanship to be a good source of damage mitigation. A concrete bond beam would be a good replacement to assure adequate workmanship.

5.2 Foundation Costs

5.2.1 Base Foundation Costs

The factors effecting foundation construction costs are many. Expenses for smaller projects are proportionally higher because of certain fixed costs (e.g. equipment mobilization). Larger projects realize an economy of scale, thus reducing cost. In this section, foundation costs are estimated for an average size project and converted into a

Table 5-3 Specifics of Wall Construction Techniques - Economic Analysis

Wall Damage Mitigation Technique	Specifics/Changes Made Over Original Foundations
Double Sill Plate	Two nominal 2 x 8 inch with no double butt joints. Decrease bolt location to 2 foot centers and assure tight fit. Nail boards together at close spacing to behave compositely
Bond Beam	Top course of block replaced with a continuous bond beam. Use one #6 bar (3/4 inch) and 3000 psi concrete
Bed Joint Horizontal Reinf	Add nominal 8 inch wide truss type wire reinforcing at every course including the footing to block bed-joint
Vertical Reinf & Grout	Embed #4 bars approximately 4 inches into footing and extend vertically to top of wall at every other block void (16 inches on center). Fill these voids with grout
CIP Reinf Concrete Wall	Replace block wall with 8 inch wide wall lightly reinforced to meet ACI 318-89 minimum requirements. Use 3000 psi concrete and add approximately 0.5 square inches of extra reinforcing at top of wall

per linear foot costs. This per foot cost is used for all size homes neglecting the effect of project magnitude. This simplification seems reasonable for all houses with the possible exception of the largest and smallest of homes.

Table 5-4 shows the assumptions used for determination of the "base foundation" costs. Also tabulated is the cost per foot estimated for the various components of the system. All of the first four items (by row) are to be added to each of the block wall systems (lower three rows) to obtain a total base foundation costs per linear foot for a specific wall system. In Table 5-5 the "base foundation" cost is compared for various size rectangular houses that have a length to width ratio of two. Figure 5-2 is a graphical representation of Table 5-5. The non-linear relationship shows that for a given length to width ratio, increasing the size of a house does not proportionally increase the foundation's costs. The perimeter (length of foundation) of the house does not increase as fast as the floor area. This figure is also useful for house sizes not tabulated in Table 5-5. An approximate correction can be made for homes that are rectangular with a length to width ratio of other than two. Rectangular homes that have a large length to width ratio will have more foundation costs relative to the square footage of the house. Since foundation costs is based only on a costs per linear foot basis, the only difference in the cost is the length of foundation. To adjust, calculate the length to width ratio and correct the cost of the foundation by multiplying the value in Table 5-5 (or Figure 5-2) by the correction ratio obtained from Figure 5-3. For example, the foundation cost for a brick veneer house that is 50 feet by 40 feet is approximately \$5,810 (L/W = 1.25; 0.95 times \$6,120).

Table 5-4 Estimate Assumptions for Base Foundations

Task	Assumptions Used in Cost Derivations (Refer to Figure 5-1)	Cost/lf Foundation
Clear and Grub	Site assumed cleared & stripped before construction began	0.00
Excavate Crawl Space	Remove and waste on-site approximately 16 inches of soil to 1 foot outside foundation perimeter. Assume machine on-site from previous grade work	1.30
Layout and Excavate Strip Footings	Grade is at top of footing before excavation and excess soil is wasted on-site. Trench serves as concrete form. Includes mobilization cost for backhoe. Includes backfill after foundation constructed	5.00
Place Footings	No formwork included. Use 3000 psi concrete. Includes key at footing top. Concrete is to be placed directly out of truck	3.12
Siding Block Wall System Economy & Average	Includes additional layout. Block and mortar delivered to site	17.56
Siding Block Wall System Custom & Luxury	Same as above	18.73
Brick Veneer Block Wall System	Same as above	22.82

Table 5-5 Base Foundation Cost for Various House Sizes

Living Space Floor Area (sf)	House Perimeter (ft)	Foundation Costs (dollars)		
		Wood, Metal or Vinyl Siding		Brick Veneer
		Econ & Avg	Cust & Lux	
800	120.0	3,240	3,380	3,870
1000	134.2	3,620	3,780	4,320
1200	147.0	3,960	4,140	4,740
1400	158.7	4,280	4,470	5,120
1600	169.7	4,580	4,780	5,470
1800	180.0	4,860	5,070	5,800
2000	189.7	5,120	5,340	6,120
2400	207.8	5,610	5,850	6,700
2800	224.5	6,060	6,320	7,240
3200	240.0	6,470	6,760	7,740

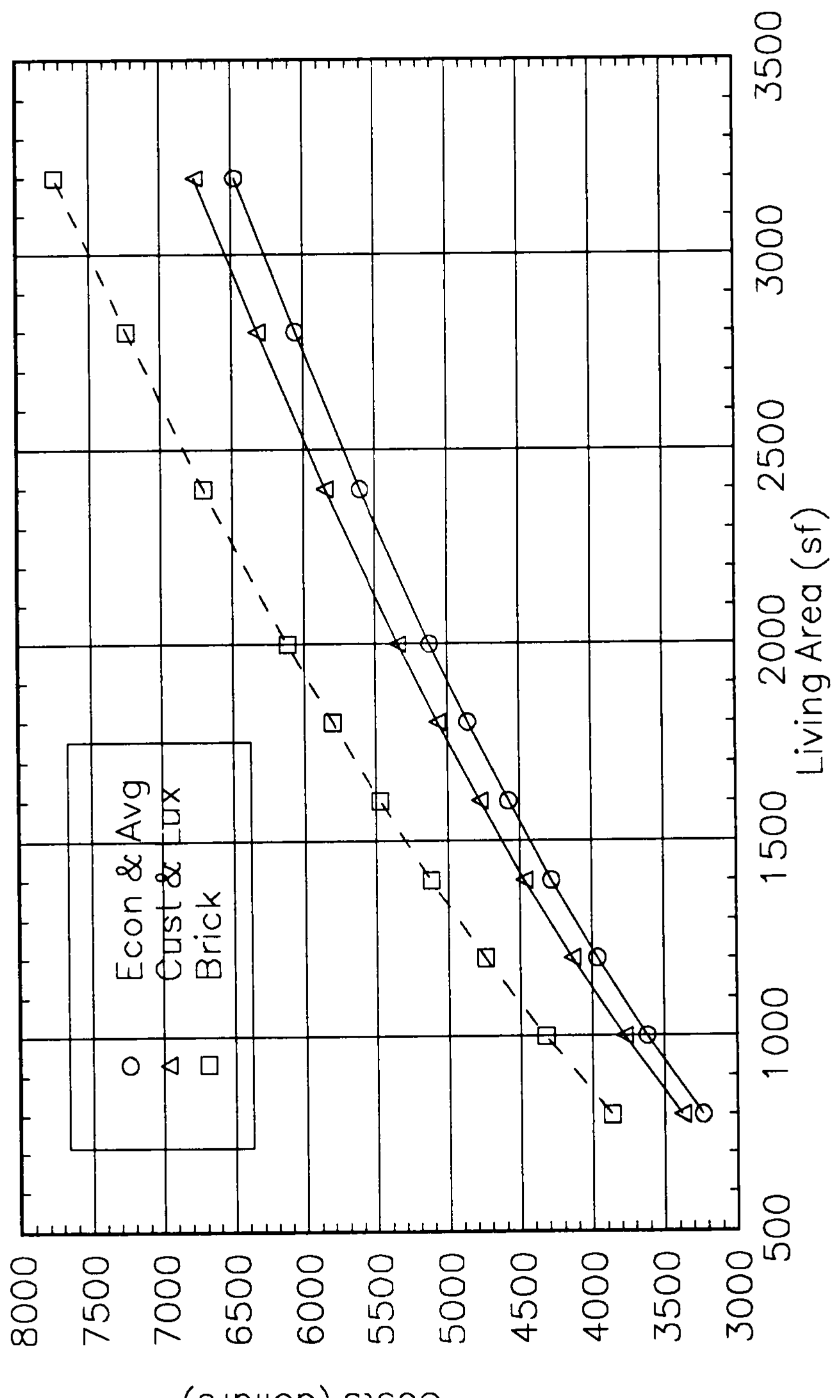

Figure 5-2 Base Foundation Costs for Various Sizes - Graphical

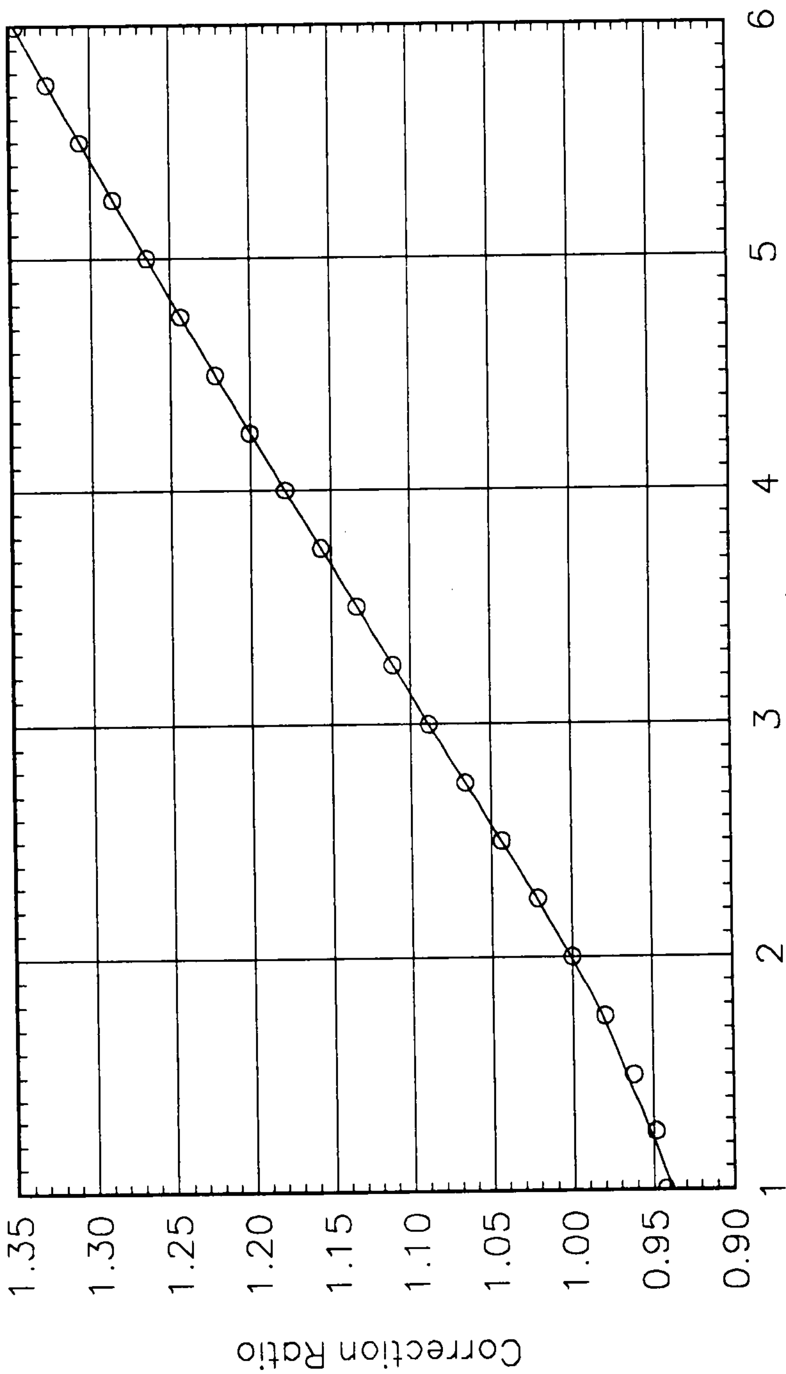

Figure 5-3 Cost Adjustment Factor for Shape of Base Foundation

5.2.2 Damage Mitigation Technique Costs

The same factors that effected the base foundation costs affect the DMT. Larger projects typically show less cost per unit prices. As above, the DMT of an average size project were converted into a per linear foot of foundation basis.

Table 5-6 and 5-7 show the assumptions made in estimating the cost of the footing and wall DMT. The total cost of these techniques for homes with a length to width ratio of two are shown in Table 5-8 and 5-9. These values are also based on a set linear foot cost and Figure 5-3 should be used to adjust for length to width ratios other than two. For example, the cost of adding both a bond beam and deformed bars to the wall and footing respectfully of a house 77 feet x 26 feet is approximately $719 (L/W = 3.0; 1.09 times ($167 + 493)).

5.3 Costs Comparisons

5.3.1 Total House Costs Assumptions

When comparisons are made between various DMT, the costs of the technique may appear expensive when compared to the cost of the foundation, but insignificant when compared to the total cost of the house. The reduction in damage from using well constructed foundations could easily offset any extra initial costs. To obtain a feel for the value of these techniques, total house costs must be determined for houses of the size mentioned previously and comparisons made to the foundation costs.

Costs for several 1000 and 2400 square foot houses of various building classes

Table 5-6 Estimate Assumptions for Footing Damage Mitigation Techniques

Footing Damage Mitigation Technique	Assumptions Used in Cost Derivations (Refer to Table 5-2)
Plastic-Soil	Assume 1 extra man-hour to pick-up plastic. Drape plastic 18 inches beyond trench both sides
Plastic-Sand	Place sand with machine that is on-site. Hand tamp. Plastic same as above
Steel Fiber	Added extra cost for placement. Add 2 man-hours to pick-up fibers from vendor
Deformed Bar	Add 1 1/2 man-hours to pick-up bars from vendor. Includes costs of chairs & transverse bars @ 8 foot centers for ease of placement
(F) Post-Tensioning	First-time workers post-tensioned. Assume freight costs for material and stressing equipment to a remote area. Extra excavation
(O) Post-Tensioning	Post-tensioning done by experienced crew with own equipment and materials purchased in bulk. Excavation as above

Table 5-7 Estimate Assumptions for Wall Damage Mitigation Techniques

Wall Damage Mitigation Technique	Assumptions Used in Cost Derivations (Refer to Table 5-3)
Double Sill Plate	Bolt length increased.
Bond Beam	Assume minimum purchase of 2 CY concrete. Majority of bond beam placed directly from truck chute
Bed Joint Reinforcing	Assume delivered with block.
Vertical Reinforcing & Grout	Assume anchor bolts placed in a grouted cell
(A) CIP Reinforced Concrete Wall	This does not have the plaster costs from the block wall subtracted. Place directly from truck chute
(E) CIP Reinforced Concrete Wall	This does have the plaster costs subtracted. Place as above

Table 5-8 Footing Damage Mitigation Techniques Costs for Various House Sizes

Living Space Floor Area (sf)	Footing Damage Mitigation Technique Cost (dollars)					
	Plastic-Soil	Plastic-Sand	Steel Fiber	Deformed Bar	(F) Post-Tensioning	(O) Post-Tensioning
800	86	216	330	106	1,020	612
1000	97	241	369	118	1,140	684
1200	106	265	404	129	1,249	750
1400	114	286	437	140	1,349	810
1600	122	305	467	149	1,442	865
1800	130	324	495	158	1,530	918
2000	137	342	522	167	1,613	968
2400	150	374	572	183	1,767	1,060
2800	162	404	617	198	1,908	1,145
3200	173	432	660	211	2,040	1,224

Table 5-9 Wall Damage Mitigation Techniques Costs for Various House Sizes

Living Space Floor Area (sf)	Wall Damage Mitigation Technique Cost (dollars)					
	Double Sill Plate	Bond Beam	Bed Joint Reinf	Vertical Reinf & Grout	(A) Cast-in-Place Reinf Concrete Wall	(E) Cast-in-Place Reinf Concrete Wall
800	408	312	156	456	641	500
1000	456	349	174	510	716	559
1200	500	382	191	558	785	613
1400	540	413	206	603	848	662
1600	577	441	221	645	906	708
1800	612	468	234	684	961	751
2000	645	493	247	721	1,013	791
2400	707	540	270	790	1,110	867
2800	763	584	292	853	1,199	936
3200	816	624	312	912	1,282	1,001

and exterior construction were estimated. The house costs were determined by using the Means (1992) square foot costs section modified by the assemblies and components sections to adjust for the differences in initial assumptions. The costs do not include any sitework (no driveway, sidewalk, septic system, landscaping, etc.) other than that listed in Table 5-4. The houses are all one story with the same assumptions as described in section 5.1.1. No utilities are included further than 5 feet outside the house perimeter. There are no garages, basements, porches, or carports included in these costs.

Most of the above mentioned exclusions are actually present when a house is constructed and should be included in the total house costs. If these costs were included, it would typically (except for the basement, garage, porch, and carport) lower the foundation's percentage of total house costs.

5.3.2 House, Foundation, and Damage Mitigation Techniques Cost Comparisons

Table 5-10 shows the estimated total house costs and the base foundation percentage of that total. This table shows that more expensive homes have a lower percentage of the total costs in the foundations. It also shows the same trend (as Figure 5-2 did) for increasing house size.

The selection of appropriate damage mitigation techniques is determined by weighing the cost and benefits. Certain techniques may be slightly less effective, but cost considerably less. Table 5-11 and 5-12 shows the percent costs of DMT with respect to the foundation and total house costs for wood siding exterior construction only. The tables show that these techniques may increase the foundation cost by a large

Table 5-10 Comparisons of Total House Costs and Base Foundation Costs

Building Class	Exterior Construction	1000 SF Living Space		2400 SF Living Space	
		House Total Costs (dollars)	Foundation Cost % of Total	House Total Costs (dollars)	Foundation Cost % of Total
Economy	Wood Siding	50,700	7.1	89,600	6.3
	Brick Veneer	54,500	7.9	95,500	7.0
Average	Wood Siding	63,200	5.7	113,700	4.9
	Brick Veneer	71,900	6.0	130,600	5.1
Custom	Wood Siding	82,400	4.6	141,900	4.1
	Brick Veneer	91,600	4.7	159,700	4.2
Luxury	Wood Siding	102,100	3.7	178,900	3.3
	Brick Veneer	106,800	4.0	186,200	3.6

Table 5-11 Footing Damage Mitigation Techniques Percentage of Costs

Footing Mitigation Technique	1000 SF Living Space				2400 SF Living Space			
	Average		Luxury		Average		Luxury	
	% Fnd	% House	% Fnd	% House	% Fnd	% House	% Fnd	% House
Plastic-Soil	2.7	0.2	2.6	0.1	2.7	0.1	2.6	0.1
Plastic-Sand	6.7	0.4	6.4	0.2	6.7	0.3	6.4	0.2
Steel Fiber	10.2	0.6	9.8	0.4	10.2	0.5	9.8	0.3
Deformed Bar	3.3	0.2	3.1	0.1	3.3	0.2	3.1	0.1
P-Tension (F)	31.5	1.8	30.2	1.1	31.5	1.6	30.2	1.0
P-Tension (O)	18.9	1.1	18.1	0.7	18.9	0.9	18.1	0.6

Table 5-12 Wall Damage Mitigation Techniques Percentage of Costs

Wall Mitigation Technique	1000 SF Living Space				2400 SF Living Space			
	Average		Luxury		Average		Luxury	
	% Fnd	% House	% Fnd	% House	% Fnd	% House	% Fnd	% House
Double Sill Plate	12.6	0.7	12.1	0.4	12.6	0.6	12.1	0.4
Bond Beam	9.6	0.6	9.2	0.3	9.6	0.5	9.2	0.3
Bed Joint Reinf	4.8	0.3	4.6	0.2	4.8	0.2	4.6	0.1
Vertical Reinf & Grout	14.1	0.8	13.5	0.5	14.1	0.7	13.5	0.4
CIP Reinf Concrete Wall	19.8	1.1	14.8	0.5	19.8	1.0	14.8	0.5

percentage, but only slightly increase the total. For example post-tensioning of the footing by an experienced crew could increase the cost of an average 2400 square foot house foundation by approximately 19%, but only increase the total costs of the house by less than a percent.

CHAPTER 6

CONCLUSIONS AND RECOMMENDATIONS

6.1 Conclusions

Subsidence damage can be minimized by using damage mitigation techniques. To select the proper technique, a cost and benefit comparison can be made between behavior, ease of construction, and costs.

The behavior of the foundations indicate which material properties are important. All structural failures (cracks) occur as a result of excessive tensile stress. Since the compressive stresses during subsidence are low, the only compressive stress-strain relationships necessary are for low stresses.

Subsidence damage concentrated in sections of the foundation. The stresses which cause damage are primarily negative bending. The post-tensioned foundation had the smallest damage and the plain concrete the largest. Deformed bars provided the second best performance which was comparable to the post-tensioned foundation. Footing interfaces slightly improved the behavior. The tension zone plastic-on-soil and plastic-on-sand interfaces reduced damage equally. Steel fibers show only a slight improvement over plain concrete. Figure 4-25 provides an accurate comparison of footing damage mitigation techniques effectiveness.

The post-tensioned foundation is much more expensive than the deformed bar foundation. The benefit does not offset the costs. The steel fiber alternative had the second largest expense and the plastic-on-sand the third. Deformed bar and plastic-on-soil have approximately equal construction costs. Figure 5-8 shows these costs relationships.

6.2 Recommendations

The compressive stress-strain relationship of concrete at low stresses is approximately linear. An appropriate modulus of elasticity would probably be the initial tangent if concrete behaved equally in tension as it does in compression. Since bending tensile stresses at cracking become increasingly non-linear at the extreme fibers, a more appropriate value would probably be the 40% secant modulus. This modulus would reflect an average of compression and tension modulii. Since no data are available for the stress-strain behavior in tension, a more refined non-linear analysis (for low subsidence stresses) is not justified.

House foundations should be constructed where the footing and wall behave compositely in resisting damage. This can be accomplished by damage mitigation techniques used in both the footing and wall. The observed behavior and economic considerations suggest that the footing should be reinforced with deformed bars. A reliable wall damage mitigation technique that is easily constructed and economical is a bond beam.

This research has provided a sound information base for footing damage mitigation. More research should be done on wall behavior.

REFERENCES

REFERENCES

ACI Committee 318 (1989). Building Code Requirements for Reinforced Concrete (ACI 318-89). American Concrete Institute, Detroit, Michigan.

American Society for Testing and Materials (1989). "Steel Strand, Uncoated Seven-Wire Stress-Relieved for Prestressed Concrete," Annual Book of ASTM Standards, 01.04, (A 416 - 88b). ASTM, Easton, MD.

American Society for Testing and Materials (1989). "Deformed and Plain Billet-Steel Bars for Concrete Reinforcement," Annual Book of ASTM Standards, 01.04, (A 615 - 87a). ASTM, Easton, MD.

American Society for Testing and Materials (1989). "Making and Curing Concrete Test Specimens in the Field," Annual Book of ASTM Standards, 04.02, (C 31 - 88). ASTM, Easton, MD.

American Society for Testing and Materials (1989). "Compressive Strength of Cylindrical Concrete Specimens," Annual Book of ASTM Standards, 04.02, (C 39 - 86). ASTM, Easton, MD.

American Society for Testing and Materials (1989). "Flexural Strength of Concrete (Using Simple Beam with Third-Point Loading)," Annual Book of ASTM Standards, 04.02, (C 78 - 84). ASTM, Easton, MD.

American Society for Testing and Materials (1989). "Sampling and Testing Concrete Masonry Units," Annual Book of ASTM Standards, 04.05, (C 140 - 75). ASTM, Easton, MD.

American Society for Testing and Materials (1989). "Slump of Hydraulic Cement Concrete," Annual Book of ASTM Standards, 04.02, (C 143 - 89a). ASTM, Easton, MD.

American Society for Testing and Materials (1989). "Flexural Strength of Concrete (Using Simple Beam with Center-Point Loading)," Annual Book of ASTM Standards, 04.02, (C 293 - 79). ASTM, Easton, MD.

American Society for Testing and Materials (1989). "Static Modulus of Elasticity and Poisson's Ratio of Concrete in Compression," Annual Book of ASTM Standards, 04.02, (C 469 - 87a). ASTM, Easton, MD.

American Society for Testing and Materials (1989). "Splitting Tensile Strength of Cylindrical Concrete Specimens," Annual Book of ASTM Standards, 04.02, (C 496 - 86). ASTM, Easton, MD.

American Society for Testing and Materials (1989). "Splitting Tensile Strength of Masonry Units," Annual Book of ASTM Standards, 04.05, (C 1006 - 84). ASTM, Easton, MD.

American Society for Testing and Materials (1989). "Test Method for Young's Modulus, Tangent Modulus, and Chord Modulus," Annual Book of ASTM Standards, 03.01, (E111). ASTM, Easton, MD.

American Society for Testing and Materials (1989). "Standard Tests Methods for Compressive Strength of Masonry Prisms," Annual Book of ASTM Standards, 04.05, (E 447 - 84). ASTM, Easton, MD.

Bennett, R. M., and Drumm, E. C., Editors (1992). "Subsidence Effects on Structures," Institute for Geotechnology Report #92-01, The University of Tennessee, 3 Volumes.

Bennett, R. M., Drumm, E. C., Johnson, D. C. (1992). "Behavior of Linear Foundations Subjected to Longwall Subsidence," Third International Workshop on Surface Subsidence due to Underground Mining. Morgantown, West Virginia, 121-128.

Fintel, M. (1985). Handbook of Concrete Engineering, Second Edition, Van Nostrand Reinhold Co., Inc., New York, NY, 172.

Hognestad, E., Hanson, N. W., and McHenry, D. (1955). "Concrete Stress Distribution in Ultimate Strength Design," Journal of the American Concrete Institute, 52(28), 472-476.

Hudgings, R. A., Bennett, R. M., Sneed, L. A. (1990). "Experimental Testing of Damage Mitigation Techniques," Mine Subsidence - Prediction and Control, Association of Engineering Geologists, 173-176.

Johnson, J. W. (1928). "Relationship Between Strength and Elasticity of Concrete in Tension and in Compression," Bulletin 90, Engineering Experiment Station, Iowa State College, Vol. XXVI. Ames, Iowa, 24-29.

MacGregor, J. G. (1988). Reinforced Concrete Mechanics and Design, First Edition, Prentice-Hall, Inc., Englewood Cliffs, New Jersey, 42-43, 51-53.

- (1992). "Means Residential Cost Data," Eleventh Annual Edition, R. S. Means Co., Kingston, Massachusetts.

Mehta, P. K. (1986). Concrete: Structure, Properties, and Materials, Prentice-Hall, Inc., Englewood Cliffs, New Jersey, 55-86.

Mirza, S. A., Hatzinikolas, M., and MacGregor, J. G. (1979). "Statistical Descriptions of Strength of Concrete," Journal of the Structural Division, ASCE, 105(ST6), 1021-1037.

Patton, M. E., and Whittaker, W. L. (1983). "Effects of Fiber Content and Damaging Load on Steel Fiber Reinforced Concrete Stiffness," Journal of the American Concrete Institute, 80(2), 13-16.

Ramakrishnan, V., Coyle, W. V., Kulandaisamy, V., and Schrader, E. K. (1981). "Performance Characteristics of Fiber Reinforced Concretes with Low Fiber Contents," Journal of the American Concrete Institute, 78(35), 388-394.

Raphael, J. M. (1984). "Tensile Strength of Concrete," Journal of the American Concrete Institute, 81(17), 158-165.

Shah, S. P., and Rangan, B. V. (1971). "Fiber Reinforced Concrete Properties," Journal of the American Concrete Institute, 68(14), 126-135.

VITA

David Charles Johnson was born on January 16, 1962 in Clinton, Tennessee. At the age of five months he moved to Jupiter, Florida and back to Clinton in 1966. He attended grammar, junior high, and high school in Clinton.

He enrolled in the University of Tennessee, Knoxville in 1984 with engineering interest. In approximately 1986 he enrolled in Civil Engineering. Soon after he went through the Cooperative Education Program employed by Kesterson Construction Company (KCC) in Maryville, Tennessee. He continued to work for KCC all through his undergraduate studies until obtaining his Bachelor of Science degree in Civil Engineering in the spring of 1990.

Before completion of his undergraduate degree, he accepted a graduate research assistance position. He completed his research and a portion of his thesis by August of 1991 and took a full-time project management position at KCC where he works today. He graduated with a Master of Science degree in Civil Engineering (concentration in structural) in the fall of 1992.